304

PREDICTION OF HEAT TRANSFER AND PRESSURE DROP DURING CONDENSATION INSIDE HORIZONTAL TUBES WITH AND WITHOUT TWISTED TAPE INSERTS

by

KONERU RAMAKRISHNA

B.E., Andhra University, Waltair, India, 1976
M. Tech., Indian Institute of Technology, Madras, India, 1978

A MASTER'S THESIS

submitted in partial fulfillment of the

requirements for the degree

MASTER OF SCIENCE

Department of Mechanical Engineering

KANSAS STATE UNIVERSITY
Manhattan, Kansas

1980

Approved by:

M. Z. Azer

Major Professor

THIS BOOK
CONTAINS
NUMEROUS PAGES
WITH THE ORIGINAL
PRINTING BEING
SKEWED
DIFFERENTLY FROM
THE TOP OF THE
PAGE TO THE
BOTTOM.

THIS IS AS RECEIVED
FROM THE
CUSTOMER.

TABLE OF CONTENTS

LIST OF TABLES

LIST OF FIGURES

ACKNOWLEDGEMENTS

I wish to express my sincere appreciation and gratitude to Prof. Naim Z. Azer for his guidance and counsel throughout the present investigation.

Thanks are extended to Prof. Leonard E. Fuller and Prof. Robert E. Crank for being on my examination committee. Thanks are also extended to Dr B.T. Beck of Department of Mechanical Engineering for several suggestions he made during the course of present investigation.

Thanks are also due to the Department of Mechanical Engineering for providing the financial support during the investigation and for other facilities.

I wish to thank Mrs. Meena B. Agrawalla for her efficient handling of the typing job.

Finally, I wish to thank my family for their patience and understanding during my graduate study.

Dedicated to my parents and Raji

CHAPTER I

INTRODUCTION

Over the past fifty years extensive studies were conducted to investigate the effects of swirl flow devices on the augmentation of heat transfer. Swirl flow can be accomplished by coiled wires, spiral fins, propellers, coiled tubes and twisted tape inserts. Most of the swirl flow devices have been shown to improve single phase and boiling heat transfer at the expense of increased pressure drop and consequently the pumping power. Improvement in heat transfer by such devices is attributed to increased velocity, secondary flow produced by radial body forces and the fin effect with certain swirl flow devices.

The success of twisted tape inserts in augmenting the single phase heat transfer and two phase boiling systems led recently to their application to condensation heat transfer inside the tubes. Royal and Bergles [58]* obtained heat transfer and pressure drop data during condensation of steam inside two similar horizontal tubes in the presence of a twisted tape insert. They used two tapes of different pitches. Luu and Bergles [60] obtained similar data for R-113 using two similar tubes and two tapes of different pitches.

Two separate correlations were developed to predict the heat transfer and pressure drop during condensation inside the

---

*Numbers in the parenthesis refer to the references in the bibliography.

tubes with twisted tapes, one for steam [58a,82] and one for R-113 [61,78]. These correlations were based on introducing modifiers to existing correlations for condensation inside smooth tubes.

The objective of present study is to attempt to develop one single correlation for heat transfer which correlates both steam and R-113 data. The objective is also to develop one single correlation for pressure drop which can correlate the data of both fluids. To achieve these objectives two different approaches were attempted.

In the first approach a suitable heat transfer correlation was identified from the existing smooth tube correlations which could correlate both steam and R-113 condensation data of Royal and Bergles [58] and Luu and Bergles [60] respectively. Modifiers were applied to these correlations to develop the desired correlations for condensation inside the tubes with twisted tape inserts. Similar procedure was adopted to obtain a desired correlation for pressure drop with twisted tape inserts that could correlate the two sets of data.

The second approach was analytical in nature in which the analogy between momentum and heat transfer in the condensate liquid film was used. This type of analogy was used with reasonable success for condensation inside the smooth tubes [68,70,72,73].

CHAPTER II

LITERATURE SURVEY

INTRODUCTION

Over the past twenty five years several reviews and surveys appeared on two phase flow in general and augmentation of single and two phase flows in particular. Gouse [1] compiled a complete bibliography of all references on two phase flow published prior to 1966. Bergles [2,3,4] published surveys on techniques to augment convective heat and mass transfer. Recently Bergles et al. [5] published a bibliography of world literature on augmentation of convective heat and mass transfer The total number of references cited was 1967. The literature was classified into passive augmentation techniques, which require no external power, and active techniques which do require external power. It was also classified according to the mode of heat transfer such as single phase flow, pool and flow boiling as well as dropwise and film condensation. Both forced and natural convective flow situations were covered. The techniques cited were surface roughness, internal and external extended surfaces, displaced promoters, swirl flow generators, surface tension devices, liquid additives,gas-liquid suspensions, fluid and surface vibrations and electro-static fields. Since the main concern of the present study is augmentation of condensation heat transfer by the use of twisted tape inserts, the emphasis of the present survey is on two-phase heat transfer augmentation with twisted tape inserts, namely,

boiling and condensation.

2.1 AUGMENTATION OF BOILING HEAT TRANSFER

One of the earliest studies on the swirl flow devices appears to be that of Larson et al.[6]. They investigated the effect of swirl flow on the forced convection boiling of R-12 inside a horizontal tube using a helical coil. They observed an increase in the heat transfer coefficients and pressure drop. Goldman [7] obtained data to show the effect of fluid spin on water boiling in tubes with short and long twisted tape inserts and with tangential inlet spinners in a small diameter,short vertical tube.For equal pumping power he obtained a 20% increase in critical heat flux (hereafter referred to as CHF). Oppenheimer [8] obtained boiling burnout data during spinning flow. He observed no effect of spinning flow on the CHF.

Gambill and Greene [9] studied the problem of burnout heat flux associated with forced convection sub-cooled and bulk nucleate boiling of water in source vortex flow (flow with tangential and axial velocity components) in small diameter horizontal tubes. They observed an increase of 400-500% in CHF compared to smooth tubes. They also studied [10] the problem of burnout of water boiling in vortex flow. They reported boiling and burnout data with spiral ramp and tangential slot vortex generators placed at the inlet of small diameter, horizontal tubes. Their data [10] showed no effect of liquid sub-cooling on the CHF.

Hoffman et al.[11] obtained experimental data on heat transfer, CHF and pressure drop for electrically heated tubes with full length twisted tape inserts during single and two phase flow of water at low and moderate pressures. They found that tighter tapes supported higher heat fluxes for a given wall superheat under local boiling conditions. They observed no effect of length-to-diameter ratio on heat transfer.

Gambill et al.[12] extended earlier studies [10] to obtain heat transfer, pressure drop, friction factors and the CHF during forced convection boiling of water with full length twisted tape inserts. They observed a 200% increase in CHF over the smooth tube values. They also observed that CHF was independent of liquid sub-cooling and system pressure. This study concluded that tapes are effective in raising the CHF of bulk boiling with net vapor generation and in local boiling with low or moderate liquid sub-cooling.

Gambill and Bundy [13] evaluated existing data on pressure drop, heat transfer and the CHF in the presence of swirl flow inside tubes and concluded that different sets of data were in some disagreement. However, they showed that twisted tape inserts improved heat transfer performance over the smooth tubes.

Hoffman et al.[14] summarised the axial and swirl flow boiling studies carried out at Oak Ridge National Laboratories with water, ethylene glycol and liquid metals.

Poppendiek et al.[15] reported experimental and analytical studies on pressure drop, velocity decay of liquid

film in swirl flow, and heat transfer during single and two phase flow of liquid metals. They used mercury for their experimental studies.

Gambill and Bundy [16] measured the local heat transfer coefficients, pressure drop and the CHF for ethylene glycol in forced convection axial and swirl flows, the latter with full length twisted tapes. The swirl flow boiling heat transfer coefficients were correlated by applying a correction factor, reflecting the acceleration induced by the swirl, to Kutateladge's [17] correlation. The swirl flow burnout heat flux data were correlated using an additive method in which boiling and non-boiling heat fluxes were separated. CHF for ethylene glycol was smaller than for water under similar conditions.

Gambill [18] conducted a series of tests in which electrical energy was dissipated in the twisted tape inserts (twist ratios 2.7-∞) than in the tube wall. He found that critical wall superheat increased with decreasing twist ratio of the twisted tape. CHF showed an optimal value between the twist ratios of 7 and 10. Inertial impingement of the liquid drops near the tube entrance and secondary flow in the rest of the tube were found to improve the performance in this case. It was concluded that CHF for other tapes can be approximated by the flat tape values.

Poppendiek and Gambill [19] reviewed the experimental and analytical studies on momentum and heat transfer in single

and two phase swirl flows.

Foure [20] identified equations to predict pressure drop inside a circular tube in which swirl flow of water is maintained by a twisted tape insert. The agreement between the predictions, taking fluid rotation, friction and form drag due to tape into account, and experimental data was better with tapes of higher pitch than for lower pitch. Foure [21] also observed experimentally fields of flow pulsations in a R-11 natural convection loop with and without twisted tape inserts and concluded that fields of pulsations are larger with tape than without tape inserts. Foure [21] also described the improvements made in the experimental determination of slip ratio in air-water systems through measuring air and water flow rates. He also compared the experimental pressure drop data on flat tape and tapes with finite pitch, with some of the correlations available in literature.

Foure et al.[22] obtained pressure drop and void fraction data with and without twisted tape inserts in circular pipes and an annulus during two phase flow of air and water. In pipes they used a single tape and in the annulus they used six tapes of three different pitches. Foure et al.[22] also studied the influence of water velocity, shape of the flow channel, the hydraulic diameter and the pitch of the tapes on single vortex (in circular tube with a tape) and bracketed vortices (in annulus with six tapes) using Martinelli and Nelson [87] parameter as the basis. Foure [23] obtained pressure drop, heat transfer coefficients and CHF during

boiling of R-11 inside a tube and an annulus in the presence of twisted tape inserts under natural and forced flow conditions. The pressure drop data agreed well with the predictions of Martinelli and Nelson [87]. Foure et al.[24] extended the work in reference [23] to water at atmospheric pressure and low flow velocities. Moussez [25] reviewed the work in references [20-24] and pointed out the difficulties involved with the measurements of pressure drop, heat transfer void fraction and the CHF with and without twisted tape inserts with different geometries.

The experiments of Foure et al.[24] were extended to higher pressures, 70 bars, in [26,27]. Three hundred burnout points were reported during axial and swirl flow boiling of water. The CHF showed a sharp decrease at a particular value of exit quality for axial and swirl flow; but occured at higher heat fluxes and qualities in swirl flow.

In the reference [28] experimental data on pressure drop, phase velocities and void fraction were reported for circular tubes, an annulus and a 4-rod cluster element with and without twisted tape inserts using air-water flow. The pressure drop and void fraction data agreed well with the predictions of Lockhart-Martinelli [83], Lottes et al.[29] and Mondin [30]. The predictions of tape data showed less deviations than the smooth tube data.

Moussez [31] reviewed the data obtained and predictions made in references [22-24,26-28]. He concluded that for a

given CHF, the flow rate can be reduced by 50% and heat transfe can be increased by 60% with the use of twisted tape inserts in two phase flow inside conduits.

Volterras and Tournier [32] conducted a series of experiments to obtain CHF during the boiling of water with and without twisted tape inserts using a 4-rod cluster of fuel elements at different pressures. All the tapes in this study had the same pitch. There was a 40% increase in CHF.

Foure et al.[33] obtained heat transfer, pressure drop and void fraction data for channels of different cross section with swirl flow. The heat transfer rates increased depending on system pressure level.

Allen [34] observed an increase of 50% in CHF of R-114 in natural convection flow inside a vertical tube with twisted tape inserts. He also observed no effect of twisted tape at low temperature drops across the liquid film during boiling. His data showed that the presence of twisted tape in the natural convection loop increased the heat transfer coefficients and the pressure drop and decreased the wall temperatures

Viskanta [35] reported CHF data in axial and swirl flow of water at 2000 psia during forced convection boiling inside the vertical tubes. He concluded that the effect of tape pitch was considerable on CHF. The maximum increase in CHF was 250% over the smooth tube value. This increase was attributed to the break up of vapor film blanketing the heated wall by centrifugal forces.

Gido and Koestel [36] developed an analytical model for heat transfer during forced convection vortex flow of mercury. They also obtained experimental data on heat transfer in swirl flow using mercury as the test fluid. Their experimental data showed an increase in swirl flow heat transfer upto 300% over the smooth tube values.

Blatt and Adt [37] investigated the effect of twisted tape inserts on heat transfer and pressure drop during boiling of water and R-11 inside a horizontal tube. They used an open loop section for water and closed loop for R-11. They covered the entire range of quality from 0 to 100%. Their results suggest that the usefulness of the tapes as augmentation devices varies with the fluid, the heat transfer rates and temperature ranges.

Berenstein et al.[38] evaluated several candidate tubes for use in once-through zero-gravity boilers and recommended serpentine tubes over the tubes with twisted tape inserts.

Moeck et al.[39] obtained CHF data for high quality steam-water mixture flowing in a vertical tube at 1000 psig with and without twisted tape inserts. Their results supported the idea that the CHF increases with the use of a twisted tape insert if the tape does not capture the liquid which would otherwise be available for impingement on the tube wall.

Pai and Pasint [40] reported the developments, at Foster and Wheeler Company, with the use of twisted tape

inserts in power boilers.

Hassida et al. [41] presented and analysed the experimental data obtained at CISE (Centro Informazioni Studi Experienze, Italy) laboratories on the possible means of increasing CHF in upward, vertical flow of steam-water mixture using small swirl promoters suitably placed along the channel. Eight hundred burnout points were reported in this paper.

Herbert and Sterns [42] presented about one hundred heat transfer data points in vertical falling films in the presence of a twisted tape insert. They noted that the heat transfer increased only at the entrance of the tube and no effect of twisted tape was observed for a length-to-diameter ratio beyond the value of 20.

Rousel and Rouvillois [43] discussed flow patterns and the CHF data in swirl flow and presented a tentative flow map for swirl flow boiling with velocity and quality as the co-ordinates.

Bergles et al. [44] presented heat transfer characteristics for dispersed flow boiling of nitrogen in the presence of swirl flow. They noted that the swirl flow minimised the thermal non-equilibrium.

Hunsbedt [45] and Hunsbedt and Roberts [46] reported heat transfer performance data for a seven tube bayonet tube forced recirculation evaporator. The departure from nucleate boiling characteristics employing swirl flow

generators and steam side heat transfer coefficients were also measured.

Lopina and Bergles [47] showed that the sub-cooled boiling tests of Gambill and Greene [10] were in fact the non-boiling tests and their superheat calculations were in error. They [47] obtained a boiling curve during swirl flow boiling with twisted tape insert and showed it to be similar to the axial flow boiling curve.

Cumo et al. [48] studied the influence of swirl flow generated by twisted tape inserts during R-12 flow in a double pipe heat exchanger. In this case R-12 was heated by forced convection flow of water in the annulus (not simply the uniform Joule heating). It was concluded that the twisted tapes increased the CHF by 200% over the smooth tube values under similar conditions.

Nooruddin and Murti [49] obtained data on heat transfer during swirl flow of an air-water system using twisted tape inserts of four different pitches. They observed two distinct heat transfer regimes.

Van der Mast et al. [50] used twisted tape inserts in desalination evaporators.

Ornatskiy et al. [51] investigated the CHF in concentric annuli of different sizes with and without swirl flow at the inlet to the tube and at different locations down stream of the inlet. Subbotin et al. [52] discussed the upper and lower limits on the tube length using augmentation devices including

swirl flow generators. Domanskiy and Sokolov [53] analysed the heat transfer problem in swirl flow of gas-liquid upward flow using a semi-empirical theory of turbulent momentum and heat transfer. Osipenko [54] studied the mass transfer problem from a thin continuous film of water evaporating on the inner wall of a tube with a swirl flow generator. Ryabov et al.[55] obtained experimental data on the temperature distribution, heat transfer rates, pressure drop and the CHF in rod bundles with different types of augmentation devices. Drizus et al.[56] measured the CHF in small diameter tubes at higher heat fluxes and mass velocities with twisted tape inserts.

While there is a considerable amount of experimental data on heat transfer, burnout and pressure drop using boiling of liquids inside channels with twisted tape inserts, very few unsuccessful attempts were made to analyse the flow phenomena associated with this type of augmentation technique. Until this can be accomplished additional experiments need to be carried out to cover wider ranges of heat fluxes, mass flow rates, with different channel sizes and geometries and different fluids.

2.2 AUGMENTATION OF CONDENSATION HEAT TRANSFER

Very few references were cited in the literature about the use of swirl flow generators in augmenting condensation heat transfer inside tubes. Lin [57] studied the augmentation of boiling and condensation heat transfer by means of static in-line mixers. His results showed that the mixers

were effective in improving the boiling and condensation heat transfer at the expense of increasing the pressure drop. In boiling the pumping power per unit heat transfer was considerably lower for the mixers compared to smooth tube values. However, the reverse was not true for condensation.

Very recently the use of twisted tape as an augmentation technique was extended to condensation heat transfer inside tubes. The only studies cited in the literature were those of Royal and Bergles [58,59], Luu and Bergles [60,61]. Royal and Bergles [58,59] reported heat transfer and pressure drop data during condensation of steam inside horizontal tubes with and without twisted tape inserts. Luu and Bergles [60,61] reported similar data for R-113 condensing inside horizontal tubes with and without twisted tape inserts. The results of these investigations will be discussed in detail later.

The objective of present study is to develop heat transfer and pressure drop correlations which predict the heat transfer and pressure drop during condensation inside tubes with twisted tape inserts.

CHAPTER III

CORRELATIONS FOR HORIZONTAL IN-TUBE CONDENSATION WITH AND WITHOUT TWISTED TAPE INSERTS

One of the approaches followed in developing the heat transfer and pressure drop design correlations for condensatior in tubes with twisted tape inserts was through applying suitabl modifiers to existing smooth tube correlations. The experimenta data obtained during condensation inside horizontal tubes, with and without twisted tape inserts by Royal and Bergles [58,59] for steam and Luu and Bergles [60,61] for R-113, were used as the source for developing these correlations.

The first step in developing the correlations being sought was to identify, among existing correlations, one single correlation to correlate the smooth tube heat transfer data of steam and R-113 and one single correlation to correlate the smooth tube pressure drop data of steam and R-113. The second step was to find suitable modifiers to these smooth tubes correlations to bring about the best possible correlation between the experimental data and the predictions of pressure drop and heat transfer for condensation in tubes with twisted tape inserts. A brief description of the two experimental investigations, mentioned above, is given in the following paragraphs.

3.1 EXPERIMENTAL DATA

Similar test sections were used by Royal and Bergles [58,59] for steam condensation and by Luu and Bergles [60,61] for R-113 condensation. Each test section was a double pipe exchanger and was divided into four, 3-foot long units to form

the test condenser sections. These sections were arranged in series, with the condensing medium flowing straight through the test tube while the coolant was diverted through mixing sections before proceeding to the next section. Thermocouples were used to measure coolant temperatures in the mixing sections at the entrance and exit of each condenser section.

Test condenser tube wall temperatures were obtained from thirty-six 30 gage copper-constantan thermocouples, spaced axially in groups of three at one-foot intervals along the test condenser. At each station, the three thermocouples were distributed circumferentially, with one at the top of the tube and the others at 90° and 180°.

For each test section, the sectional condensation heat transfer coefficient was obtained

$$h_z = \left[\frac{2\pi r_o \Delta z \, (\bar{t}_{sat} - \bar{t}_{wo})}{q_o} - \frac{r_o}{K_o} \ln\left(\frac{r_o}{r_o + a'}\right) \right]^{-1} \qquad (3\text{-}1)^*$$

where

h_z = sectional average heat transfer coefficient

r_o = inner tube inside radius

Δz = length of each single section of the test condenser

$\bar{t}_{wo}$ = average outside wall temperature of each section

q_o = sectional heat transfer obtained by measuring coolant temperature rise through each section and its flow rate

$\bar{t}_{sat}$ = average saturation temperature in each section

---

*See Nomenclature for the definition of symbols.

K_o = thermal conductivity of tube wall

a' = thickness of the tube wall

In Eq (3-1) the average wall temperatures were obtained by first averaging the circumferential temperatures at each station, using Simpson's rule and then linearly averaging the circumferential averages for each section. The average saturation pressure for each section was obtained by linearly averaging the static pressures of the condensing medium at each section's entrance and exit.

The overall heat transfer coefficient was also calculated from Eq (3-1) using the arithmetic average of the sectional average wall temperatures and linearly averaging $\bar{t}_{sat}$ for the inlet and outlet pressures of the entire condenser tube.

In each of the above investigations [59,61] one set of data was obtained for smooth tube pressure drop and heat transfer, and two sets of data were obtained for tubes with twisted tape inserts. The ranges of geometric and flow parameters covered are given in Tables 3.1 and 3.2 respectively. Any further details about these two investigations can be found in references [59,61].

3.2 SMOOTH TUBE CORRELATIONS

3.2.1 HEAT TRANSFER

Several correlations [62-76] are available in the literature to predict local and mean heat transfer coefficients during condensation inside tubes. Some of these correlations are based on single phase heat transfer analogy, some are based on the boundary layer treatment and analogy between heat

TABLE 3.1

SELECTED GEOMETRIC PARAMETERS OF THE EXPERIMENTAL TUBES

Test Fluid	Steam			R-113		
Type of Tube	Smooth	Twisted Tape # 1	Twisted Tape # 2	Smooth	Twisted Tape # 1	Twisted Tape # 2
Tube Number	2	3	4	1	2	3
Material	Cu[+]	Cu, SS[++]	Cu, SS	Cu	Cu, SS	Cu, SS
Outside diameter	0.625	0.625	0.625	0.625	0.625	0.625
Inside diameter	0.545	0.545	0.545	0.527	0.527	0.527
Wall Thickness	0.040	0.040	0.040	0.049	0.049	0.049
Tape Thickness	N.A.[*]	0.015	0.015	N.A.	0.020	0.020
Tape Pitch per 180°	N.A.	1.8	3.8	N.A.	1.467	2.425

*N.A. = not applicable

+ Cu = Copper ++ SS = Stainless Steel

Units are in inches

TABLE 3.2

SELECTED FLOW PARAMETERS RANGES FOR EXPERIMENTAL DATA

Test Fluid	Steam	R-113
Mass Velocity (lbm/ft^2 hr)	110,000-420,000	63,700-560,000
Overall Condensing Heat Transfer Coefficients ($Btu/ft^2 hr\ ^oF$)	3200-19,000	200-1200
Inlet Coolant Temperature (^oF)	270-340	50-219
Inlet Test Fluid Pressure (psia)	41.5-81.5	35-95
Inlet Test Fluid Superheat (^oF)	0-28	0-7
Exit Quality	-0.019 - +0.041	-0.052 - +0.06

and momentum transfer in the condensate (liquid) film. These correlations differ widely in their predictions and no single correlation predicts well the data obtained by different investigations. Some of these correlations are described in Appendix A.

Royal and Bergles [58,59] compared their smooth tube he transfer data for steam with several of in-tube condensation heat transfer correlations [63-66,72]. They found that the correlations of Akers et al. [63] and Soliman et al. [66] were reasonable predictors of their smooth tube heat transfer data of steam. The correlation of Akers et al. [63] predicte the sectional average heat transfer coefficients within ± 30% for about 60% of the data points and the overall values were predicted within ± 15% for most of the data points. In general this correlation predicted values slightly higher than the experimental values.

The correlation of Akers et al. [63] for the smooth tub can be written as:

$$\bar{h}_{TP} = 0.0265 \frac{K_l}{D} \left(\frac{G_e D}{\mu_l} \right)^{0.8} Pr_l^{0.4} \qquad (3\text{-}2)$$

where

h_{TP} = mean condensation heat transfer coefficient for smooth tube

K_l = thermal conductivity of the saturated liquid

μ_l = dynamic viscosity of the saturated liquid

Pr_l = Prandtl number of the saturated liquid

D = tube inside diameter

G_e = equivalent mass velocity

$$= G_t \left[\bar{x} \left(\frac{\rho_l}{\rho_v}\right)^{0.5} + (1-\bar{x}) \right]$$

$\bar{x}$ = arithmetic average of inlet and outlet qualities

G_t = total mass velocity

Royal [59] found that the correlation of Soliman et al. [66] best predicted the sectional heat transfer coefficients during steam condensation inside smooth tube.

Luu and Bergles [77,78] compared their smooth tube heat transfer data of R-113 with the predictions of the correlations in the references [62-67, 69,71,72,74,76]. They concluded that Shah [76], Traviss et al. [72] and Boyko and Kruzhilin [65], in that order, were the best predictors of their experimental data. Since Boyko and Kruzhilin [65] correlations is a average correlation, they adopted it with suitable modification to correlate their data of R-113 with twisted tape inserts.

The correlation of Boyko and Kruzhilin [65] for smooth tube can be written as:

$$\bar{h}_{TP} = 0.024 \frac{K_l}{D} \left(\frac{G_t D}{\mu_l}\right)^{0.8} Pr_l^{0.43} \frac{\left[(\rho/\rho_m)_{in}^{0.5} + (\rho/\rho_m)_{out}^{0.5}\right]}{2} \qquad (3\text{-}3)$$

where the symbols were defined earlier and

$$(\rho/\rho_m) = 1 + x \left(\frac{\rho_l}{\rho_v} - 1 \right) \qquad (3\text{-}4)$$

Eq (3-3) predicted the sectional and mean heat transfer coefficients for smooth tube data of R-113 within ± 30%.

In a recent study Shah [76] developed a correlation to predict local and mean heat transfer coefficients during film condensation inside tubes. The correlation was tested against 474 data points from twenty-one independent investigations, covering a wide range of conditions encountered in practice. The mean deviation between the predictions and experimental data was within 15%.

Shah's correlation [76] is an extension of the one he developed to predict the heat transfer coefficients during boiling inside tubes [79]. The latter correlation [79] was developed for saturated flow boiling for two regimes :
a) nucleate boiling in which bubble activity is predominant
b) pure convection boiling, also known as fully developed boiling, in which the bubble activity is completely suppressed.

In developing the boiling correlation, Shah [79] defined the following non-dimensional parameters:

$$\phi = h_z/h_l \qquad (3\text{-}5a)$$

Bo = Boiling number

$$= q_o/G_t\, h_{fg} \qquad (3\text{-}5b)$$

Co = Convection number

$$= \left(\frac{1-x}{x}\right)^{0.8} \left(\frac{\rho_v}{\rho_l}\right)^{0.5} \qquad (3\text{-}5c)$$

where

h_z = local heat transfer coefficient

h_l = liquid superficial heat transfer coefficient that is, heat transfer coefficient assuming liquid alone is flowing in the pipe at its mass flow rate

h_{fg} = latent heat of vaporisation of the fluid

q_o = heat flux at the inner side of the tube

At low qualities, that is higher values of convection number, Co, the nucleate boiling effects are important and the correlation is given by [79]

$$\phi = 230\ Bo^{0.5} \qquad (3\text{-}6)$$

At high qualities, that is low values of convection number, Co, the pure convection boiling exists and the correlation takes the following form:

$$\phi = 1.8\ Co^{-0.8} \qquad (3\text{-}7)$$

Eq (3-7) represents the condition of pure boiling in which the bubble nucleation is suppressed and is applicable if the following conditions are met : a) there is no bubble nucleation and b) the entire tube wall is wetted by the liquid film. These two conditions are also met in film condensation inside tubes. So Shah extended Eq (3-7) to film condensation inside tubes [76]. Eq (3-7) deviated by as much as 50% from experimental measurements when applied to the condensation data. The trend of the data indicated that the density ratio in the convection number, Co, is best represented by the reduced pressure, p_r. Therefore the correlation variable for condensation inside the tubes was given by:

$$Z = \left(\frac{1-x}{x}\right)^{0.8} p_r^{0.4} \qquad (3\text{-}8)$$

By analysing condensation experimental data, the correlation was obtained as :

$$\phi = \left[1 + 3.8\ Z^{-0.95}\right] \qquad (3\text{-}9)$$

ϕ is defined by Eq (3-5a) and includes the local condensation heat transfer coefficient.

Using Eqs (3-8) and (3-9), the calculation procedure for local heat transfer coefficients, during condensation inside tubes, can be summarized as given below:

1. Knowing the condensing fluid and the saturation pressure, the transport and thermodynamic properties can be obtained [80,81].
2. For a specified dryness fraction, x, the superficial heat transfer coefficient, h_l, of the liquid phase is calculated from

$$h_l = h_L\ (1-x)^{0.8} \qquad (3\text{-}10)$$

where h_L is the heat transfer coefficient assuming all the mass is flowing as a liquid and is given by Dittus-Boelter equation

$$h_L = 0.023\ Re_L^{0.8}\ Pr_l^{0.4}\ K_{l/D} \qquad (3\text{-}11)$$

where

Re_L = Reynolds number assuming all the mass is flowing as liquid

$$= \left[\frac{G_t\ D}{\mu_l}\right]$$

Shah [76] recommended that Eq (3-11) be used for $Re_L > 350$.

3. The parameter Z and ϕ are then calculated from Eqs (3-8) and (3-9) respectively. Using Eqs (3-8) to (3-10) the local condensation heat transfer coefficient is given by:

$$h_z = h_L \left[(1-x)^{0.8} + 3.8\, x^{0.76}(1-x)^{0.04} p_r^{-0.38}\right] \quad (3\text{-}12)$$

Mean Heat Transfer Coefficients

The mean heat transfer coefficients can be defined in different ways as given below:

$$\bar{h}_{TP} = \frac{1}{(x_{in}-x_{out})} \int_{x_{out}}^{x_{in}} h_z \, dx \quad (3\text{-}13)$$

or

$$\bar{h}_{TP} = \frac{1}{(L_2 - L_1)} \int_{L_1}^{L_2} h_z \, dz \quad (3\text{-}14)$$

$$\frac{1}{\bar{h}_{TP}} = \frac{1}{(x_{in} - x_{out})} \int_{x_{out}}^{x_{in}} \frac{dx}{h_z} \quad (3\text{-}15)$$

where L_1 and L_2 are the axial co-ordinates, measured from tube inlet, where the condensation process started and where it is completed, respectively. If condensation is not complete L_2 is at tube outlet.

Eq (3-15) is a result of the energy balance over a differe ntial length of the tube and which if integrated will result in an overall average for the entire tube.

All these definitions of the mean heat transfer coefficients, generally, involve numerical integration.However,with the use of certain assumptions the above integrals can be evaluated in a closed form. For example, assuming linear variation of quality with axial distance and complete condensation, Shah

[76] showed that the mean heat transfer coefficient defined by Eq (3-14) is given

$$\bar{h}_{TP} = h_L (0.55 + 2.09\ p_r^{-0.38}) \qquad (3.16)$$

In deriving Eq (3-16), from Eq (3-14), x_{in} was taken as 1.0 and x_{out} as 0.0.

Shah [76] showed that there is a mean value of quality, $\bar{x}$, that can be used in the local condensation heat transfer coefficient equation, given by Eq (3-12), to obtain the mean condensation heat transfer coefficient. For the above assumptions of linear quality variation and complete condensation, Shah [76] used $\bar{x}$ equals to 0.5 in Eq (3-12) to calculate the mean condensation heat transfer coefficient and the value differed from the one calculated using Eq (3-16) by only 5%.

The choice of correct mean quality, $\bar{x}$, depends on the rate of cooling and is usually less than 0.5. For the purpose of present study a value of 0.4 was selected for $\bar{x}$. When this value was substituted in Eq (3-12), the following equation resulted for the mean condensation heat transfer coefficient

$$\bar{h}_{TP} = h_L (0.665 + 1.86\ p_r^{-0.38}) \qquad (3-17)$$

where h_L is calculated from Eq (3-11).

3.2.1.1 RESULTS AND DISCUSSION

The correlation of Akers et al. [63] as given by Eq (3-2) was used to predict the mean heat transfer coefficients for the smooth tube data of Royal and Bergles [58,59] for

steam and Luu and Bergles [60,61] for R-113. Properties were evaluated at inlet saturation pressures from the references [80,81] for all the correlations tested or proposed in this report. In all the experimental runs the inlet quality was nearly 100% and the exit quality was nearly 0.0. Therefore, a value of 0.5 was used for $\bar{x}$ in Eq (3-2). The results of the predictions are compared in Figs (3-1) and (3-2). The results in both the figures show that Akers et al. [63] correlation predicted values lower than the experiments. The disagreement was within 35% for R-113 and 25% for steam data. In a few instances the disagreement exceeded these limits.

The Boyko and Kruzhilin [65] correlation was not used to evaluate the smooth tube data. The reason for this becomes evident in section (3.3.1.2).

Eq (3-12) averaged by Eq (3-15), Eq (3-16) and Eq (3-17) were used in the present study to predict the steam and R-113 smooth tube heat transfer data. It was found that Eq (3-17) resulted in the best correlation for both sets of data. The results of the predictions of Eq (3-17), using Eq (3-11) for h_L, are compared with the experimental data in Figs (3-3) and (3-4). The disagreement between the predicted and experimental values is between 5% and -15% for steam and within $\pm$20% for R-113. In both cases, the correlation predicted slightly higher values than the experimental data.

It can be concluded that Shah's [76] correlation predicted best the mean heat transfer coefficients during condensation of steam and R-113 inside smooth horizontal tubes

THIS BOOK CONTAINS NUMEROUS PAGES WITH DIAGRAMS THAT ARE CROOKED COMPARED TO THE REST OF THE INFORMATION ON THE PAGE.

THIS IS AS RECEIVED FROM CUSTOMER.

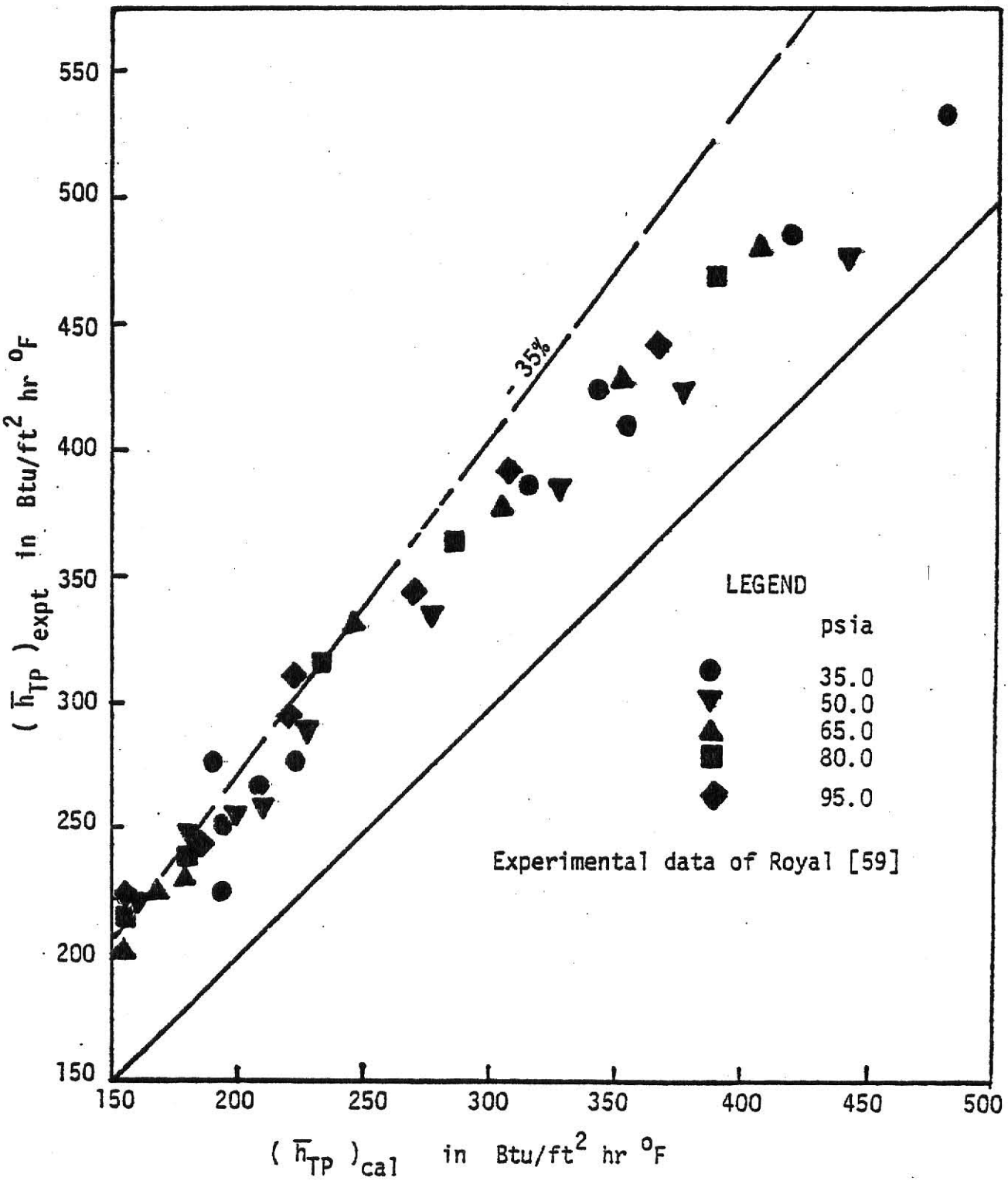

Fig (3-1) Comparison Between Calculated and Experimental Mean Heat Transfer Coefficents for Smooth Tube Data of R - 113, Using Akers et al. [63] Correlation.

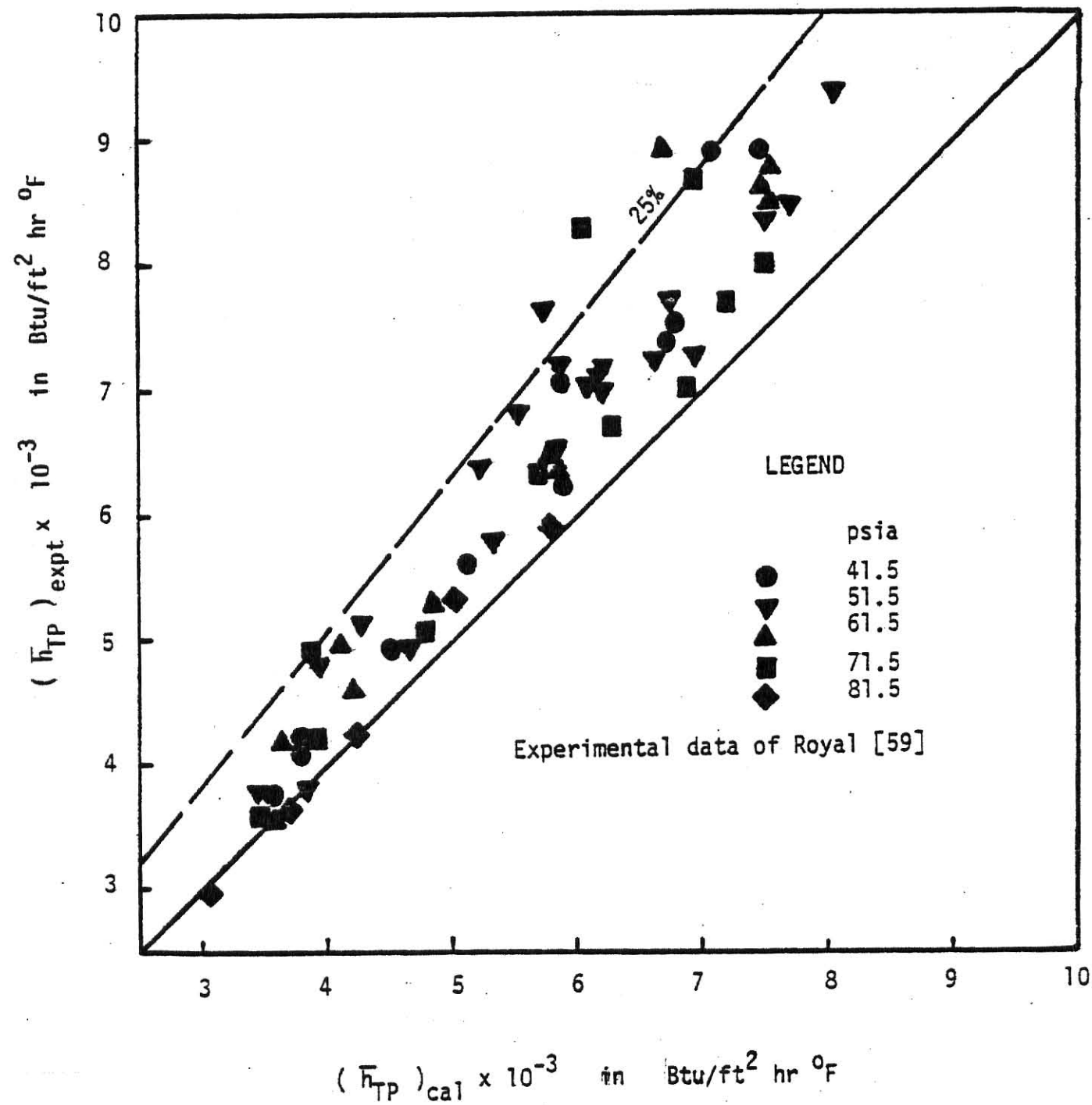

Fig (3-2) Comparision Between Calculated and Experimental Mean Heat Transfer Coefficents for the Smooth Tube Data of Steam Using Akers et al. [63] Correlation.

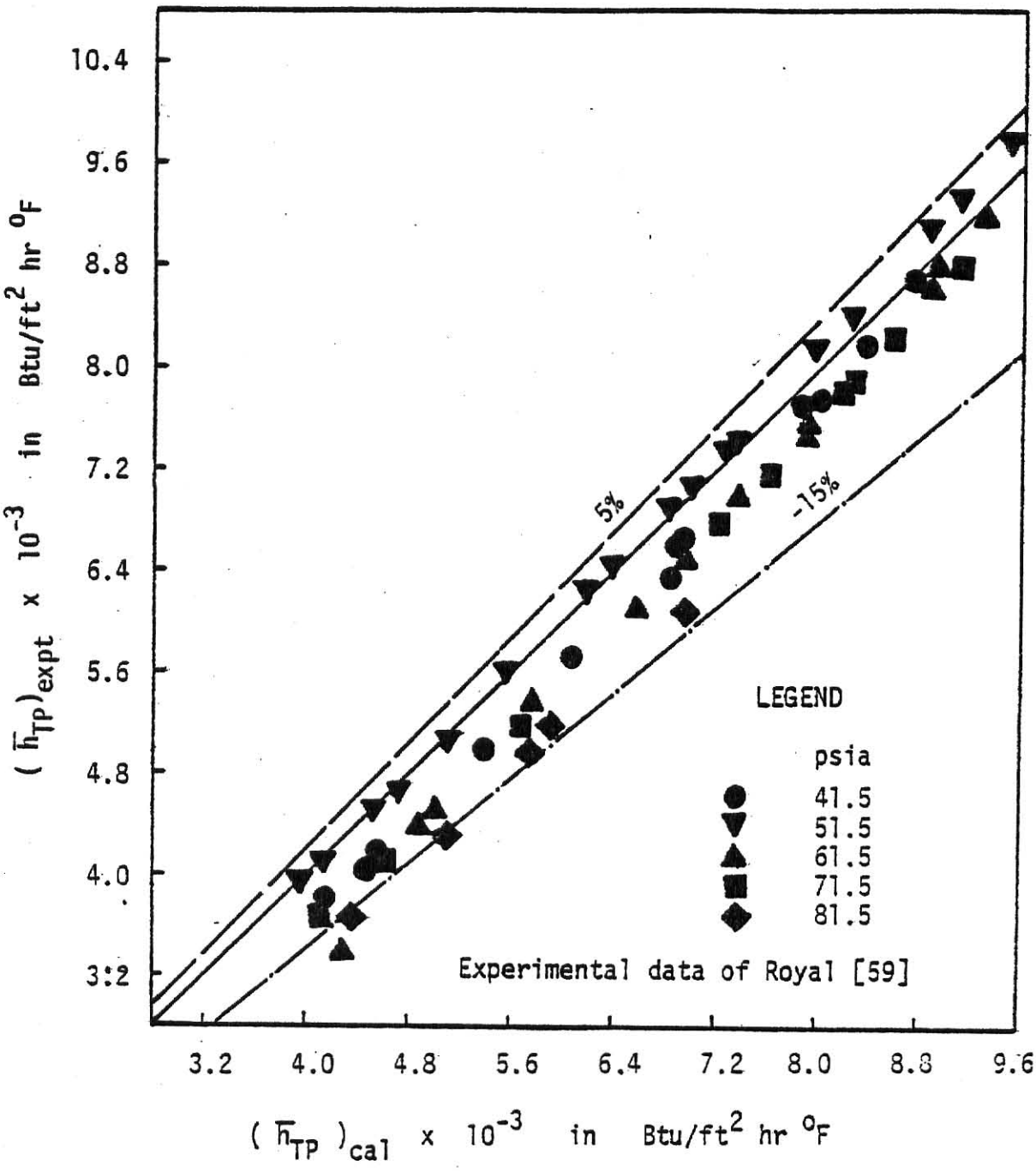

Fig (3-3) Comparison Between Calculated and the Experimental Mean Heat Transfer Coefficents for the Smooth Tube Data of Steam Using Shah's Correlation, Eq (3-17).

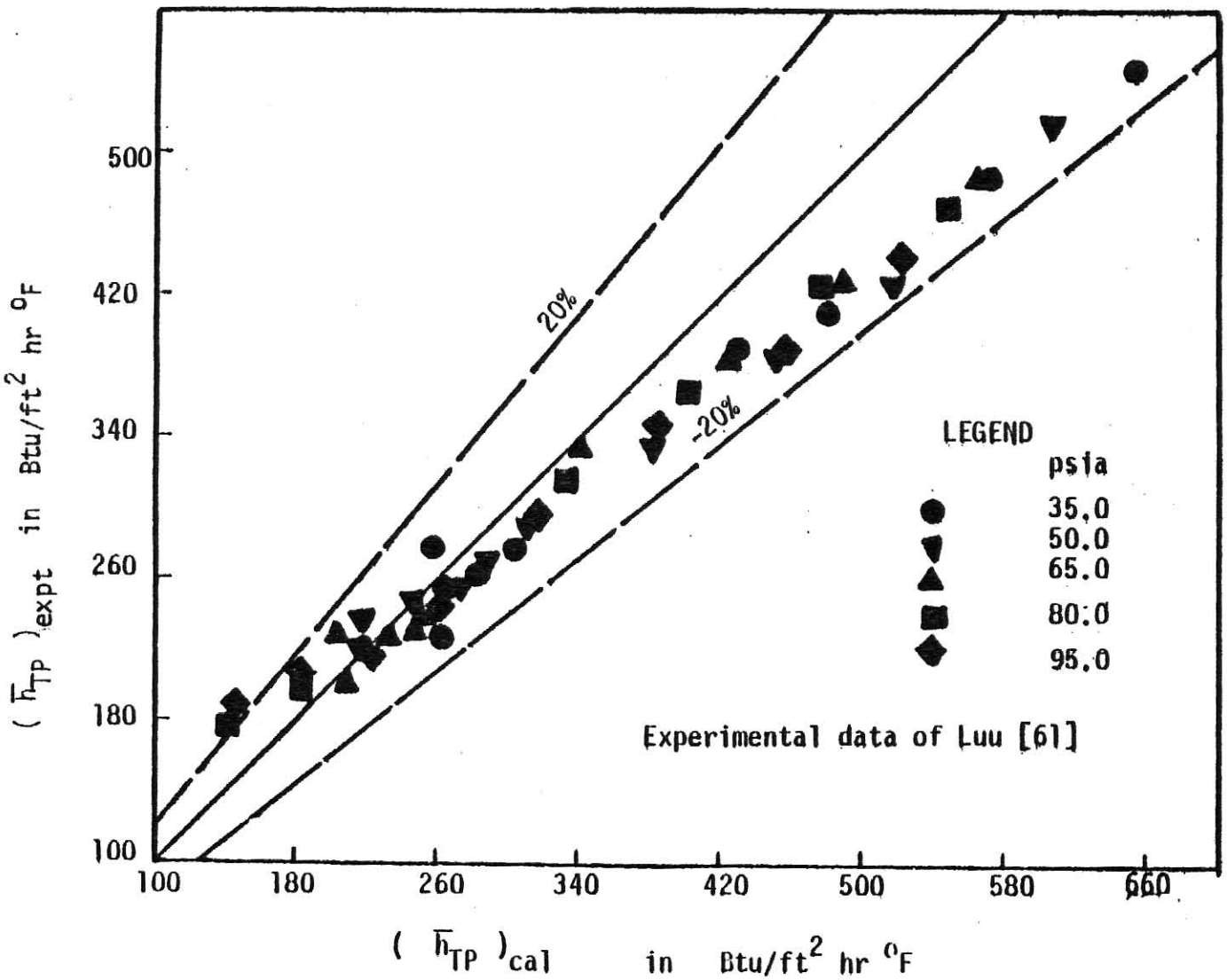

Fig (3-4) Comparison Between Calculated and Experimental Mean Heat Transfer Coefficents for the Smooth Tube Data of R-113 Using Shah's Correlation, Eq (3-17)

compared to the other existing correlations.

3.2.2 PRESSURE DROP

Two-phase pressure gradient for flow inside smooth horizontal tubes can be written as a sum of frictional and momentum terms. Therefore,

$$\left(\frac{dp}{dz}\right) = \left(\frac{dp}{dz}\right)_{TPF} + \left(\frac{dp}{dz}\right)_{M} \qquad (3\text{-}18)$$

where $\left(\frac{dp}{dz}\right)$ = total pressure gradient

$\left(\frac{dp}{dz}\right)_{TPF}$ = two-phase frictional pressure gradient

and $\left(\frac{dp}{dz}\right)_{M}$ = two-phase pressure gradient due to momentum changes.

The momentum pressure gradient can be written as:

$$\left(\frac{dp}{dz}\right)_{M} = -\frac{G_t^2}{g_c}\frac{dx}{dz}\left[-\frac{2(1-x)}{\rho_l(1-\psi)} + \frac{2x}{\rho_v\psi}\right.$$

$$\left. + \frac{\psi(1-x)}{\rho_l\, x(1-\psi)} - \frac{x\,(1-\psi)}{\rho_v\psi(1-x)}\right] \qquad (3\text{-}19)$$

where ψ is the void fraction.

The details of the derivation of Eq (3-19) are given in the next chapter.

To evaluate the frictional and momentum pressure gradients, a two-phase friction factor for frictional pressure gradient

and an expression for void fraction for momentum pressure gradient are needed. Also, the knowledge of quality gradient is necessary.

Royal and Bergles [82] identified five correlations [83-86] including a homogeneous model [95,96] for two-phase frictional pressure gradient and seven void fraction correlations [83,90-94] including a homogeneous model [95,96] to correlate their [59] pressure drop measurements of steam condensation inside smooth, horizontal tube. A summary of these correlations is given in Apendices B and C.

All the possible combinations of frictional pressure drop and void fraction correlations were tested with the smooth tube pressure drop data of steam [59]. Royal and Bergles [82] found that the combination of frictional pressure drop correlation of Dukler et al. [86] and void fraction correlation of Hughmark [90] was the best predictor of their [59] smooth tube pressure drop data.

The Hughmark correlation [90] for void fraction is described in Appendix C. In the following paragraphs Dukler et al. [86] correlation for frictional pressure drop is described.

Applying the dynamic similarity principle to two-phase flow in a conduit, Dukler et al. [86] arrived at the following equations:

$$Re_{TP} = \frac{\ell V_m \rho_{TP}}{\mu_{TP}} \qquad (3\text{-}20)$$

and

$$f_{TP} = \frac{1}{2} \left[\frac{\left(\frac{dp}{dz} \right)_{TPF}}{\left(\frac{\rho_{TP} V_m^2}{g_c \ell} \right)} \right] \qquad (3\text{-}21)$$

where

ℓ = characteristic dimension

Re_{TP} = two-phase Reynolds number

f_{TP} = two-phase friction factor

V_m = mean two-phase velocity

ρ_{TP} = two-phase density

μ_{TP} = two-phase dynamic viscosity

ρ_{TP} and μ_{TP} can be given by:

$$\rho_{TP} = \left[\frac{\rho_l \lambda^2}{(1 - \psi)} + \frac{\rho_v (1 - \lambda)^2 c_1}{\psi} \right] \qquad (3\text{-}22)$$

$$\bar{\mu}_{TP} = \left[\mu_l \lambda + \mu_v (1 - \lambda) c_2 \right] \qquad (3\text{-}23)$$

$$\lambda = \left[\frac{\text{Volumetric flow rate of liquid}}{\text{Total volumetric flow rate}} \right]$$

c_1, c_2 = constants

The problem now reduces to finding c_1 and c_2. Dukler et al. [86] considered four special cases for c_1 and c_2 and developed correlations for friction pressure gradient in two-phase flow, for two of these special cases. Those two correlations are described below:

CASE - I: Homogeneous two phase flow is assumed and there is no slip between the two phases. In this case,

$$c_1 = 1.0$$

$$c_2 = 1.0$$

and $$\lambda = (1 - \psi) \qquad (3\text{-}24)$$

Using the inside diameter for the characteristic length, ℓ, Eqs (3-20) to (3-23) can be written as:

$$Re_{NS} = \left[\frac{4\ W_t}{\pi D\ \mu_{NS}}\right] \qquad (3\text{-}25)$$

$$f_{NS} = \left[\frac{\left(\frac{dp}{dz}\right)_{TPF}}{\left(\frac{2\ G_t^2}{g_c\ D\ \rho_{NS}}\right)}\right] \qquad (3\text{-}26)$$

$$\rho_{NS} = \left[\rho_l \lambda + \rho_v (1 - \lambda)\right] \qquad (3\text{-}27)$$

and

$$\mu_{NS} = \left[\mu_l \lambda + \mu_v (1 - \lambda)\right] \qquad (3\text{-}28)$$

The subscript "NS" refers to no-slip or homogeneous condition.

The above equations describe the two-phase, no-slip parameters.

The assumption of homogeneous flow permits the treatment of a two-phase mixture as an equivalent single phase fluid. Thus the correlation can be given by the single phase friction factor-Reynolds number relation as:

$$f_{NS} = \left[0.0014 + \frac{0.125}{Re_{NS}^{0.32}} \right] \qquad (3\text{-}29)$$

Parameters used in Eqs (3-29) are defined by Eqs (3-25), (3-27) and (3-28).

CASE - II: This is a special case in which slip takes place; but c_1 and c_2 are assumed to be equal to unity. This is true when the ratio of each phase velocity to the average velocity remains constant over the flow cross-section. In such a case,

$$Re_{TP} = Re_{NS}\ \beta \qquad (3\text{-}30)$$

and

$$f_{TP} = \frac{f_{NS}}{\beta} \qquad (3\text{-}31)$$

where

$$\beta = \left[\frac{\rho_l}{\rho_{NS}} \frac{\bar{\lambda}^2}{(1-\bar{\psi})} + \frac{\rho_v}{\rho_{NS}} \frac{(1-\bar{\lambda})^2}{\bar{\psi}} \right] \qquad (3\text{-}32)$$

ρ_{NS}, f_{NS} and Re_{NS} are no-slip parameters defined by Eqs (3-25) to (3-27).

Using the definition of Reynolds number and friction factor given by Eqs (3-30) and (3-31), the two-phase frictional pressure drop was given as:

$$\left(\frac{dp}{dz} \right)_{TPF} = - \frac{2\ G_t^2\ f_o\ \alpha\ \beta}{g_c\ D\ \rho_{NS}} \qquad (3\text{-}33)$$

f_o in Eq (3-33) is single phase friction factor evaluated at

two-phase Reynolds number, Re_{TP}, the latter being defined by Eq (3-30). f_o can be calculated using Eq (3-29) with Re_{TP} in place of Re_{NS}.

α in Eq (3-33) is the ratio of f_{TP} to f_o. By using four hundred data points Dukler et al. [86] arrived at the following equation

$$\alpha(\lambda) = \frac{f_{TP}}{f_o} = 1 - \frac{\ln \lambda}{[1.281 + 0.478 \ln \lambda + 0.444 (\ln \lambda)^2 + 0.094 (\ln \lambda)^3 + 0.00843 (\ln \lambda)^4]} \quad (3\text{-}34)$$

By using Eqs (3-27), (3-28), (3-25), (3-32), (3-30), (3-29) and (3-34) into Eq (3-33), the frictional pressure gradient can be calculated for a given mass flow rate, quality and saturation pressure.

Royal and Bergles [82] used the Dukler et al. [86] and Hughmark [90] combination for frictional pressure gradient and void fraction respectively, for smooth tube pressure drop data of steam. They [82] assumed a constant quality gradient for each sub-section of the test condenser. This constant was determined from the enthalpy changes of the coolant in each sub-section of the condenser. They [82] divided each sub-section into ten increments for computer estimation of total pressure drop.

Royals and Bergles [82] concluded that Dukler et al. [86] and Hughmark combination predictions were higher than experimental data and the disagreement was as high as 40%. The reasons for this can be attributed to following:

1. The momentum pressure gradient is of the same order of magnitude as the frictional pressure gradient for all the steam data. There are uncertainities involved in the momentum model and void fraction correlations.
2. The frictional pressure gradient was calculated using the friction factor developed for adiabatic two-phase, two-component systems. The friction factor in condensation was shown to be higher than the friction factor in adiabatic flow by Linehan et al. [97].

Using all possible combinations of frictional pressure drop correlations [72,83,86,88,89] including a homogeneous model [95,96] and seven void fraction correlations [83,90-94] including a homogeneous model [95,96], Luu and Bergles [77] compared their smooth tube condensation pressure drop data of R-113 with the predictions of the above combinations. However they introduced a correction factor, suggested by Silver and Wallis [98], to the adiabatic friction factor calculated from the above mentioned frictional pressure drop correlations. The correction factor can be obtained as described below:

$$\frac{f_c}{f_{ad}} = \left[\exp\left(\bar{\zeta}/2\, f_{ad} \right) - \left(\zeta/f_{ad} \right) \right] \qquad (3\text{-}35)$$

where

f_c = friction factor in the presence of condensation

f_{ad} = adiabatic friction factor

$$\zeta = \frac{D}{2x}\frac{dx}{dz}\left[\frac{\psi - 0.5x\frac{d\psi}{dx}}{\sqrt{\psi}}\right] \qquad (3\text{-}36)$$

ψ = Void fraction

From their comparisons, Luu and Bergles [77] concluded that the combination of Lockhart-Martinelli correlation [83] for the frictional pressure gradient and the momentum pressure gradient based on a homogeneous flow model described best their experimental smooth tube pressure drop data of R-113.

In another study Luu and Bergles [78] using all the combinations cited above concluded that Lockhart-Martinelli correlation [83] predicted the experimental smooth tube pressure drop data of R-113 slightly better than Duckler et al. [86] correlation. It is to be noted at this point that Traviss et al. [72] correlation is a combination of Lockhart-Martinelli correlation [83] and Zivi's correlation [93].

3.2.2.1 PRESSURE DROP CORRELATION

In the present study the frictional pressure gradient was calculated using Lockhart-Martinelli correlation [83] along with the correction factor suggested by Silver and Wallis [98]. The void fraction was calculated using the correlation of Zivi [93]. The void fraction is given by:

$$\psi = \frac{1}{\left[1 + \left(\frac{1-x}{x}\right)\left(\frac{\rho_v}{\rho_l}\right)^{2/3}\right]} \qquad (3\text{-}37)$$

This equation is simple to use and involves no iteration as in Hughmark's correlation [90].

The Lockhart-Martinelli correlation [83] was developed for two-component, two-phase flow inside tubes. The correlation is described below:

The parameter X was defined as:

$$X = \left[\left(\frac{dp}{dz}\right)_l / \left(\frac{dp}{dz}\right)_v\right]^{0.5} \qquad (3\text{-}38)$$

where

$\left(\frac{dp}{dz}\right)_l$ = frictional pressure gradient assuming that liquid alone is flowing in the pipe.

$\left(\frac{dp}{dz}\right)_v$ = frictional pressure gradient assuming that vapor (or gas) alone is flowing in the pipe.

The frictional pressure gradients due to single phase flow of liquid and vapor (or gas) depend upon the type of flow if each phase is alone flowing in the tube. Thus each phase could be in laminar or turbulent flow. For turbulent flow of both phases, X in Eq (3-38) is designated by the subscript tt and is given by:

$$X_{tt} = \left(\frac{W_l}{W_v}\right)^{0.9} \left(\frac{\mu_l}{\mu_v}\right)^{0.1} \left(\frac{\rho_v}{\rho_l}\right)^{0.5} \qquad (3\text{-}39)$$

For a two-phase condensing system with a given qualtiy, x, Eq (3-39) can be replaced by:

$$X_{tt} = \left(\frac{1-x}{x}\right)^{0.9} \left(\frac{\mu_l}{\mu_v}\right)^{0.1} \left(\frac{\rho_v}{\rho_l}\right)^{0.5} \qquad (3\text{-}40)$$

Another parameter, ϕ_v, was defined as

$$\phi_v = \left\{\left(\frac{dp}{dz}\right)_{TPF} / \left(\frac{dp}{dz}\right)_v\right\}^{0.5} \qquad (3\text{-}41)$$

where

$\left(\frac{dp}{dz}\right)_{TPF}$ = two-phase frictional pressure gradient.

In general, ϕ_v, is a function of X. Therefore,

$$\phi_v = f(X) \qquad (3\text{-}42)$$

Analysing adiabatic two-component, two-phase experimental data on pressure drop inside tubes, Lockhart and Martinelli [83] presented a family of curves for ϕ_v vs X. Soliman et al. [66] approximated the curve for ϕ_v vs X_{tt} for turbulent flow of both phases by:

$$\phi_v = \left[1 + 2.85\, X_{tt}^{0.523}\right] \qquad (3\text{-}43)$$

The frictional pressure gradients, due to vapor (or gas) flowing alone in the tube, can be calculated from the well established equations of single phase turbulent flow. In such a case,

$$\left(\frac{dp}{dz}\right)_v = - \frac{2 f G_t^2 x^2}{g_c \rho_v D} \qquad (3\text{-}44)$$

where

G_t = total mass velocity

D = inside diameter of the tube

f = friction factor

The friction factor, f, in Eq (3-44) for adiabatic two-phase system is designated as f_{ad} and is given by:

$$f_{ad} = \left[\frac{0.045}{Re_v^{0.2}}\right] \qquad (3\text{-}45)$$

where

$$Re_v = \left[\frac{G_t x D}{\mu_v}\right] \qquad (3\text{-}46)$$

To account for condensation, f_{ad}, is corrected by Eqs(3-35) and (3-36) and the resulting friction factor, f_c, is used in Eq (3-44) a condensing fluid.

After obtaining the frictional pressure gradient due to vapor flow, the two-phase frictional pressure gradient can be obtained from the following equation:

$$\left(\frac{dp}{dz}\right)_{TPF} = \phi_v^2 \left(\frac{dp}{dz}\right)_v \qquad (3\text{-}47)$$

where ϕ_v is calculated using Eqs (3-40) and (3-43).

3.2.2.2 SUMMARY OF CALCULATIONS OF PRESSURE DROP

1. Assume the quality as

$$\frac{dx}{dz} = -\frac{1}{L}$$

where L = length of the condenser tube.

This assumption implies constant cooling rate.

2. For a specified condensing pressure and quality compute the following:

$$\psi = \frac{1}{1 + \left(\frac{1-x}{x}\right)\left(\frac{\rho_v}{\rho_l}\right)^{2/3}}$$

$$\frac{d\psi}{dx} = \frac{\psi^2}{x^2}\left(\frac{\rho_v}{\rho_l}\right)^{2/3}$$

$$\zeta = \frac{D}{2x}\frac{dx}{dz}\left[\frac{\psi - 0.5x\frac{d\psi}{dx}}{\sqrt{\psi}}\right]$$

3. For a specified mass velocity and tube inside diameter compute the following:

$$Re_v = \frac{G_t x D}{\mu_v}$$

$$f_{ad} = \frac{0.045}{Re_v^{0.2}}$$

$$\frac{f_c}{f_{ad}} = \left[\exp\left(\zeta/2f_{ad}\right) - \left(\zeta/f_{ad}\right)\right]$$

4. From the above information compute the following:

$$\left(\frac{dp}{dz}\right)_v = - \frac{2 f_c G_t^2 x^2}{g_c \rho_v D}$$

$$X_{tt} = \left(\frac{1-x}{x}\right)^{0.9} \left(\frac{\mu_l}{\mu_v}\right)^{0.1} \left(\frac{\rho_v}{\rho_l}\right)^{0.5}$$

$$\phi_v = \left[1 + 2.85\, X_{tt}^{0.523}\right]$$

5. Finally, the two-phase frictional pressure gradient can be computed by:

$$\left(\frac{dp}{dz}\right)_{TPF} = \phi_v^2 \left(\frac{dp}{dz}\right)_v$$

The two-phase momentum pressure gradient can be computed by:

$$\left(\frac{dp}{dz}\right)_{\dot{M}} = - \frac{G_t^2}{g_c} \frac{dx}{dz} \left[- \frac{2(1-x)}{\rho_l(1-\psi)} + \frac{2x}{\rho_v \psi} + \frac{\psi(1-x)}{\rho_l\, x(1-\psi)} - \frac{x(1-\psi)}{\rho_v \psi\,(1-x)} \right]$$

and

$$\left(\frac{dp}{dz}\right) = \left(\frac{dp}{dz}\right)_{TPF} + \left(\frac{dp}{dz}\right)_{\dot{M}}$$

3.2.2.3 RESULTS AND DISCUSSION

For each experimental run of Royal and Bergles [58,59] for steam, and Luu and Bergles [60,61] for R-113, the entire

test section was divided into twenty incremental lengths. For steam and R-113 the quality gradient was assumed as in step 1, given in the previous section. The inlet quality in all the runs was nearly 100%. By using the assumed quality gradient and 100% inlet quality, the average quality for a given incremental length was calculated. The pressure drop for each incremental length was calculated using the above scheme. The total pressure drop was sum of the pressure drops of all the incremental lengths.

This scheme was implemented in a digital computer program and comparisons were made, between the predicted and experimental data for steam data of Royal and Bergles [58,59] and R-113 data of Luu and Bergles [60,61], in Figs (3-5) and (3-6) respectively.

The results show that the proposed correlation predicts pressure drop values lower than the experimental values, for steam. For R-113 the disagreement between predicted and experimental data is within ± 35% for a majority of the points except at low flow rates where the disagreement exceeded these limits. Several reasons could have contributed to this disagreement. First uncertainity is the assumption of constant quality gradient, as in step 1, and second is the uncertainity in the experimental results.

3.3 CORRELATIONS FOR TUBES WITH TWISTED TAPE INSERTS

3.3.1 HEAT TRANSFER

Studies on the effect of twisted tape inserts on condensation heat transfer appeared in the literature recently and are

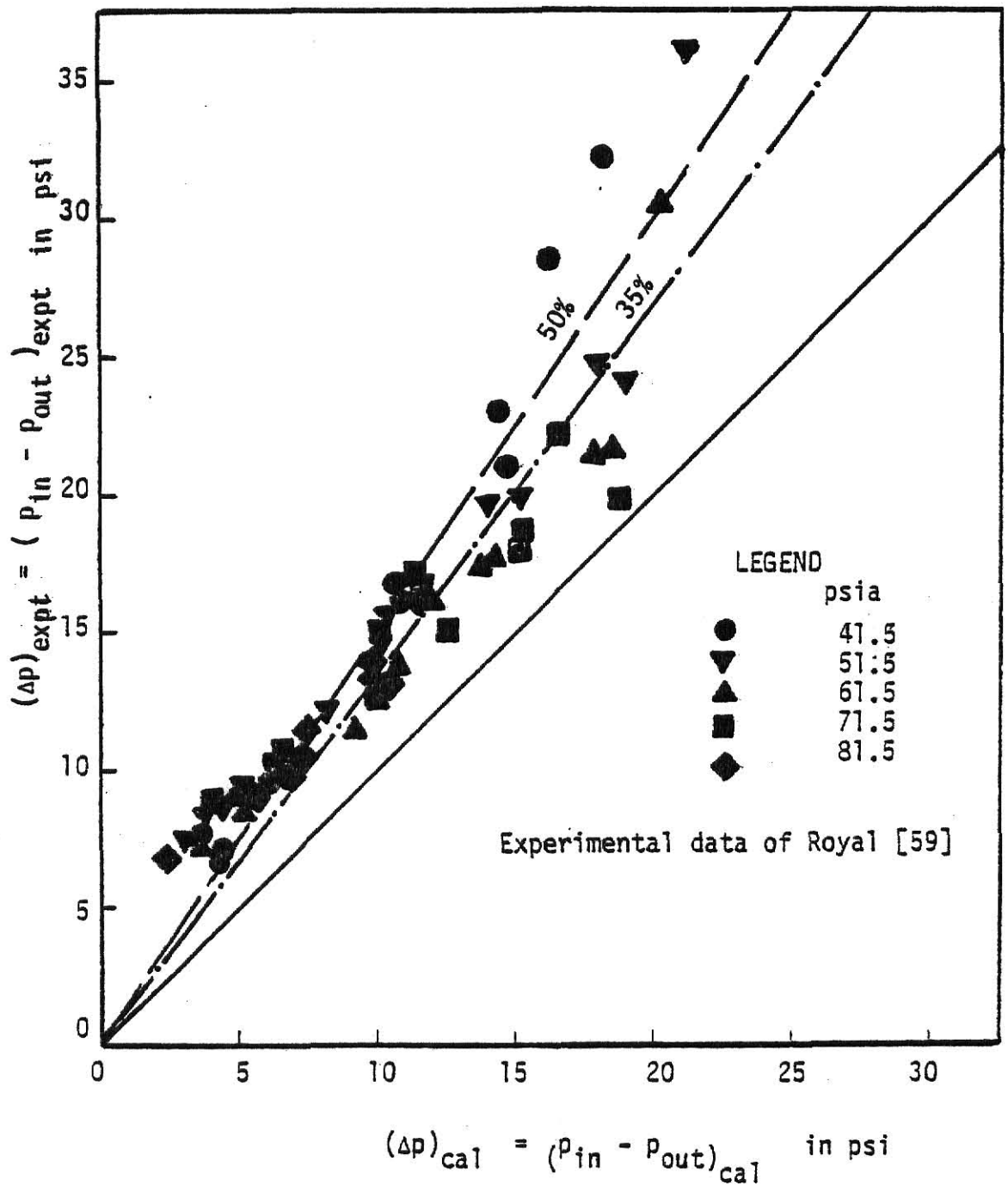

Fig (3-5) Comparison Between Calculated and Experimental Pressure Drop for The Smooth Tube Data of Steam.

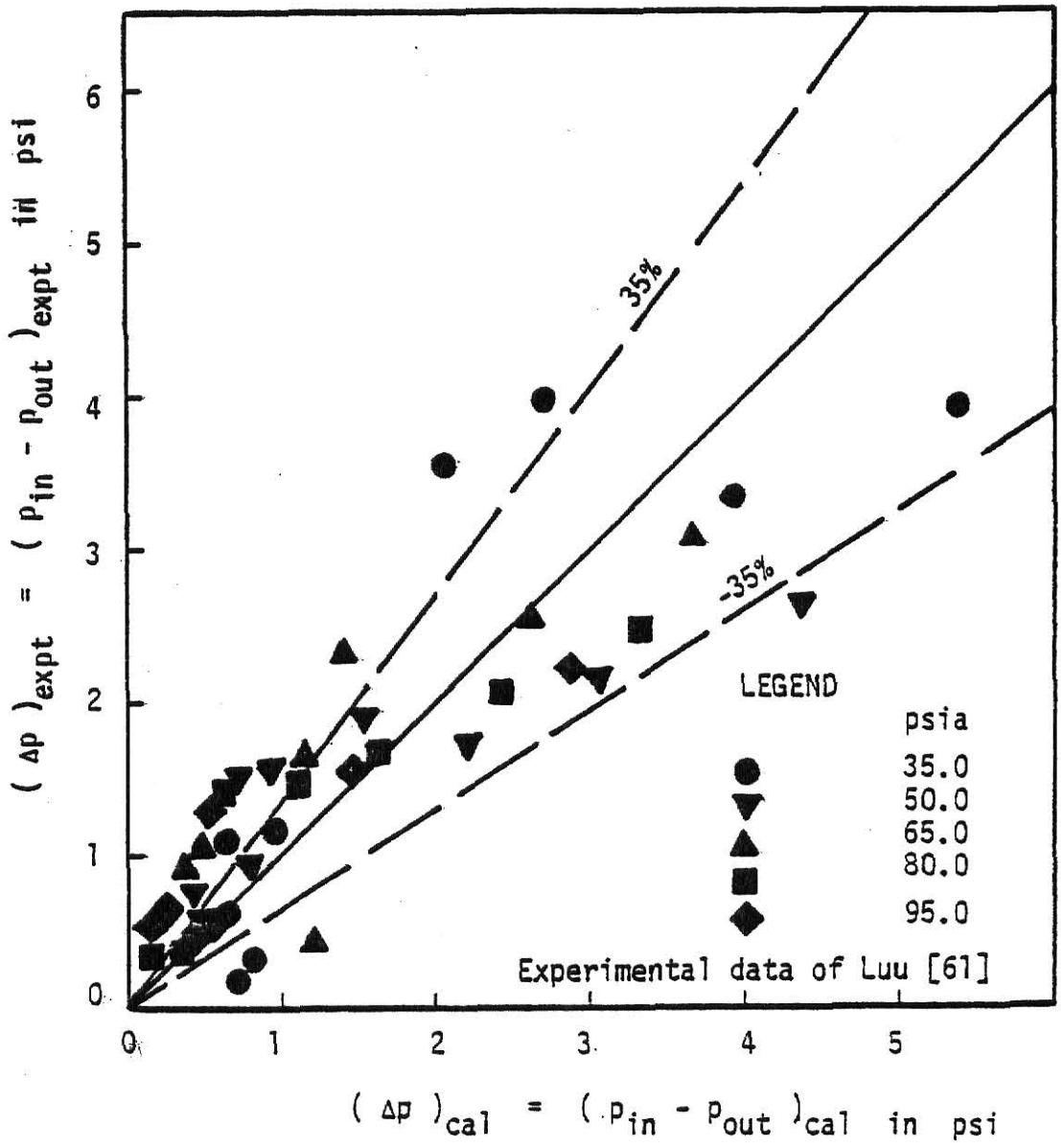

Fig (3-6) Comparison Between Calculated and Experimental Pressure Drop for Smooth Tube Data of R-113.

very few in number. Royal and Bergles [58,59] and Luu and Bergles [60,61] obtained heat transfer and pressure drop data with twisted tape inserts for low pressure steam and R-113 respectively. These investigations were discussed at the beginning of this chapter.

Royal and Bergles [58a] selected Akers et al. [63] correlation, the best predictor of their smooth tube steam heat transfer data, to modify for the purpose of predicting heat transfer coefficients, local and mean, during condensation of steam inside tubes with twisted tape inserts. They identified the effects of twisted tapes on pressure drop and heat transfer. These effects are: 1. Tangential velocity effects 2. Tape fin effects and 3. Wall shear effects. These effects are discussed in the following paragraphs.

1. Tangential Velocity Effects: The twisted tape induces swirl in the flow and a tangential velocity is added to the velocity vector, which is otherwise axial. The tangential velocity is a function of the radius from the axis. This additional component of velocity is needed to maintain the mass flow rate in the presence of a twisted tape inside the tube. The flow velocity in the presence of a twisted tape is the vectorial sum of axial and tangential components. This increased velocity, due to the presence of tangential component, is a function of radius. The tangential velocity component is given by:

$$u_t = u_a\left[\frac{\pi r}{2Yr_o}\right] \qquad (3\text{-}48)$$

where

u = the velocity

a,t = refer to axial and tangential components respectively.

Y = reduced half pitch of the tape, also known as twist ratio, defined as pitch of the tape per 180^{o}/Inside diameter of the tube.

The total velocity, u, is obtained by vectorially adding u_t and u_a respectively. Therefore,

$$u = u_a\left[\frac{\pi^2}{4}\left(\frac{r}{Yr_o}\right)^2 + 1\right]^{0.5} \qquad (3\text{-}49)$$

Since the interfacial shear stress is a function of velocity at the interface, Eq (3-49) has to be evaluated at the interfacial radius. Interfacial shear stress is important to the heat transfer process. Since finding the interfacial radius requires the knowledge of the liquid film thickness, the calculation procedure of which is tedious, Eq (3-49) can be evaluated at the tube inner radius. This involves a small error because the film thickness is small compared to the tube radius. Now defining velocity correction factor as the ratio of total velocity to the axial velocity, it can be written that

$$F_t = \left(\frac{u}{u_a}\right)$$

where,

F_t = velocity correction factor.

Evaluating u in Eq (3-49) at r_o, F_t can be given by

$$F_t = \frac{1}{2Y}\left[\pi^2 + 4Y^2\right]^{0.5} \qquad (3\text{-}50)$$

Since F_t characterises the velocity increase due to the presence of a twisted tape, it should be applied to the Reynold number of interest in the correlation.

2. Fin Effects: A twisted tape in contact with the wall behaves like a fin of length equal to the radius of the tube. Assuming that the tape is in good thermal contact with the wall and the tip of the fin, which is in the axial plane of the tube, is thermally insulated, the fin effectiveness can be given by [99]

$$\eta = \frac{\tanh(m\, r_o)}{m\, r_o} \qquad (3\text{-}51)$$

where

$$m = \left(\frac{2\, h_c}{K_{tt}\, \delta_{tt}}\right)$$

h_c = heat transfer coefficient over the twisted tape surface

K_{tt} = thermal conductivity of tape material

δ_{tt} = thickness of the twisted tape

To compute the effectiveness of the tape as a fin, the heat transfer coefficient over the tape surface needs to be determined. This involves an iteration process. Instead of this approach a reasonable value for the effectiveness can be assumed without a serious error.

Defining the fin effect correction factor, F_{tt}, as the

ratio of heat transferred with fin effect to heat transferred without the fin effect, results in

$$F_{tt} = 1 + \frac{2}{\pi} \left\{ \frac{\pi}{2} - \frac{\delta_{tt}}{D} \right\} \qquad (3\text{-}52)$$

The fin effect of the twisted tape increases the heat transfer rate. Therefore the correction factor, F_{tt}, is multiplied by the smooth tube heat transfer coefficient to yield the heat transfer coefficient in the presence of a twisted tape insert.

3. Wall Shear Effects: The presence of a twisted tape reduces the flow cross sectional area and increases the wetted perimeter. The tape increases the wall shear and hence the total pressure loss. This is accounted for by the use of a twisted tape friction factor correction. Lopina and Bergles [100] presented one such correction for single phase flow of water and it was adopted for two phase flow. Therefore,

$$F_f = \frac{f_{tt}}{f_c} = 2.75\ Y^{-0.406} \qquad (3\text{-}53)$$

where f = friction factor

tt and c = refer to twisted tape and smooth tube respectively

Y = twist ratio per 180° rotation

The changes in flow area and wetted perimeter is accounted for by the use of an equivalent diameter in the calculations. Neglecting the area occupied by the tape in relation to the cross sectional area of the pipe, the equivalent diameter can

be written as:

$$D_e = \frac{\pi D^2}{\{ \pi D + 2(D-\delta_{tt}) \}} \qquad (3\text{-}54)$$

Incorporating the corrections discussed above into the smooth tube correlation of Akers et al. [63], Royal and Bergles [58a,59] gave a correlation for the mean heat transfer coefficients in the presence of a twisted tape insert. The modified Akers et al. correlation as used by Royal and Bergles [58a] is given below:

$$\bar{h}_{tt} = 0.0265 \frac{K_l}{D_e} \left[\frac{F_t \, G_e \, D_e}{\mu_l} \right]^{0.8} Pr_l^{0.4} F_{tt} \qquad (3\text{-}55)$$

where

$$G_e = G_t \{ \bar{x} \, (\frac{\rho_l}{\rho_v})^{0.5} + (1-\bar{x}) \}$$

$\bar{x}$ = arithmetic mean of inlet and outlet qualities

Eq (3-55) predicted the heat transfer coefficients during condensation of steam in the presence of a twisted tape insert within ± 30% of the experimental values.

Luu and Bergles [78] modified the Boyko and Kruzhilin [65], the best predictor of their smooth tube data for R-113, on the same lines as discussed above. They, however, made a few changes which are discussed below:

1. They evaluated the velocity in Eq (3-49) as an average rather than at the inner wall. Therefore,

$$F_t = \frac{8Y^2}{3\pi^2}\left\{\left[\frac{1}{4}\left(\frac{\pi}{Y}\right)^2 + 1\right]^{1.5} - 1\right\} \qquad (3\text{-}56)$$

2. The fin effect correction factor was given by

$$F_{tt} = 1 + \frac{2}{\pi}\left[\left\{\frac{\eta(4Y^2 + \pi^2)^{0.5}}{2Y}\right\} - \frac{\delta_{tt}}{D}\right] \qquad (3\text{-}57)$$

They used 0.97 for the fin effectiveness, η.

3. The equivalent diameter was defined taking the tape area into account. Therefore,

$$D_e = \frac{\{\pi D^2 - 4D\delta_{tt}\}}{\{\pi D + 2(D - \delta_{tt})\}} \qquad (3\text{-}58)$$

Following these changes the Boyko and Kruzhilin correlation [65] was given as [78]:

$$\bar{h}_{tt} = 0.024 \frac{K_l}{D_e} F_{tt} \left[\frac{F_t G_e D_e}{\mu_l}\right]^{0.8} Pr_l^{0.43} \frac{\left[(\rho/\rho_m)_{in}^{0.5} + (\rho/\rho_m)_{out}^{0.5}\right]}{2} \qquad (3\text{-}59)$$

where

$$(\rho/\rho_m) = \left[1 + x\left\{\left(\frac{\rho_l}{\rho_v}\right) - 1\right\}\right]$$

The modified Boyko and Kruzhilin correlation predicted the experimental heat transfer data of R-113 with tapes within

± 30%.

3.3.1.1 CORRELATION FOR TWISTED TAPES

In the present study a heat transfer correlation was developed utilizing the heat transfer data for steam condensation inside horizontal tubes with twisted tape inserts.

For each experimental run with a twisted tape, the mass flow rate and saturation pressure were identified. For these conditions, for each run, a smooth tube mean heat transfer coefficient was calculated using Eq (3-17) with the inside diameter of the tube, as the characterstic dimension. The ratio of the experimental mean heat transfer coefficient with twisted tape to the corresponding calculated smooth tube mean heat transfer coefficient was calculated. This ratio was identified as R.

$$R = \left\{ \frac{\bar{h}_{tt}}{\bar{h}_{TP}} \right\}_{\text{at the same conditions}} \qquad (3\text{-}60)$$

It was assumed that R, in general, is a function of:

1. The Reynolds number (Re_L) assuming that all the mass is flowing as liquid, that is

$$Re_L = \left[\frac{G_t \, D}{\mu_l} \right]$$

2. the half pitch, Y
3. the liquid Prandtl number, Pr_l

and 4. the reduced pressure p_r.

Therefore, in general, it can be written that

$$R = f\,(Re_L,\ Y,\ Pr_l,\ p_r)$$

Various correlation functions were attempted. After several trials it appeared that the reduced pressure, p_r, and the liquid Prandtl number, Pr_l, had little effect on R. It was finally decided to correlate R with the ratio (Re_L/Y). This same parameter was used by Lopina and Bergles [101] and Hong and Bergles [102] to correlate heat transfer data in single phase flow inside the tubes with twisted tape inserts. As a result the following correlation function was used.

$$R = \left[1 + a_o \left\{\frac{Re_L}{Y}\right\}^{a_1}\right] \qquad (3\text{-}61)$$

Due to the fact that steam data of Royal and Bergles [58a,59] showed a definite effect for the twist ratio of the tape, while R-113 data [60,61] didn't show the effect, the constants a_o and a_1 in Eq (3-61) were determined by using steam data alone. Least squares regression analysis was used to determine a_o and a_1. The result was:

$$R = \frac{\bar{h}_{tt}}{\bar{h}_{TP}} = \left[1 + 0.02 \left\{\frac{Re_L}{Y}\right\}^{0.19}\right] \qquad (3\text{-}62)$$

Eq (3-62) was then used to correlate R-113 data.

3.3.1.2 RESULTS AND DISCUSSION

The modified correlation of Akers et al., Eq (3-55), was tested for its capability to predict the twisted tape data of R-113 [61]. A value of 0.97 was used for the fin effectiveness

as suggested by Luu and Bergles [78]. Equivalent diameter was determined from Eq (3-54). The Akers et al. [63] correlation doesn't contain any friction factor term. So there was no necessity to calculate F_f. The results of these computations are shown in Fig (3-7). The agreement between calculation and experiment is within ± 20%. The modified Akers et al. correlation was used to calculate mean heat transfer coefficients during condensation of steam in the presence of a twisted tape insert. These results are shown in Fig (3-8). The disagreement between predicted and experimental values is within 15% and -30%. Most of the predictions were higher than the experimental values.

The Boyko and Kruzhilin correlation [65] was modified by Luu and Bergles [78] to predict the mean heat transfer coefficients during condensation of R-113 with twisted tape inserts and was given by Eq (3-59). Eq (3-59) was used to predict the condensation heat transfer data of steam with twisted tape inserts. Using the local quality values from the experimental data of steam with twisted tape inserts, a fourth order polynomial interpolation function was obtained to calculate intermediate values of quality for each experimental run. The fin effectiveness of the tape was taken as 0.97. Using twelve incremental lengths for the entire length of condenser and Eq (3-59) local heat transfer coefficients were calculated. The mean heat transfer coefficient was obtained by using Eq (3-15). The numerical integration was carried out by a modified trapezoidal rule [103]. The predictions were higher than experimental values and the error was in the range of 60

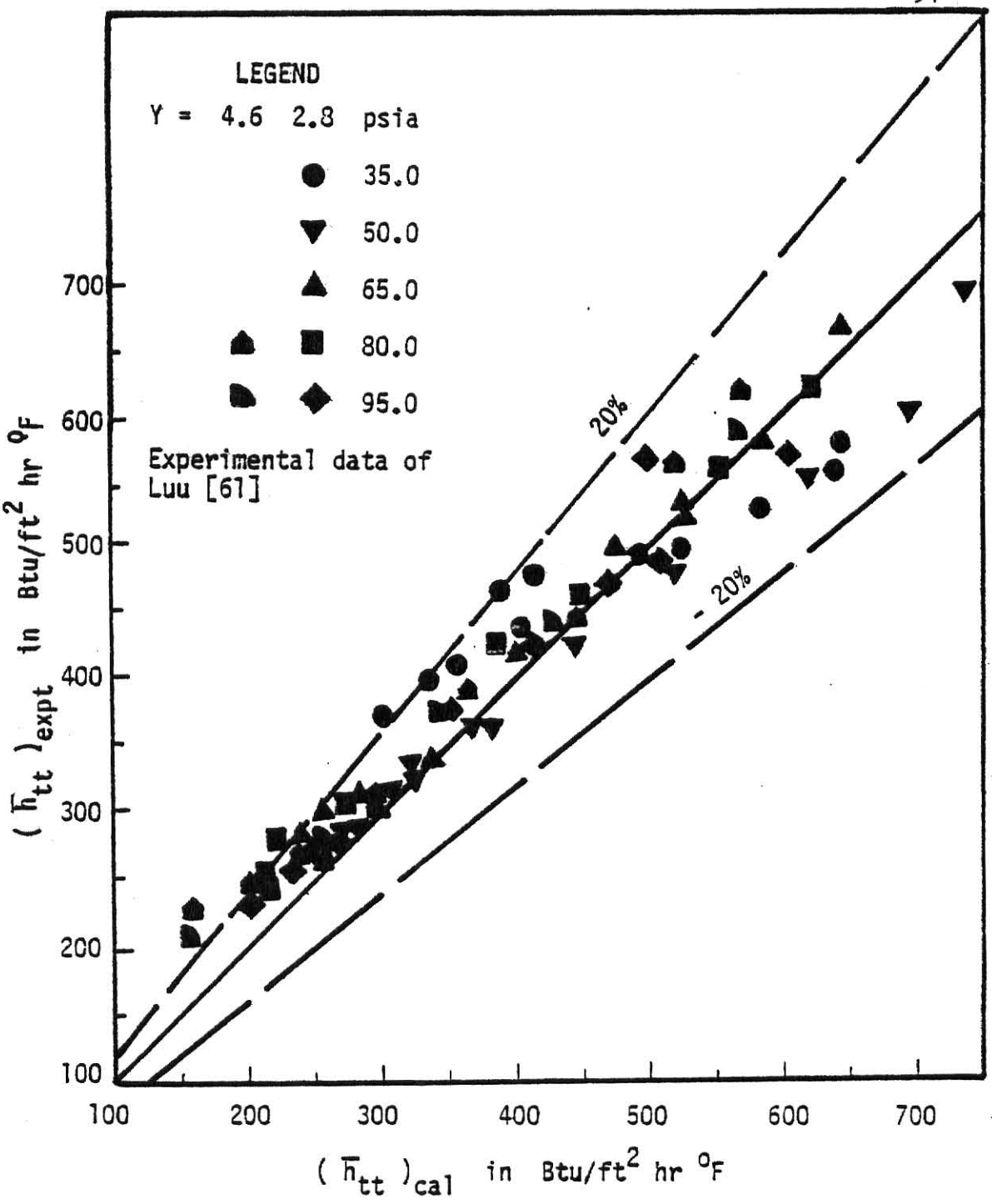

Fig (3-7) Comparison Between Calculated and Experimental Mean Heat Transfer Coefficents for Twisted Tape Data of R-113 Using Modified Correlation of Akers et al. [58a], Eq (3-55).

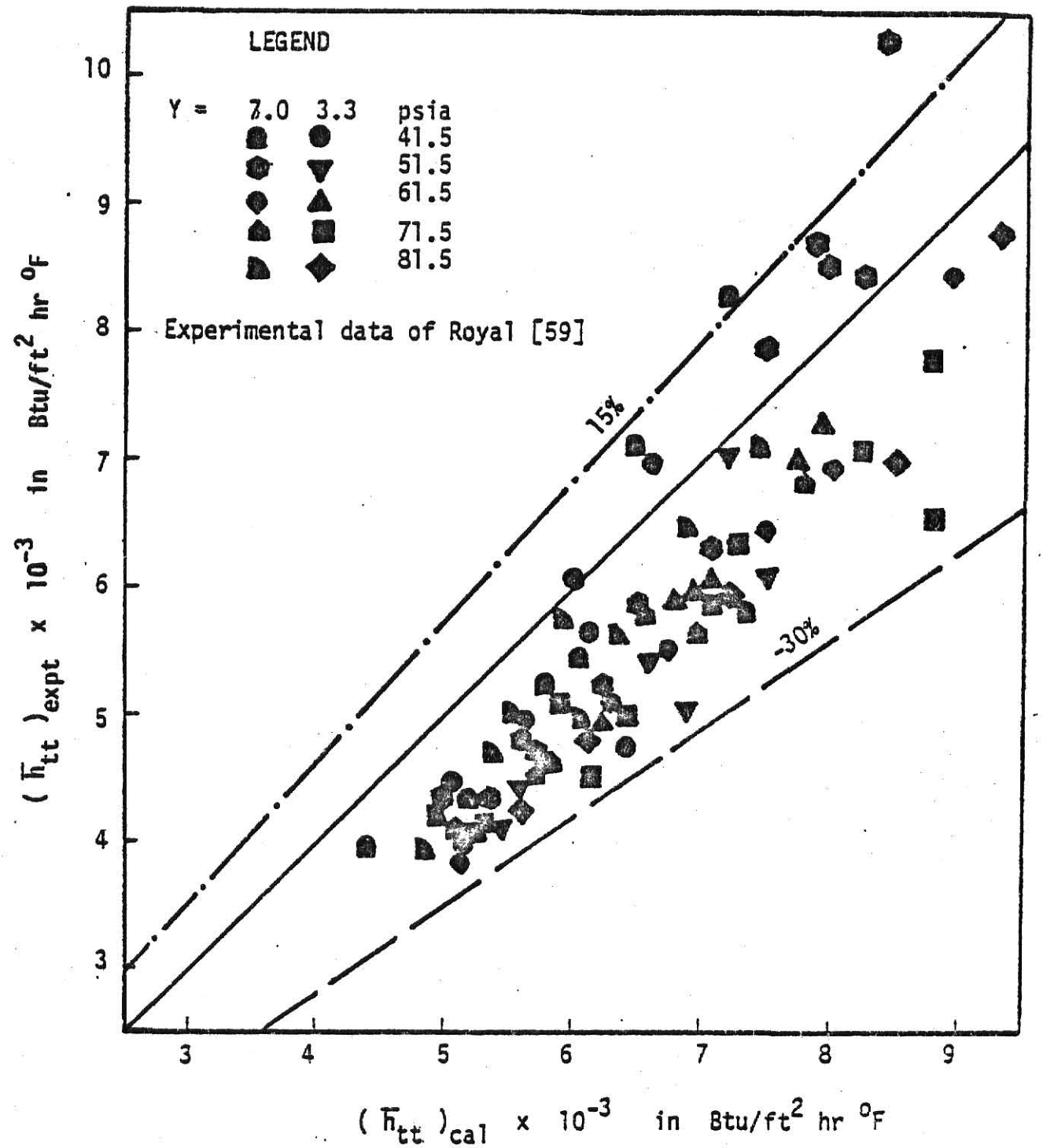

Fig (3-8) Comparison Between Calculated and Experimental Mean Heat Transfer Coefficents for the Twisted Tape Data of Steam Using Modified Correlation of Akers et al. [58a], Eq (3-55).

to 90%. For this reason Boyko and Kruzhilin correlation [65] was not used to predict the smooth tube heat transfer data of steam and R-113.

Figs (3-9) and (3-10) show the comparisons between experimental measurements of steam and R-113 respectively with the predictions of Eq (3-62). The disagreement between measurements and predictions is within ± 20% for steam and within + 25% and -10% for R-113.

Therefore, it can be concluded that when both sets of data are combined the proposed correlation agrees within ±25% of the experimental measurements.

3.3.2 PRESSURE DROP CORRELATION FOR TUBES WITH TWISTED TAPES INSERTS.

The approach to the pressure drop calculation for tubes with twisted tape inserts is similar to the one used for smooth tubes. The total pressure gradient is expressed as a sum of frictional and momentum pressure gradients. However, the presence of a twisted tape increases the friction factor over the smooth tube condensation friction factor. It also decreases the flow area and increases the wetted perimeter. This is usually taken care of by the use of an equivalent diameter in place of inside diameter.

Royal and Bergles [82] modified the Dukler et al. correlation for frictional pressure gradient [86] and used Hughmark correlation [90] for void fraction, in order to correlate their pressure drop data during condensation of steam in the presence of a twisted tape insert. The following modifications to the Dukler et al. [86] correlation were

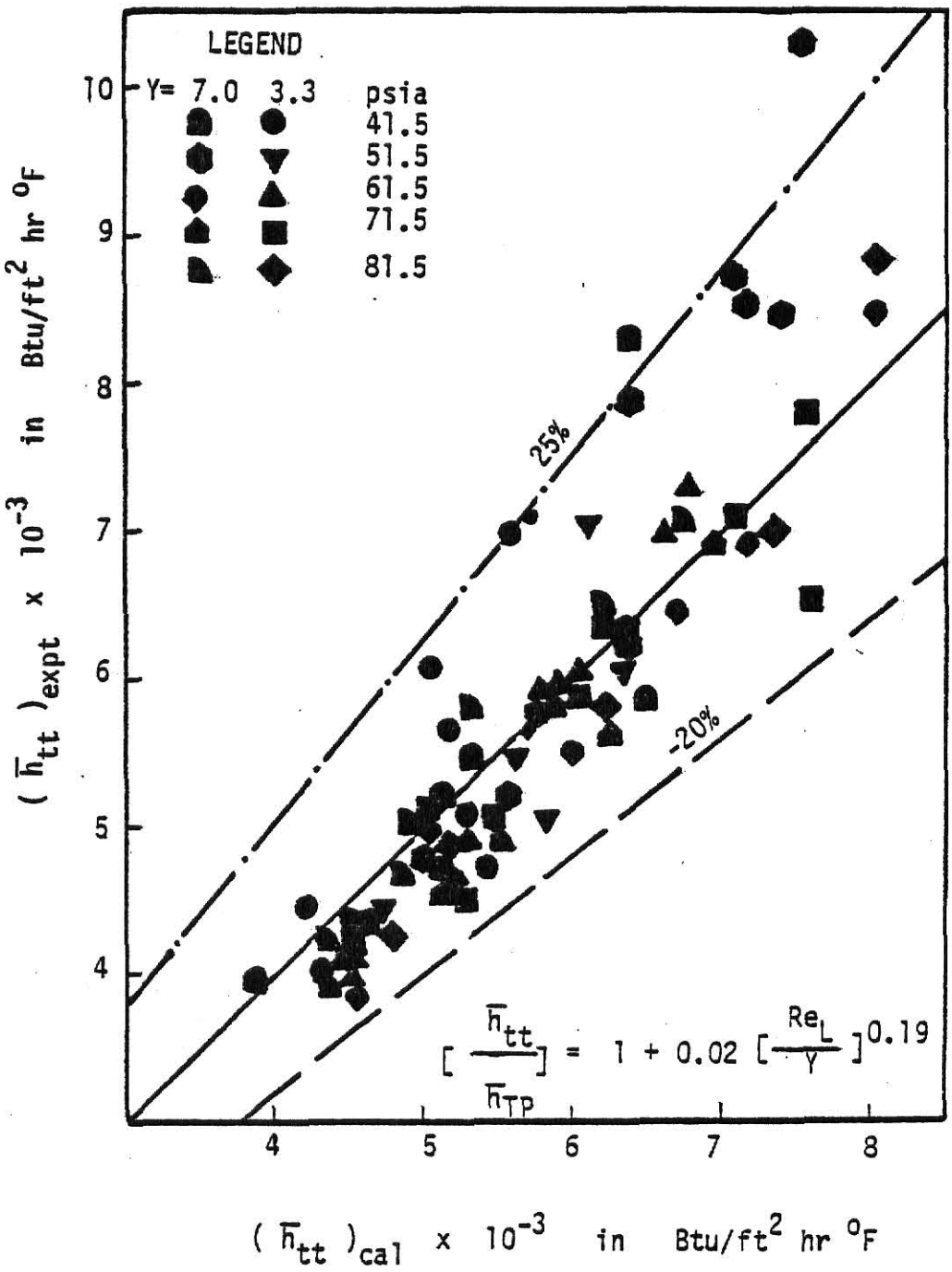

Fig (3-9) Comparison Between Calculated and Experimental Mean Heat Transfer Coefficents for Twisted Tape Data of Steam Using Modified Correlation of Shah.

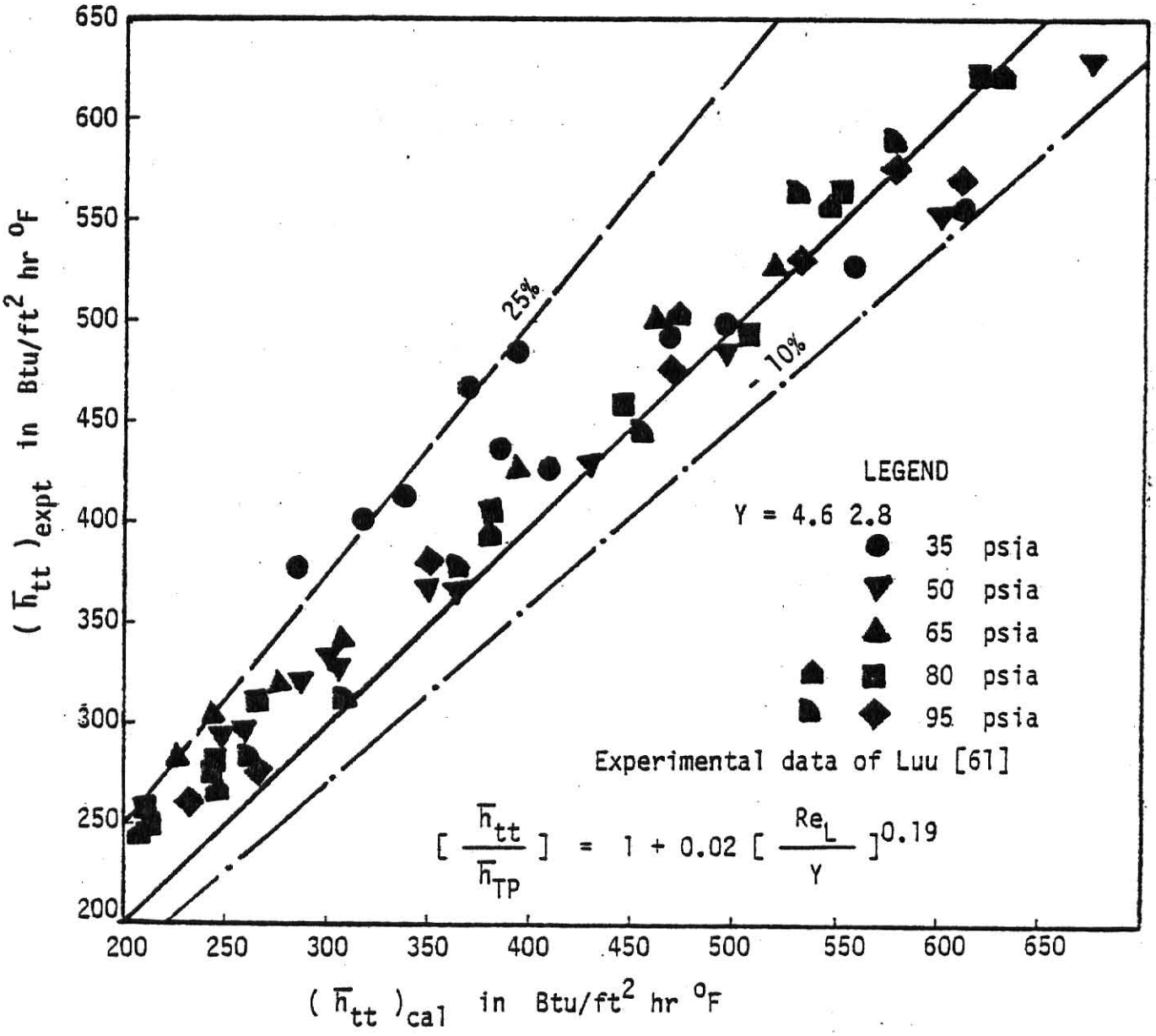

Fig (3-10) Comparison Between Calculated and Experimental Mean Heat Transfer Coefficents for Twisted Tape Data of Steam Using Modified Correlation of Shah.

applied:

1. The use of equivalent diameter as defined by Eq (3-54) in place of inside diameter as the characteristic length in Eqs (3-25) and (3-33).
2. The use of a wall shear correction factor, F_f, as given by Eq (3-53) to the adiabatic friction factor used in the smooth tube pressure drop predictions.

It is to be noted here that Royal and Bergles [82] did not apply a correction factor to the adiabatic friction factor to take care of the effect of condensation on the friction factor as was done by Luu and Bergles [78] for R-113 for smooth tube. Using these modifications to the smooth tube correlations, Royal and Bergles [82] predicted the pressure drop during condensation of steam in the presence of a twisted tape insert. Their predictions were lower than the experimental data, and the disagreement was as high as 50%.

Luu and Bergles [77] modified the Traviss-Rohsenow [72] correlations to predict the pressure drop during condensation of R-113 in the presence of a twisted tape insert. The following modifications were introduced:

1. the use of an equivalent diameter, defined by Eq (3-58), in place of inside diameter, as the characteristic dimension.
2. the use of wall shear correction factor, F_f, as defined by Eq (3-53), to the condensation friction factor, f_c obtained from Eqs (3-36) and (3-35).

It is to be noted here that

1. The Traviss-Rohsenow correlation [72] is nothing but the Lockhart-Martinelli correlation [83].

2. Luu and Bergles [77] applied correction to the adiabatic friction factor to account for condensation, in smooth tube pressure drop predictions.
3. They [77] also used a homogeneous momentum equation for momentum pressure gradient in smooth tube pressure drop calculations.

Using the above mentioned modifications to the smooth tube pressure drop predictions, Luu and Bergles [77] predicted pressure drop during condensation of R-113 in the presence of twisted tape inserts. The agreement was within about 40%. The predictions were lower than the experimental data.

In another report, Luu and Bergles [78] modified Dukler et al. correlation [86] to which the following modifications were introduced:

1. The use of an equivalent diameter, as defined by Eq (3-58) in place of inside diameter
2. The use of a correction factor, Eqs (3-36) and (3-35), to adiabatic friction factor to account for condensation.
3. The use of wall shear correction factor, F_f, given by Eq (3-53), to the condensation friction factor to account for the increased friction due to the presence of tape.

These above mentioned modifications resulted in pressure drop predictions which were within $\pm$ 40% of their experimental data.

3.3.2.1 PRESSURE DROP WITH TWISTED TAPE INSERTS

In the present study Lockhart-Martinelli correlation [83], described in section (3.2.2.1), for frictional pressure drop was modified by:

1. the use of equivalent diameter, as defined by Eq (3-54), in place of inside diameter in Eqs (3-46) and (3-44).
2. use of correction factor to adiabatic friction factor, given by Eqs (3-36) and (3-35), to account for condensation.
3. use of wall shear correction factor, F_f, given by Eq (3-53), to account for increased friction due to the presence of twisted tape.

The momentum pressure gradient was calculated using Eq (3-19) and the void friction was calculated by Zivi's [93] expression of Eq (3-37).

3.3.2.2 RESULTS AND DISCUSSION

Using the above modifications to the smooth tube pressure drop prediction procedure, (section 3.2.2.1) the pressure drops during condensation of R-113 and steam were predicted. The entire tube length was divided into twenty incremental lengths and the total pressure drop was the sum of pressure drops in the twenty sub-sections. This scheme was discussed in detail in section (3.2.2.2).

The predicted and experimental pressure drop are compared in Fig (3-11) for steam and Fig (3-12) for R-113. The disagreement between predictions and experimental data is within +25% for steam. The predictions were lower than the experimental data. The R-113 predictions agreed within $\pm$40% with the experimental data. The larger error in this case could be due to uncertainities in the pressure measurements.

3.4 SUMMARY

The results of this chapter can be summarized as follows:

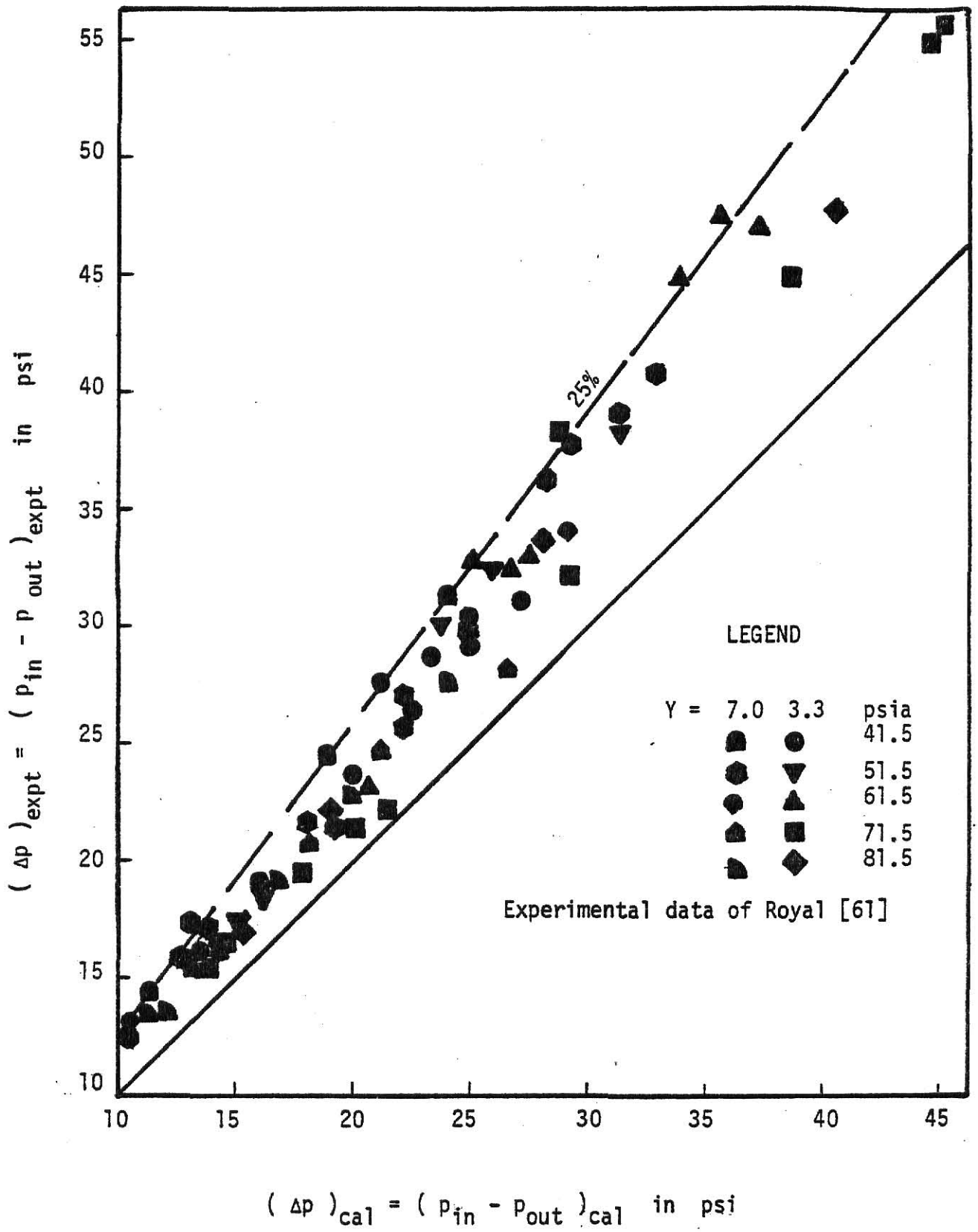

Fig (3-11) Comparison Between Calculated and Experimental Pressure Drop for the Twisted Tape Data of Steam.

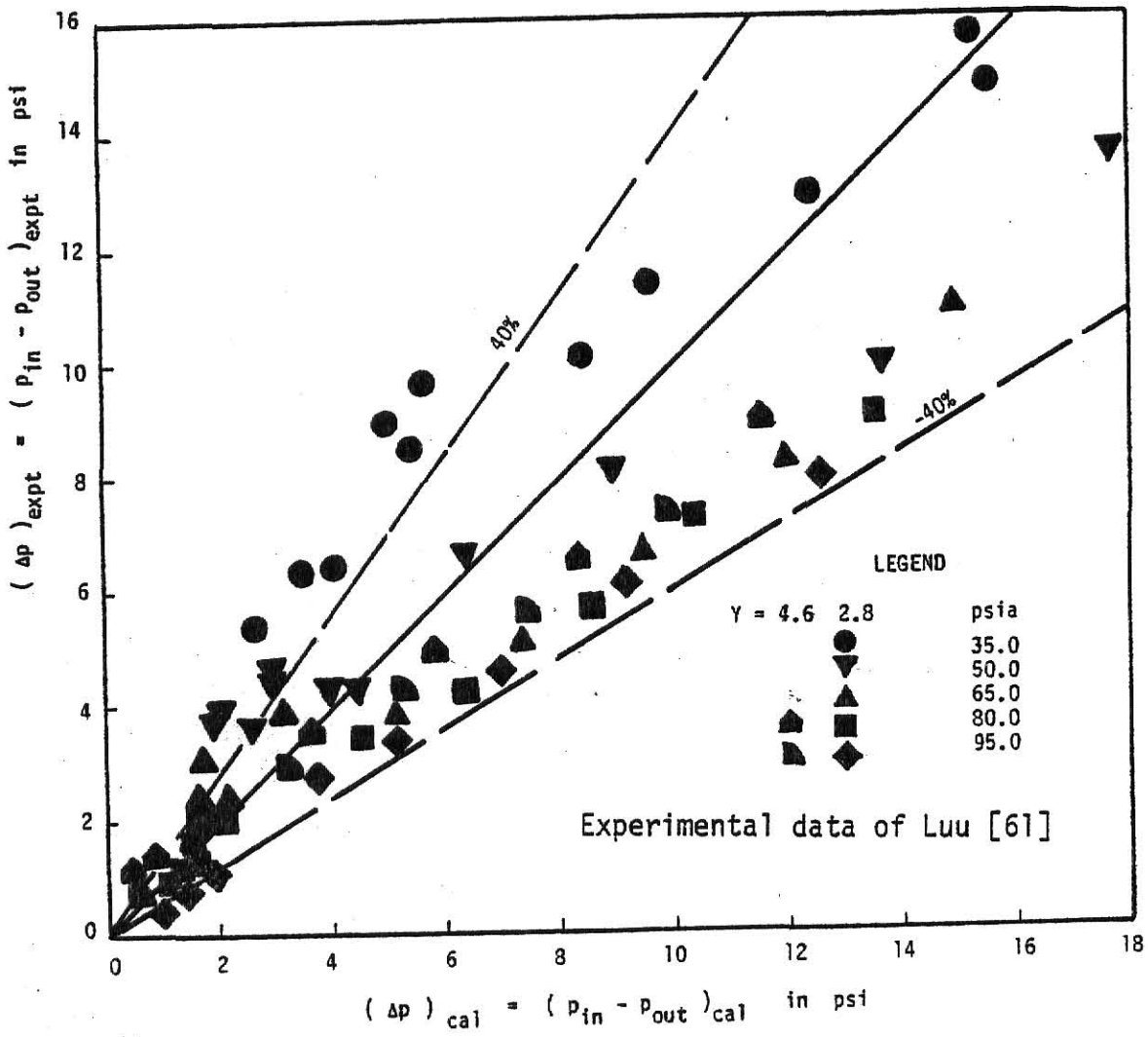

Fig (3-12) Comparison Between Calculated and Experimental Pressure Drop for the Twisted Tape Data of R - 113.

1. Shah's [76] correlation, given by Eq (3-17), can be used to predict the mean heat transfer coefficients during condensation inside smooth horizontal tubes.
2. Eqs (3-17) and (3-62) can be used to predict mean heat transfer coefficients during condensation inside horizontal tubes with twisted tape inserts.
3. Lockhart-Martinelli [83] correlation with the modifications suggested in Section (3.2.2.1) and Zivi [93] correlation for void fraction can together be used to predict smooth tube pressure drop during condensation.
4. Lockhart-Martinelli [83] correlation in item 3, given above, with further modifications proposed in Section (3.3.2.1) can be used to predict pressure drop during condensation inside horizontal tubes with twisted tape inserts.

3.5 CONCLUSIONS

The proposed correlation for pressure drop and heat transfer predictions during condensation inside tubes with twisted tape inserts can by no means be considered as the final word on this subject. Their validity needs to be tested with more experimental data of different fluids, tubes and twisted tape geometries. The validity of some of the correlations used for two-phase,diabatic flow friction factor and void fraction is questionable. For example, the definition of void fraction in two-phase adiabatic and diabatic flows in smooth tubes is well established and can be measured. In the presence of a twisted tape insert the definition of void fraction needs to be re-examined. No experimental data on this

subject are available at the present time to verify these expressions in the present study. Until such time the proposed correlation can serve as reference for future studies. No claim can be made about the superiority over the ones developed by Royal and Bergles [58,59] for steam data and Luu and Bergles [60,61] for R-113 data. The advantage of the present correlations is that one correlation for heat transfer and one correlation for pressure drop could correlate two sets of data of steam and R-113. Also, the proposed correlations bring about a closer agreement between predictions and experimental data.

CHAPTER IV

ANALYSIS OF CONDENSATION HEAT TRANSFER INSIDE A SEMI-CIRCULAR TUBE

INTRODUCTION

The problem of condensation heat transfer inside tubes is difficult to analyse because of the complex nature of the phenomena connected with phase changes. Moreover, there are no adequately accurate methods to evaluate the pressure drop and void fraction during phase changes in two-phase, diabatic systems. Because of such difficulties only a few attempts were made in the past to analyse the problem of forced convection condensation inside circular tubes.

Azer et al. [70] analysed the problem assuming annular flow with axi-symmetric liquid film surrounding the vapor core. They used a modified Lockhart-Martinelli parameter [104], obtained from the experimental data of R-12, to compute two-phase friction pressure gradient and Zivi's equation [93] for void fraction. They were successful in predicting the local heat transfer coefficients during condensation of R-12 [104] and R-22 [105].

Bae et al. [68,105] and Traviss et al. [72,106] analysed the problem as flow over a flat plate, thus neglecting the curvature effects. Their analyses were mainly for the refrigerants. Making use of the range of physical properties of refrigerants, Traviss et al. [72] introduced certain simplifications so that the final heat transfer equation can be used in the design of condensers. They used Lockhart-Martinelli [83] and Zivi [93] correlations for frictional pressure

drop and void fraction, respectively.

To the author's knowledge the analysis of the problem of condensation inside semi-circular tubes with twisted tape inserts has never been attempted. It has been shown by Royal and Bergles [58,59] and Luu and Bergles [60,61] that the use of twisted tape inserts augment the condensation heat transfer. Royal and Bergles [58,59] showed a definite effect of twist ratio, (pitch of the tape per 180° rotation of tape/ inside diameter of the tube), on heat transfer. As the twist ratio increases, the tape becomes straight and the flow inside the tube will be similar to the flow inside semi-circular tubes. As a starting point to the analysis of the problem of condensation inside a tube with a twisted tape insert, the problem of condensation inside a semi-circular tube is analysed in the present study.

4.1 PHYSICAL MODEL

Assuming that the modified Baker's flow regime map of Soliman [107] holds good for the semi-circular tube, it can be shown that, for high velocity vapor flow, annular flow exists over a major portion of the tube. Therefore, in the present analysis annular flow model is assumed without any liquid entrainment into the vapor core. A smooth interface is assumed to exist between vapor and liquid phases. Therefore, the model to be analysed is that of condensation inside a semi-circular tube, where a continuous liquid film flows along the semi-circular boundary while the remaining straight boundary is insulated,as shown in Fig (4-1). No liquid film exists on the insulated surface. It is assumed that inertial

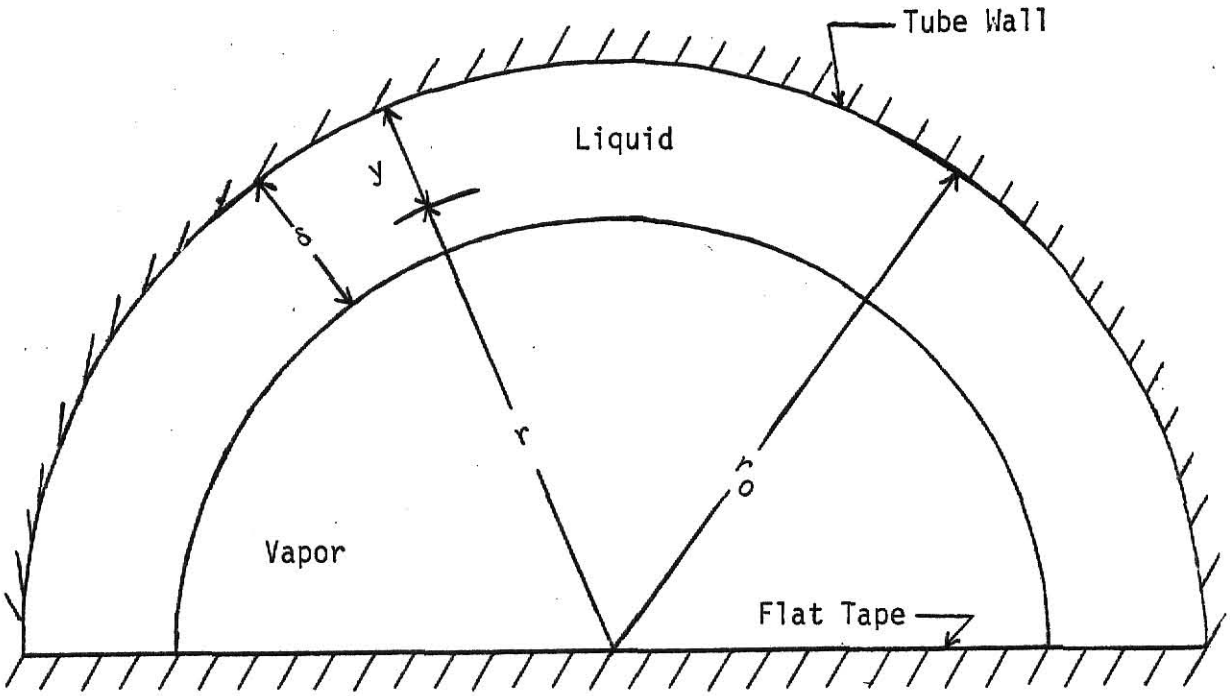

Fig (4-1) Schematic Diagram of Two-Phase, Annular Flow Model During Condensation Inside a Semi-Circular Tube with Axisymmetric Liquid Film.

and shear forces dominate the flow. The analysis is based on the following assumptions:

1. The vapor phase is at the saturation temperature and the interfacial temperature drop is negligible.
2. The flat surface is assumed to be adiabatic.
3. The flow is steady and one dimensional. The liquid and vapor velocities are in the axial direction.
4. The liquid film is axi-symmetric.
5. The liquid film is in turbulent motion. von Karman velocity profile is assumed to describe the liquid film flow.
6. The static pressure is uniform at a given axial location.
7. The thermodynamic and transport properties of both phases are assumed to be constant.
8. Eddy diffusivities for momentum and energy transfer are assumed to be equal for the liquid film.
9. Axial heat conduction in the liquid film is negligible.

4.2 MODEL DEVELOPMENT

The governing equations for momentum and energy transfer in turbulent flow in the liquid film are:

$$\tau = \frac{1}{g_c} \left[\mu_l + \rho_l \, \varepsilon_M \right] \left[\frac{du_l}{dy} \right] \qquad (4\text{-}1)$$

$$q = - \left[K_l + \rho_l \, C_l \, \varepsilon_H \right] \left[\frac{dt}{dy} \right] \qquad (4\text{-}2)$$

where

τ = shear stress at a distance y from the wall

q = heat flux at y

u_l = axial velocity of liquid at y

μ_l = dynamic viscosity of the liquid

ρ_l = density of the liquid

ε_M = eddy diffusivity for momentum transfer

ε_H = eddy diffusivity for energy transfer

K_l = thermal conductivity of liquid

C_l = specific heat of the liquid

g_c = gravitational constant

and t = temperature at y

To solve Eqs (4-1) and (4-2) the shear stress and heat flux distributions across the liquid film and the ratio of the eddy diffusivities for momentum and energy transfer need to be determined.

In single phase turbulent flow, for fluids of Prandtl number greater than unity, assuming that ε_M and ε_H are equal, introduces little error in the computation of Nusselt number. In the present analysis also it is assumed that ε_M equals ε_H for the liquid film.

Eqs (4-1) and (4-2) can be rewritten in dimensionless form as:

$$\tau/\tau_o = (1 + \varepsilon_M/\nu_l)\left[\frac{du^+}{dy^+}\right] \qquad (4-3)$$

$$q/q_o = \left(\frac{1}{Pr_l} + \frac{\varepsilon_M}{\nu_l}\right)\left[\frac{dt^+}{dy^+}\right] \qquad (4-4)$$

where

τ_o = wall shear stress

q_o = heat flux at the wall

ν_l = kinematic viscosity of the liquid film

Pr_l = Prandtl number of the liquid film

$$u^+ = \frac{u_l}{V^*}$$

$$V^* = (\tau_o g_c/\rho_l)^{0.5}$$

$$y^+ = \frac{y\ V^*}{\nu_l}$$

and

$$t^+ = \frac{\rho_l\ C_l\ V^*\ (t_o - t)}{q_o}$$

Solving Eq (4-3) for ε_M^+/ν_l and substituting the result in Eq (4-4) yields

$$\frac{q}{q_o} = \left[\frac{1}{Pr_l} + \frac{(\tau/\tau_o)}{\left(\frac{du^+}{dy^+}\right)} - 1\right]\left[\frac{dt^+}{dy^+}\right] \qquad (4\text{-}5)$$

The initial condition for this first order equation is:

$$t^+ = 0 \quad \text{at} \quad y^+ = 0 \qquad (4\text{-}6)$$

Integration of Eqs (4-5) with the initial condition in Eq (4-6) yields the dimensionless temperature drop across the liquid film, t_δ^+. Using t_δ^+ the local Nusselt number can be determined as will be shown in a latter section.

In order to integrate Eq (4-5) the following quantities have to be determined.

1. The velocity distribution across the liquid film
2. The shear stress distribution across the liquid film
3. The local liquid film thickness, and
4. The heat flux distribution across the liquid film.

These distributions will be determined in the following sections.

4.2.1 THE VELOCITY DISTRIBUTION ACROSS THE LIQUID FILM

von Karman velocity profile yielded reasonable results for Nusselt number in annular flow condensation [72,73,104, 105]. The same velocity distribution is used in the present analysis to describe the liquid film velocity distribution.

The von Karman velocity profile is given by the following equations:

$$\begin{aligned} u^+ &= y^+ && 0 < y^+ < 5 \\ u^+ &= -3.05 + 5 \ln y^+ && 5 < y^+ < 30 \\ u^+ &= 5.5 + 2.5 \ln y^+ && y^+ > 30 \end{aligned} \qquad (4\text{–}7)$$

4.2.2 THE SHEAR STRESS DISTRIBUTION ACROSS THE LIQUID FILM

The shear stress distribution can be obtained by writing the momentum equation for the liquid differential element at a radius r from the tube axis as shown in Fig (4–2). Referring to Fig (4–3) the momentum equation for the differential element can be written as:

$$\Sigma \dot{M}_{out} - \Sigma \dot{M}_{in} = \Sigma F_z \qquad (4\text{–}8)$$

The momentum flux rate into the element is given by:

$$\Sigma \dot{M}_{in} = \frac{1}{g_c} [u_l W_l + u_i dW_l] \frac{A_r}{A_l} \qquad (4\text{–}9)$$

where

u_i = velocity of the condensing particles leaving the vapor core and entering the liquid film at liquid-vapor interface.

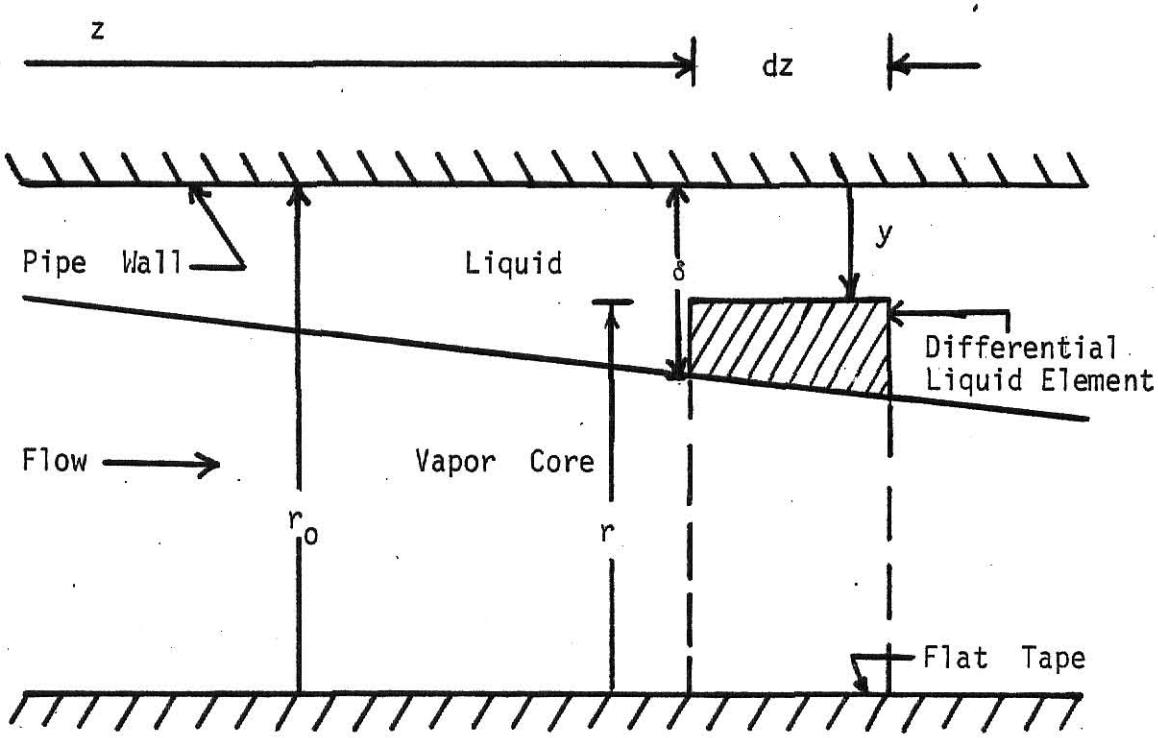

Fig (4.2) Basic Co-ordinate System of Two - Phase Annular Flow Model For The Semi - Circular Tube.

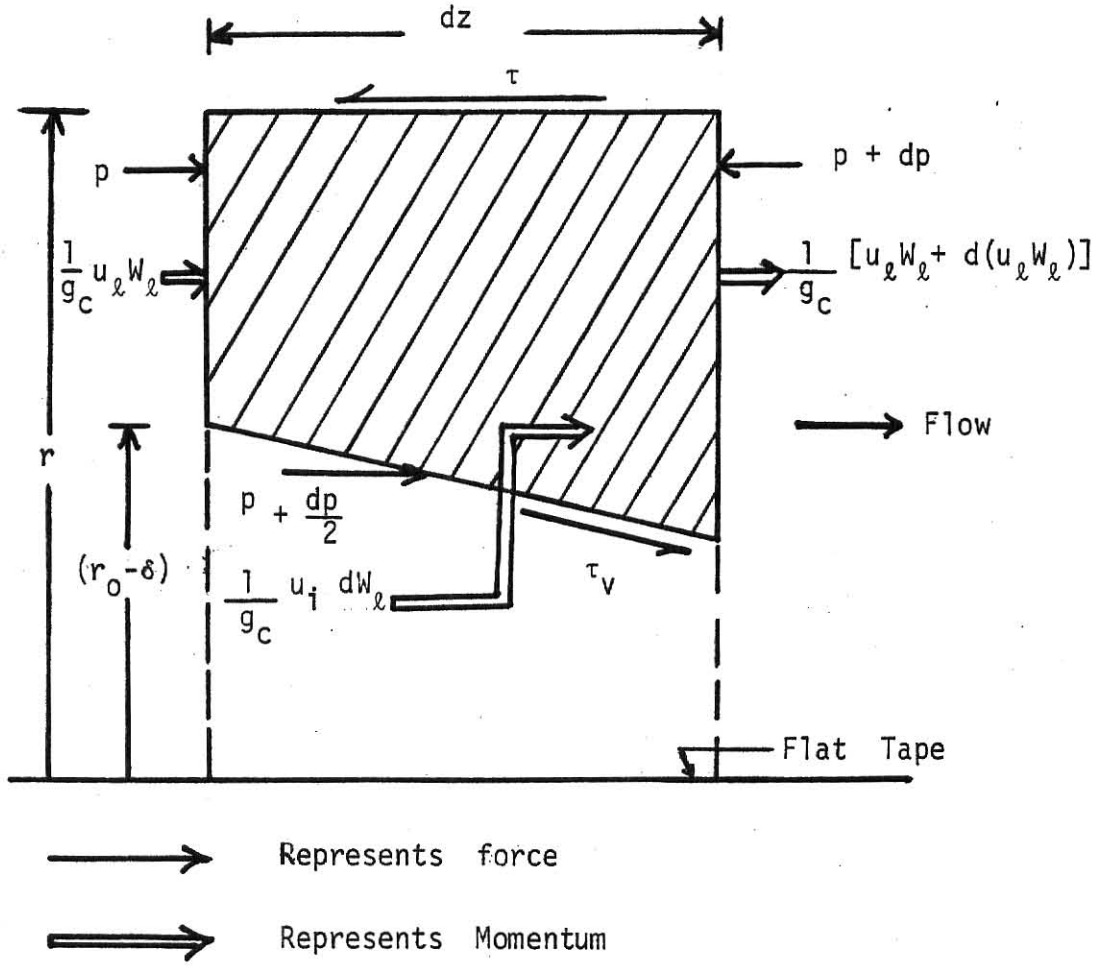

Fig (4-3) The Differential Liquid Element with Forces and Momenta.

The momentum flux rate leaving the element is given by:

$$\Sigma \dot{M}_{out} = \frac{1}{g_c} \left[u_1 W_1 + d(u_1 W_1) \right] \frac{[A_r + dA_r]}{[A_1 + dA_1]} \qquad (4\text{–}10)$$

The sum of all the forces acting in the axial direction on the liquid element is given by:

$$\Sigma F_z = - A_r \, dp - \tau \pi r \, dz + \tau_v \pi (r_o - \delta) dz \qquad (4\text{–}11)$$

where

τ_v = interfacial shear stress

δ = local liquid film thickness

The areas A_r and A_1 used in Eqs (4–9) and (4–10) are given by:

$$A_r = \frac{\pi}{2} \left[r^2 - (r_o - \delta)^2 \right] \qquad (4\text{–}12)$$

$$A_1 = \frac{\pi}{2} \left[r_o^2 - (r_o - \delta)^2 \right] \qquad (4\text{–}13)$$

Since δ is small compared to r_o, neglecting higher order terms, one can write as :

$$\frac{A_r}{A_1} = \frac{\left[(r^+/r_o^+)^2 + 2\,\delta^+/r_o^+ - 1 \right]}{2\,\delta^+/r_o^+} \qquad (4\text{–}14)$$

Also,

$$A_r + dA_r = \frac{\pi}{2} \left[r^2 - (r_o - (\delta + d\delta))^2 \right]$$

$$\text{and} \quad A_1 + dA_1 = \frac{\pi}{2} \left[r_o^2 - (r_o - (\delta + d\delta))^2 \right] \qquad (4\text{–}15)$$

By assuming that the changes in the film thickness are gradual and smooth, by neglecting higher order terms and noting

that $d(\delta/r_o) \ll (\delta/r_o)$, it can be shown that:

$$\frac{A_r + dA_r}{A_1 + dA_1} = \frac{A_r}{A_1} \tag{4-16}$$

Substitution of Eqs (4-12), (4-13), (4-16), (4-10) and (4-11) into Eq (4-8) yields:

$$\frac{[(r^+/r_o^+)^2 + 2\delta^+/r_o^+ - 1]}{2g_c[\delta^+/r_o^+]} \left[\frac{d}{dz}(u_1 W_1) - u_i \frac{dW_1}{dz}\right]$$

$$= \frac{\pi}{2}[r^2 - (r_o - \delta)^2]\left(\frac{dp}{dz}\right) - \tau\pi r + \tau_v \pi (r_o - \delta) \tag{4-17}$$

Solving Eq (4-17) for τ yields

$$\tau = \frac{[(r^+/r_o^+)^2 + 2\delta^+/r_o^+ - 1]}{2\pi r g_c[\delta^+/r_o^+]} \left[u_i \frac{dW_1}{dz} - \frac{d}{dz}(u_1 W_1)\right]$$

$$- \frac{1}{2}\left[r - \frac{(r_o - \delta)^2}{r}\right]\left(\frac{dp}{dz}\right) + \tau_v \frac{(r_o - \delta)}{r} \tag{4-18}$$

Since

$$y = r_o - r$$
$$y^+ = r_o^+ - r^+ \tag{4-19}$$

and since $(y^+/r_o^+)^2 \ll 1$ it can be shown that

$$\tau = \frac{[1-(y^+/\delta^+)]}{\pi r_o g_c [1-(y^+/r_o^+)]} \left[u_i \frac{dW_l}{dz} - \frac{d}{dz}(u_l W_l) \right]$$

$$- \frac{r_o}{2}\left(\frac{dp}{dz}\right)\left\{ (1-\delta^+/r_o^+) \left[\frac{(1-y^+/r_o^+)}{(1-\delta^+/r_o^+)} - \frac{(1-{}^+/r_o^+)}{(1-y^+/r_o^+)} \right] \right\}$$

$$+ \tau_v \left[\frac{(1-\delta^+/r_o^+)}{(1-y^+/r_o^+)} \right] \qquad (4-20)$$

Soliman et al. [66] assumed that

$$u_i = \beta u_l \qquad (4-21)$$

Bae et al. [105] obtained a relationship between β and δ^+ using a value for u_l averaged, across the film thickness. They used the von Karman velocity profile to find an average liquid velocity and obtained three equations for β as a function δ^+ depending on the value δ^+. An integrated average value of β from their equations for δ^+ values upto 500 is 1.38. Traviss et al. [106] used the same equations obtained by Bae et al. [105]. Azer et al. [70], Soliman et al. [66] and Soliman [107] used a constant value of 1.25 for β. In the present analysis this constant value is used for β. Therefore

$$u_i = 1.25\, u_l \qquad (4-22)$$

With the use of Eq (4-22), and Zivi's equation [93] for void fraction, Eq (4-20) can be written as

$$\tau = \frac{[1-y^+/\delta^+]}{[1-y^+/r_o^+]}\left[-\left[\frac{G_t^2\, r_o(1-x)}{2\,\rho_l g_c(1-\psi)}\right]\frac{dx}{dz}\left\{-0.75+\frac{(1-x)}{(1-\psi)}\right.\right.$$

$$\left.\left.\frac{(\rho_v/\rho_l)^{2/3}}{\left[x+(1-x)\left(\frac{\rho_v}{\rho_l}\right)^{2/3}\right]^2}\right\}\right] - \frac{r_o}{2}\left(\frac{dp}{dz}\right)\left\{(1-\delta^+/r_o^+)\right.$$

$$\left.\left[\frac{(1-y^+/r_o^+)}{(1-\delta^+/r_o^+)} - \frac{(1-\delta^+/r_o^+)}{(1-y^+/r_o^+)}\right]\right\} + \tau_v\left[\frac{(1-\delta^+/r_o^+)}{(1-y^+/r_o^+)}\right] \qquad (4\text{–}23)$$

where

G_t = total mass velocity

ρ = density

x = local quality

$\frac{dx}{dz}$ = quality gradient

ψ = void fraction

The details of the derivation of Eq (4–23) from Eq (4–20) are given in Appendix D.

4.2.2.1 THE INTERFACIAL SHEAR STRESS

The wall shear stress, τ_o can be obtained from Eq (4–23) as the shear stress at $y^+ = 0$. Therefore,

$$\tau_o = \left[-\left[\frac{G_t^2 r_o(1-x)}{2\rho_l g_c(1-\psi)}\right]\frac{dx}{dz}\left\{-0.75 + \frac{(1-x)}{(1-\psi)}\right.\right.$$

$$\left.\left.\frac{(\frac{\rho_v}{\rho_l})^{2/3}}{[x + (1-x)(\frac{\rho_v}{\rho_l})^{2/3}]^2}\right\}\right] - \frac{r_o}{2}\frac{dp}{dz}[1 - (1-\delta^+/r_o^+)^2]$$

$$+ \tau_v(1-\delta^+/r_o^+) \qquad (4-24)$$

Solving Eq (4-24) for τ_v, interfacial shear stress can be written as:

$$\tau_v = \left[\tau_o + \frac{r_o}{2}\frac{dp}{dz}[1 - (1-\delta^+/r_o^+)^2] + \frac{G_t^2 r_o(1-x)}{2\rho_l g_c(1-\psi)}\right.$$

$$\left.[-0.75 + \frac{(1-x)}{(1-\psi)}\left\{\frac{(\frac{\rho_v}{\rho_l})^{2/3}}{(x+(1-x)(\frac{\rho_v}{\rho_l})^{2/3})^2}\right\}]\right] /(1-\delta^+/r_o^+)$$

(4-25)

In order to calculate the interfacial shear stress, τ_v, from Eq (4-25), it is necessary to obtain the wall shear stress, τ_o, and the local pressure gradient, $(\frac{dp}{dz})$.

4.2.2.2 DETERMINATION OF PRESSURE GRADIENT, $\frac{dp}{dz}$ AND WALL SHEAR STRESS, τ_o.

Referring to Fig (4-4) the momentum equation can be written for an elemental volume of radius r_o and length dz,

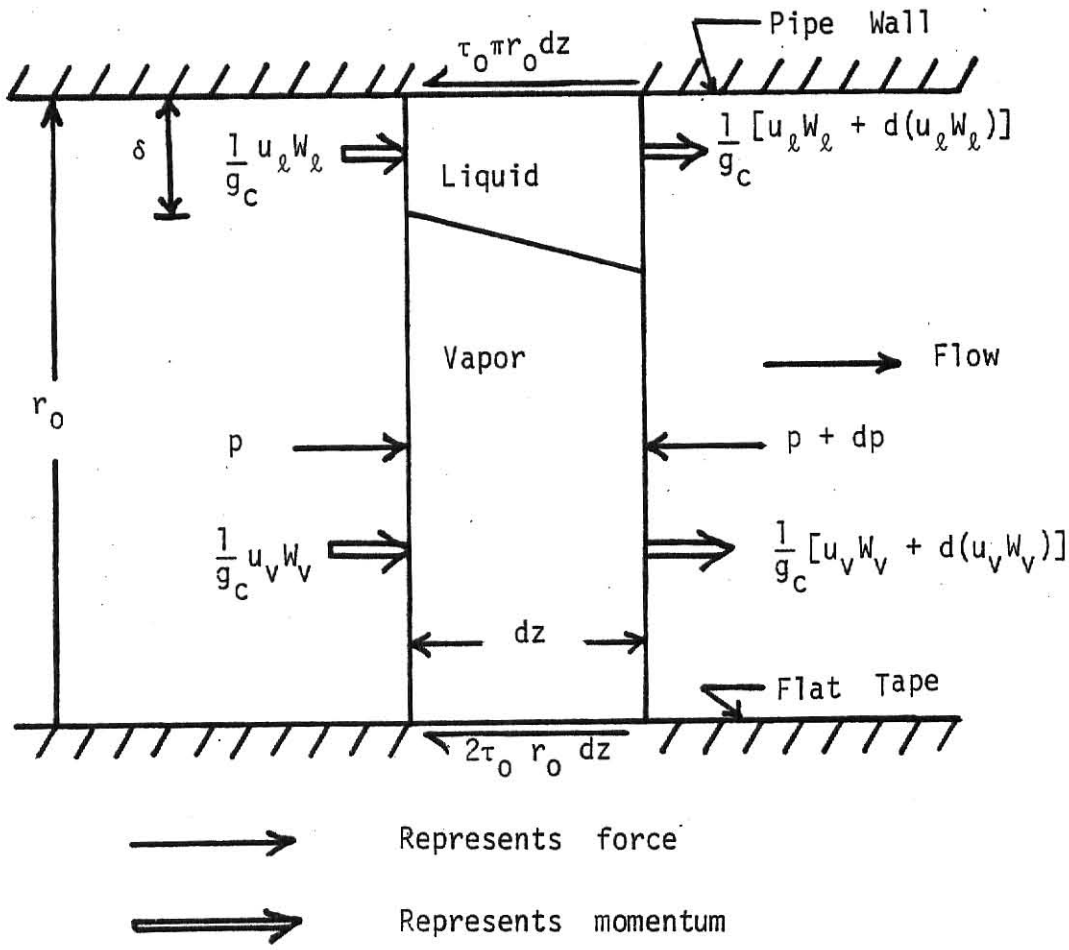

Fig (4-4) The Differential Element of Vapor and Liquid with Forces and Momenta.

which includes both the vapor and the liquid phases.

$$\Sigma \dot{M}_{out} - \Sigma \dot{M}_{in} = \frac{1}{g_c} d[u_l W_l + u_v W_v]$$

$$= \Sigma F_z \qquad (4\text{-}26)$$

where subscript v refers to the vapor phase.

In the present analysis, it is assumed that the wall shear stress, τ_o, is uniform and equal around the circumference of the semi-circular boundary and on the flat diametrical surface. As a result, the summation of forces is given by:

$$\Sigma F_z = -\frac{\pi r_o^2}{2} dp - \tau_o r_o (2 + \pi) dz \qquad (4\text{-}27)$$

From Eqs (4-26) and (4-27) one can write:

$$\left(\frac{dp}{dz}\right) = -\frac{1}{A g_c} d[u_l W_l + u_v W_v] - \frac{2\tau_o}{r_o}(1 + 2/\pi) \qquad (4\text{-}28)$$

where

A is the cross-sectional area of the duct.

It was shown earlier that

$$\left(\frac{dp}{dz}\right) = \left(\frac{dp}{dz}\right)_{\dot{M}} + \left(\frac{dp}{dz}\right)_{TPF} \qquad (4\text{-}29)$$

where subscript $\dot{M}$ refers to momentum term and TPF refers to two-phase friction.

By comparing Eqs (4-28) and (4-29), the momentum and frictional terms of the pressure gradient can be separated as:

$$\left(\frac{dp}{dz}\right)_M = -\frac{1}{Ag_c}\frac{d}{dz}\left[u_l W_l + u_v W_v\right] \qquad (4-30)$$

and

$$\left(\frac{dp}{dz}\right)_{TPF} = -\frac{2\bar{\tau}_o}{r_o}(1 + 2/\pi) \qquad (4-31)$$

The momentum pressure gradient can be written as:

$$\left(\frac{dp}{dz}\right)_M = -\frac{G_t^2}{g_c}\frac{dx}{dz}\left[-\frac{2(1-x)}{\rho_l(1-\psi)} + \frac{2x}{\rho_v\psi} + \frac{\psi(1-x)}{\rho_l x(1-\psi)} - \frac{x(1-\psi)}{\rho_v\psi(1-x)}\right] \qquad (4-32)$$

The derivation of Eq (4-32) is given in Appendix E. Evaluation of momentum pressure gradient needs an equation for local void fraction. In the present analysis Zivi's equation [93], as given by Eq (4-33), was used for void fraction.

$$\psi = \frac{1}{\left[1 + \left(\frac{1-x}{x}\right)\left(\frac{\rho_v}{\rho_l}\right)^{2/3}\right]} \qquad (4-33)$$

There are several correlations available in the literature [83-88] to predict the frictional pressure gradients in two-phase flow. As shown in Chapter III the Dukler et al. [86] predicted well the pressure drop data during condensation of steam [59] and R-113 [61] with and without twisted tape inserts.

The frictional pressure gradient correlation of Dukler et al. [86], described in section (3.2.2), was basically developed for two-phase, two-component adiabatic flow and was used with limited success for two-phase, one-component, diabatic systems, specifically for condensation. What is needed for the present analysis is a correlation capable of predicting pressure gradient in a semi-circular conduit during condensation. Such a correlation does not exist at the present time. To surmount this difficulty it was postulated that the two-phase frictional pressure drop correlation of Dukler et al. [86] developed for smooth tubes could be applied to the two-phase flow inside a semi-circular tube by replacing the tube inside diameter by equivalent diameter of the semi-circular tube. In such a case

$$D_e = D/(1+2/\pi) \qquad (4-34)$$

In Eq (4-34) the equivalent diameter is defined as:

$$D_e = 4 \times \left[\frac{\text{flow cross-sectional area}}{\text{wetted perimeter}}\right] \qquad (4-35)$$

In calculating flow cross-sectional area and wetted perimeter the thickness of the tape (flat surface in this case) was neglected.

4.2.3 THE LIQUID FILM THICKNESS

Referring to Fig (4-5) and from the continuity equation of the liquid layer, it can be shown that

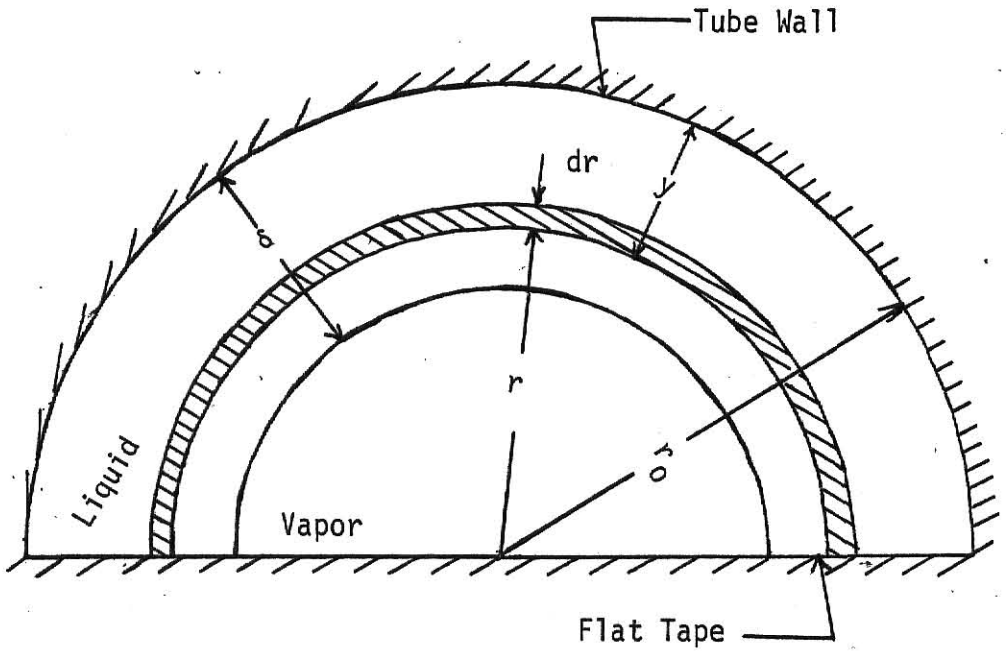

Fig (4-5) Differential Liquid Element for Liquid Continuity Equation.

$$W_l' = \int_{(r_o-\delta)}^{r_o} \pi r u_l \rho_l dr \qquad (4\text{-}36)$$

where

W_l' = liquid mass flow rate through the semi-circular tube.

Eq (4-36) can be rewritten as:

$$W_l = \frac{2\pi\rho_l \nu_l^2}{V^*} \int_0^{\delta^+} (r_o^+ - y^+)u^+ dy^+ \qquad (4\text{-}37)$$

where W_l = liquid mass flow rate through the entire cross section.

Since

$$W_l = (1-x)W_t \qquad (4\text{-}38)$$

Eq (4-37) becomes

$$W_t = \frac{2\pi\rho_l \nu_l^2}{(1-x)V^*} \int_0^{\delta^+} (r_o^+ - y^+)u^+ dy^+ \qquad (4\text{-}39)$$

The determination of δ^+ involves an iteration procedure. In such a case the total mass flow rate, W_t, condensing pressure, p_{sat}, and local quality, x, need to be specified. The properties ρ_l and ν_l, can be determined corresponding to p_{sat}. V^* and r_o^+ can be determined as discussed in previous sections. Since the velocity profile across the liquid film is described by Eq (4-7), the right hand side of Eq (4-39) can be determined after numerically evaluating the integral for an assumed value of δ^+. This value is then compared to the total mass flow rate, W_t. If the agreement is not within a prescribed limit a new value of δ^+ is assumed and the right hand side of Eq (4-39) is determined. The procedure continues until the error criterion for W_t is met.

4.2.4 THE HEAT FLUX DISTRIBUTION ACROSS THE LIQUID FILM

By applying energy balance on an elemental volume of liquid, as shown in Fig (4–6), one can write

$$q\pi r + W_1'' C_1\left(\frac{t + t_o}{2} - t_o\right) = q_o \pi r_o dz + W_1'' C_1 \left(\frac{t + t_o}{2} - t_o\right) + d\left[W_1'' C_1\left(\frac{t + t_o}{2} - t_o\right)\right] \quad (4\text{–}40)$$

where

W_1'' = mass flow rate of liquid into the elemental volume

q_o = heat flux at the inside tube wall

t = temperature of liquid at a radius r

t_o = wall temperature

q = heat flux at a radius, r

r_o = tube inside radius

C_1 = specific heat of saturated liquid

The energy balance in Eq (4–40) is based on the mean enthalpy of the liquid in the elemental volume. Eq (4–40) can be rewritten as:

$$\frac{q}{q_o} = \frac{r_o}{r} + \frac{1}{2\pi r q_o} \frac{d}{dz} \left[W_1'' C_1 (t - t_o)\right] \quad (4\text{–}41)$$

The ratio W_1''/W_1 is equal to the ratio of respective flow areas. Thus,

$$\frac{W_1''}{W_1} = \frac{\left[1 - (r/r_o)^2\right]}{\left[1 - (1-\delta/r_o)^2\right]} \quad (4\text{–}42)$$

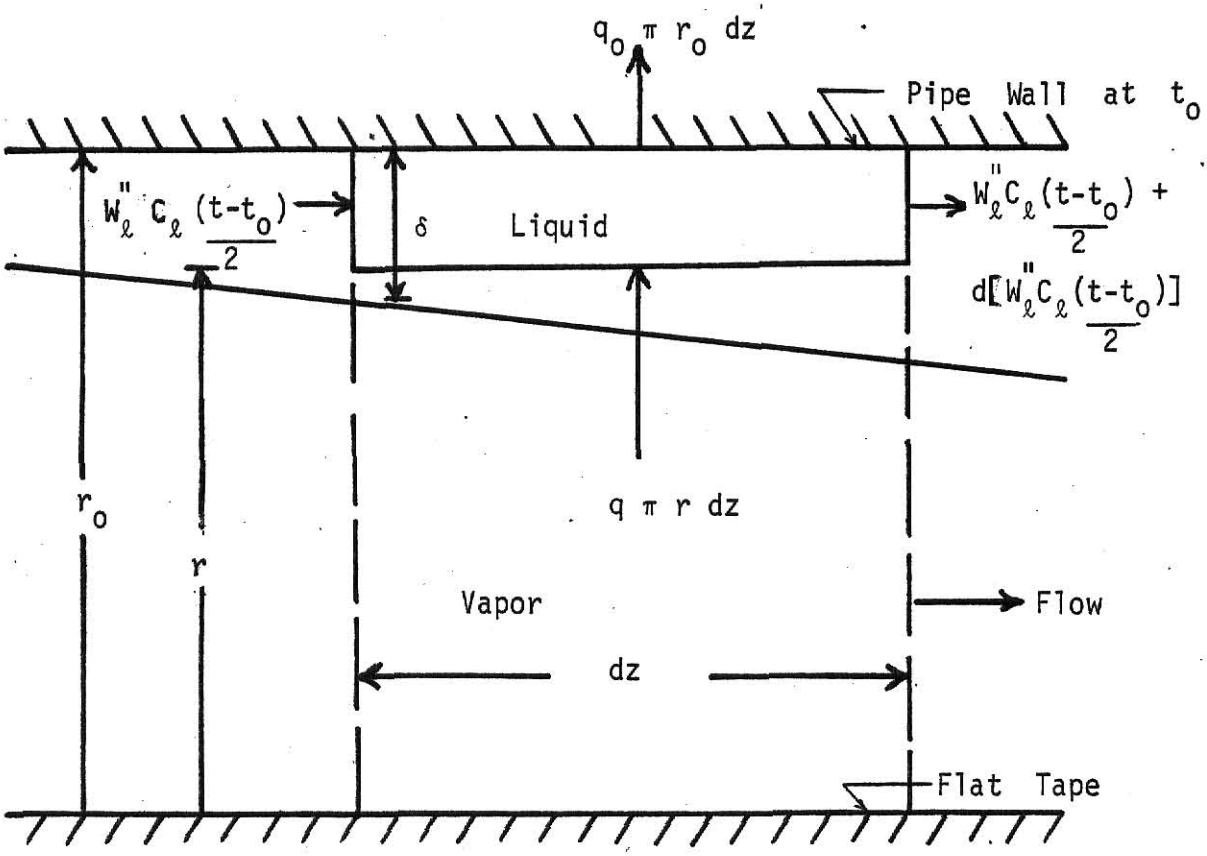

Fig (4-6) The Liquid Differential Element for Energy Balance.

By using Eqs (4-38) and (4-42) in Eq (4-41) it can be written as:

$$\frac{q}{q_o} = \frac{r_o}{r} + \frac{W_t\, C_1 \left[1 - (r/r_o)^2\right]}{2\pi r q_o} \frac{d}{dz} \left\{ \frac{(1-x)(t-t_o)}{\left[1 - (1-\delta/r_o)^2\right]} \right\} \tag{4-43}$$

The derivative on the right hand side of Eq (4-43) can be written as:

$$\frac{d}{dz}\left[\frac{(1-x)(t-t_o)}{\left[1-(1-\delta/r_o)^2\right]}\right] = \frac{(t_o-t)}{\left[1-(1-\delta/r_o)^2\right]}\frac{dx}{dz}$$

$$+ \frac{(1-x)}{\{1-(1-\delta/r_o)^2\}}\frac{d}{dz}(t-t_o) + (1-x)(t-t_o)$$

$$\frac{d}{dz}\left\{\frac{1}{1-(1-\delta/r_o)^2}\right\} \tag{4-44}$$

In the present analysis it is assumed that $(t-t_o)$ is independent of z. Therefore the second term on the right hand side of Eq (4-44) can be eliminated. Also assuming that neglecting the third term involves little error, Eq (4-44) can be written as:

$$\frac{d}{dz}\left\{\frac{\left[(1-x)(t-t_o)\right]}{\left[1-(1-\delta/r_o)^2\right]}\right\} = \left\{\frac{(t_o-t)}{\left[1-(1-\delta/r_o)^2\right]}\right\}\frac{dx}{dz} \tag{4-45}$$

Since

$$r = r_o - y$$

$$r^+ = r_o^+ - y^+$$

$$r/r_o = r^+/r_o^+$$

$$(y^+/r_o^+)^2 \ll 1$$

and

$$(\delta^+/r_o^+)^2 \ll 1$$

the heat flux equation can be expressed by:

$$\frac{q}{q_o} = \frac{1}{(1-y^+/r_o^+)} + \frac{W_t C_l}{2\pi r q_o \delta^+} \frac{dx}{dz} y^+ (t_o - t) \qquad (4-46)$$

Since

$$W_t = G_t \frac{\pi r_o^2}{2} ,$$

Eq (4-43) can be rewritten as:

$$\frac{q}{q_o} = \frac{1}{(1-y^+/r_o^+)} \left\{ 1 + \left[\frac{G_t r_o}{4\rho_l V^* \delta^+}\right] \frac{dx}{dz} t^+ y^+ \right\} \qquad (4-47)$$

Equating Eqs (4-5) and (4-47) and rearranging the terms results in,

$$\frac{dt^+}{dy^+} = \frac{\{1 + \alpha' t^+ y^+\}}{\left[1-y^+/r_o^+\right] \left[\frac{1}{Pr_l} + \frac{(\tau/\tau_o)}{(du^+/dy^+)} - 1\right]} \qquad (4-48)$$

Where

$$\alpha' = \frac{G_t\, r_o}{4\rho_l V^* \delta^+} \frac{dx}{dz} \qquad (4\text{-}49)$$

The initial condition for (4-48) is given by

$$t^+ = 0 \quad \text{at } y^+ = 0$$

Eq (4-48) is non-separable, non-linear, first order, ordinary differential equation which needs to be solved numerically.

4.2.5 LOCAL HEAT TRANSFER COEFFICIENT AND NUSSELT NUMBER

By the definition of local heat transfer coefficient

$$h_z = \frac{q_o}{(t_o - t_{sat})} \qquad (4\text{-}50)$$

where

t_{sat} = saturation temperature

From the definition of t^+ at δ^+ (that is t^+_δ)

$$(t_o - t_{sat}) = \frac{t^+_\delta\, q_o}{\rho_l C_l V^*} \qquad (4\text{-}51)$$

Substituting Eq (4-51) into Eq (4-50) the local heat transfer can be written as:

$$h_z = \frac{\rho_l\, C_l\, V^*}{t^+_\delta} \qquad (4\text{-}52)$$

and Nusselt number is given by

$$Nu_z = \frac{h\, D_e}{K_l} = \frac{\rho_l\, C_l\, V^* D_e}{K_l\, t^+_\delta} \qquad (4\text{-}53)$$

or

$$Nu_z = \frac{V^* De}{\alpha_l t_\delta^+} \qquad (4\text{-}54)$$

where

α_l = thermal diffusivity of the liquid film

4.3 RESULTS AND DISCUSSION

The computational steps for determining local condensation heat transfer coefficients inside the semi-circular tube under consideration are summarized in Appendix F. To start with the computational process, the length and inside diameter of the semi-circular tube, D, the total mass velocity of condensing fluid, G_t, the local quality x, and an assumption on quality gradient, $\frac{dx}{dz}$, need to be known. With such information, steps 1 through 16 in Appendix F can be executed. δ^+ in step 18 is then determined through the iteration procedure outlined in section(4.2.3) by using the velocity profile given in step 17. Simpson's one-third rule was used for numerical integration. δ^+ was divided into 100 intervals. A difference of 0.01 lbm/hr, between the total mass flow rate obtained by the integration process of the right hand side of the equation in step 18 and the actual total mass flow rate, W_t, was selected as the convergence criterion. To avoid the iteration process another approach was developed to determine δ^+. In this approach δ^+ is expressed by:

$$\delta^+ = 0.902\ Re_l^{0.5} \qquad 0 \leq Re_l < 30 \qquad (4\text{-}55)$$

$$\delta^+ = 0.6133\ Re_l^{0.5907} \qquad 30 \leq Re_l \leq 685 \qquad (4\text{-}56)$$

$$\delta^+ = 0.121\ Re_l^{0.8284} \qquad 685 < Re_l \leq 23{,}000 \qquad (4\text{-}57)$$

where

$$Re_l = \left[\frac{G_t\ (1-x)\ D_e}{\mu_l}\right] \qquad (4\text{-}58)$$

The basis for the above equations is given in Appendix G. Using these expressions caused no significant change in the computed heat transfer coefficients determined using δ^+ obtained by the iteration procedure.

Once δ^+ is known, steps 19 and 20 can be executed. In step 21, the numerical itegration was carried out using a Runge-Kutta-Gill scheme with 100 intervals for δ^+. This step yields the dimensionless temperature drop across the liquid film, t^+_δ, which can be used in step 22 to determine the local heat transfer coefficient and Nusselt number.

A computer program was written in FORTRAN language to implement the above procedure on ITEL/AS5 digital computer. A listing of the computer program is given in Appendix H. The computation procedure begins for an initial quality of 0.99 since a value of 1.0 represents a singular point in the analysis.

All thermodynamic and transport properties of the saturated liquid and vapor of the condensing fluid were determined at inlet saturation pressure from the references [80,81]. The quality gradient was assumed to be equal to (-1/L). This amounts to assuming a constant rate of cooling.

The steps outlined in Appendix F can be used for computig the local heat transfer coefficients inside a circular tube during annular flow, with only three changes in the above procedure. The first one is to replace the equivalent diameter, D_e, by the inside diameter of the tube, D, in all the equations. The second change is to replace the expression for τ_o in step 14 by the following expression:

$$\tau_o = -\frac{r_o}{2}\left(\frac{dp}{dz}\right)_{TPF} \qquad (4\text{-}59)$$

The third change is to replace the non-dimensional film thickness, δ^+, equations for semi-circular tube, Eqs (4-55) to (4-58), by the equations for circular-tube. These equations were developed by Traviss et al. [106] and are given below:

$$\delta^+ = 0.7071\ Re_l^{0.5} \qquad 0 \leq Re_l \leq 50 \qquad (4\text{-}60)$$

$$\delta^+ = 0.4818\ Re_l^{0.585} \qquad 50 < Re_l \leq 1125 \qquad (4\text{-}61)$$

$$\delta^+ = 0.095\ Re_l^{0.812} \qquad 1125 < Re_l \qquad (4\text{-}62)$$

where

$$Re_l = \left[\frac{G_t(1-x)D}{\mu_l}\right] \qquad (4\text{-}63)$$

To test the validity of the present analysis, which is essentially an extension of the analysis of Abis [104], comparisons were made between its predictions and the experimental measurements reported by Abis [104]. Abis [104] reported the local heat transfer coefficients during conden-

sation of R-12 inside a horizontal tube. Figs (4-7) and (4-8) show such comparisons for the parameters indicated in the figures. The results show, qualitatively, that both analytically predicted values and experimental data show the same trend. Quantitatively, near the entrace region of the tube, where the quality is in the vicinity of 1.0, the analytical predictions are lower than the experimental values. Downstream from the entrance, where the lower quality flow occurs, the analysis predicts local heat transfer coefficients higher than the experimental values. This type of behaviour can be attributed to the following reasons:

1. Near the entrance of the tube the presence of interfacial waves and a thinner liquid film, with possible dry patches, give rise to higher experimental heat transfer coefficients. These effects were neglected in the present analysis.
2. The present analysis assumes that annular flow exists over the entire length of the condenser tube. At lower qualities the flow pattern is either wavy or slug flow in which the experimental heat transfer coefficients are lower than in annular flow. This explains why the analysis over-predicts the experimental data at lower qualities.
3. The friction factors used in the present analysis to calculate the frictional pressure gradients were originally developed for adiabatic, two-phase flow conditions. It was shown by Linehan et al. [97] that condensation friction factors are higher than the two-phase flow,

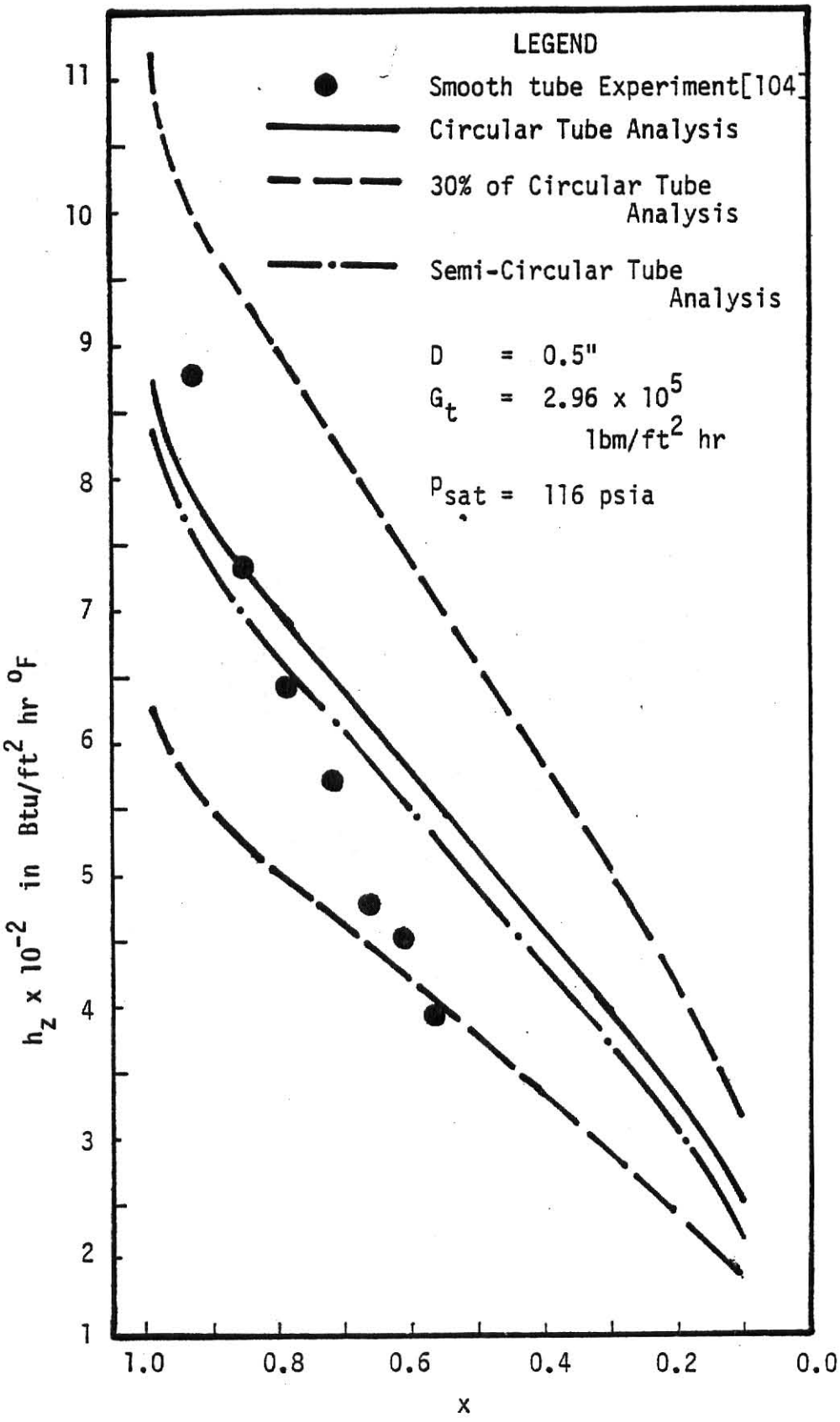

Fig (4-7) Comparison of Circular Tube Analysis with Experiment [104] and Analysis of Semi-Circular Tube for R - 12.

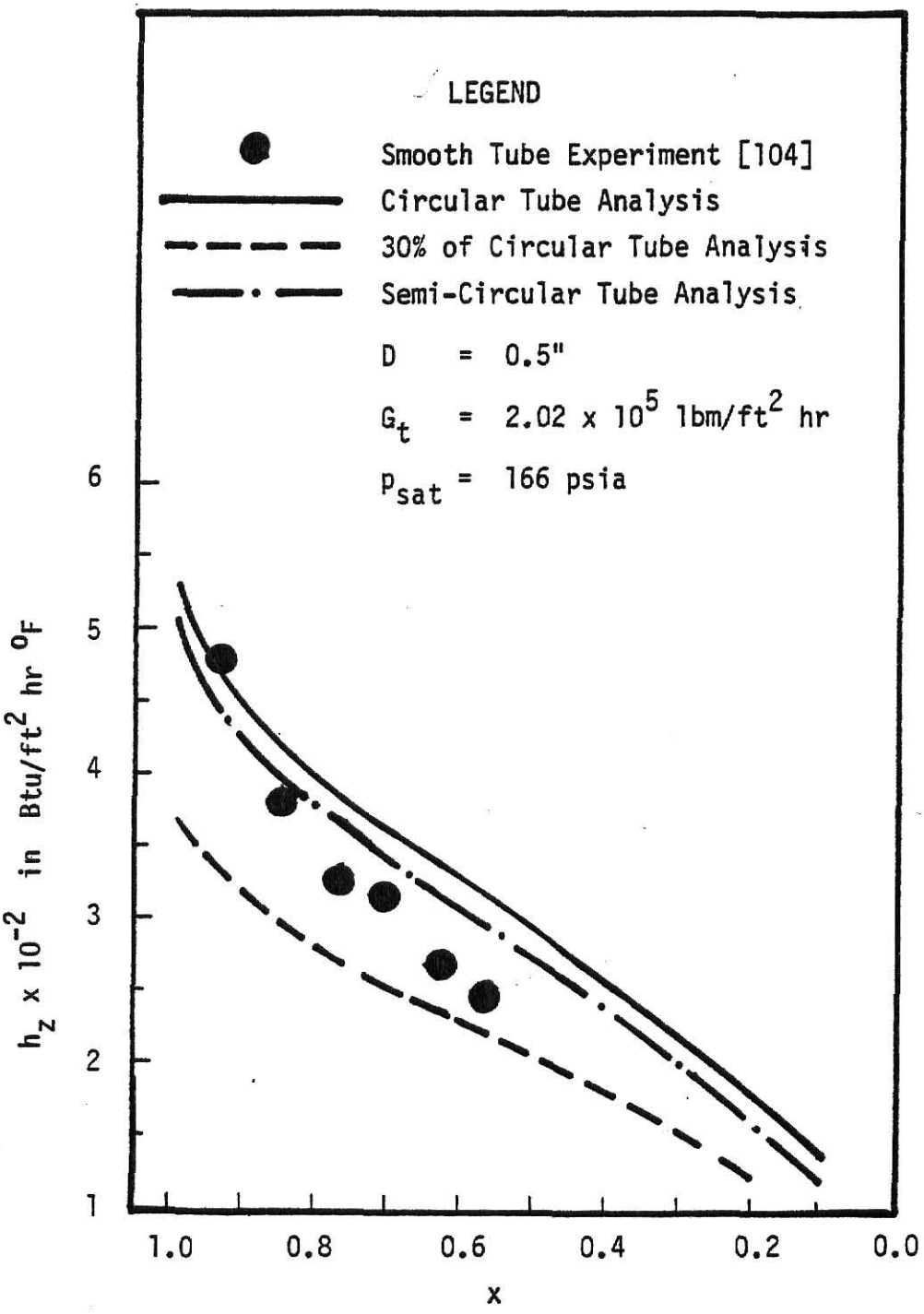

Fig (4-8) Comparison of Circular Tube Analysis with Experiment [104] and Analysis of Semi-Circular Tube for R - 12.

adiabatic values.

4. The assumption of constant quality is not true. The knowledge of true quality gradient requires the knowledge of the rate of cooling or condensing heat transfer coefficient, which is the quantity being sought from this analysis.

Despite these uncertainities in the analysis the results in Figs (4-7) and (4-8) show that the disagreement between the analysis and experiment is within ±30%.

Comparisons were also made between the predicted mean condensation heat transfer coefficients using the present analysis for smooth tube and the experimental mean values reported by Royal [59] for steam and Luu [61] for R-113. The mean heat transfer coefficients in the present analysis were determined by averaging the local values as shown below:

$$\bar{h}_{TP} = \frac{1}{(x_{in}-x_{out})} \int_{x_{out}}^{x_{in}} h_z \, dx \qquad (4\text{-}64)$$

Simpson's rule [103] was used to evaluate the integral in Eq (4-64). The results of these comparisons are shown in Fig (4-9) for steam and Fig (4-10) for R-113. In general, the predicted values are higher than the experimental measurements. The difference is within -50% for steam and within +15% and -30% for R-113. In a few instances the experimental values are higher than the predicted values for R-113. Despite the uncertainities in the analysis, outlined earlier, the tendency of the predictions to be higher than the experimental data was

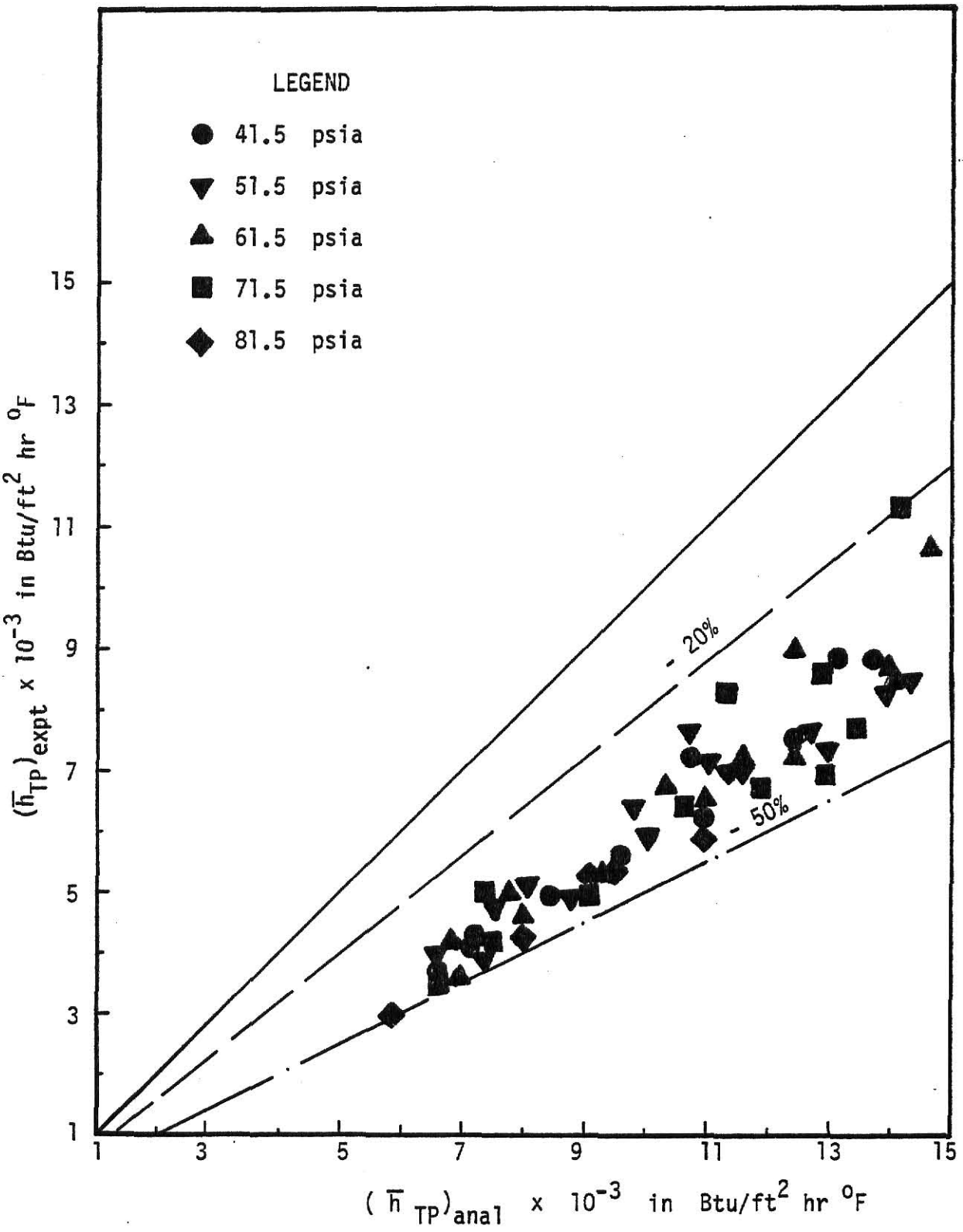

Fig (4-9) Comparison Between Analytical and Experimental [59] Mean Heat Transfer Coefficents During Condensation of Steam Inside a Smooth Tube.

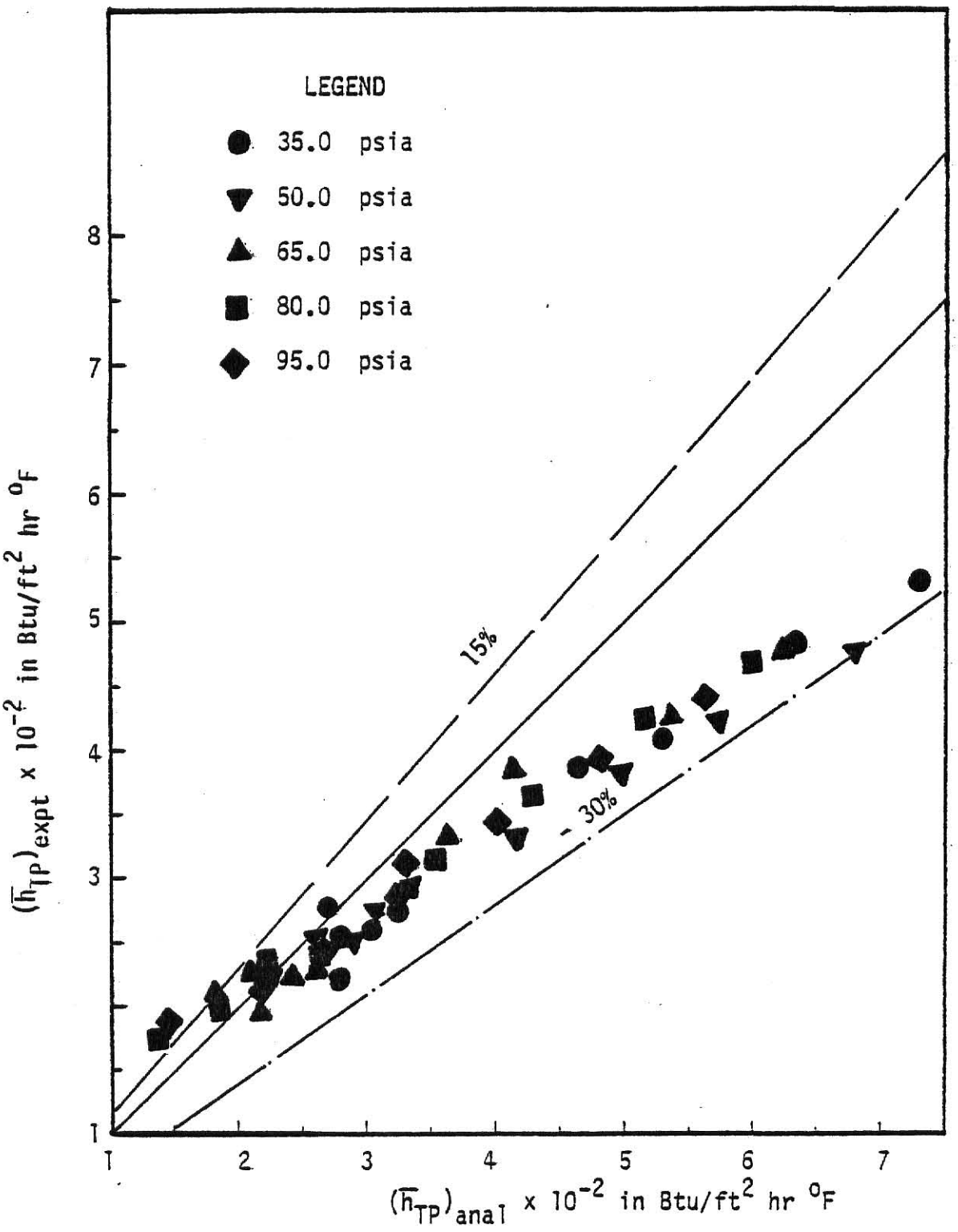

Fig (4-10) Comparison Between Analytical and Experimental [61] Mean Heat Transfer Coefficents During Condensation of R - 113 Inside a Smooth Tube.

anticipated. The reason for this is that the analysis is based on the assumption of annular flow throughout the entire length of tube. In reality annular flow occurs only in the upstream section of the tube and is followed by wavy or slug flow toward the downstream section. It is well known that the condensation heat transfer coefficients are higher in annular flow regime than in wavy or slug flow regimes.

For the sake of comparison, local heat transfer coefficients during condensation inside a semi-circular tube were calculated using the present analysis for the same flow conditions as in Figs (4-7) and (4-8). Similar comparisons were made for steam and R-113. The results are shown in Figs (4-11) and (4-12). The results of these comparisons indicate that local values for semi-circular tubes are lower than circular tubes. This can be explained in the following way:

According to Eq (4-52) the local heat transfer coefficient, h_z, is directly proportional to the local shear velocity, V^*, and inversely proportional to the local non-dimensional temperature drop across the liquid film, t^+_δ. The local shear velocity, V^*, is defined in terms of the local wall shear stress, which is dependent upon the local frictional pressure drop. For the same flow conditions the local frictional pressure gradient for semi-circular tube is higher than for circular tube, according to Eq (3-33). However, it can be shown that the shear velocity, V^*, is directly proportional to the friction factor, f_o, evaluated at two-phase Reynolds number, Re_{TP}. Since f_o is inversely proportional to Re_{TP} and for a given set of

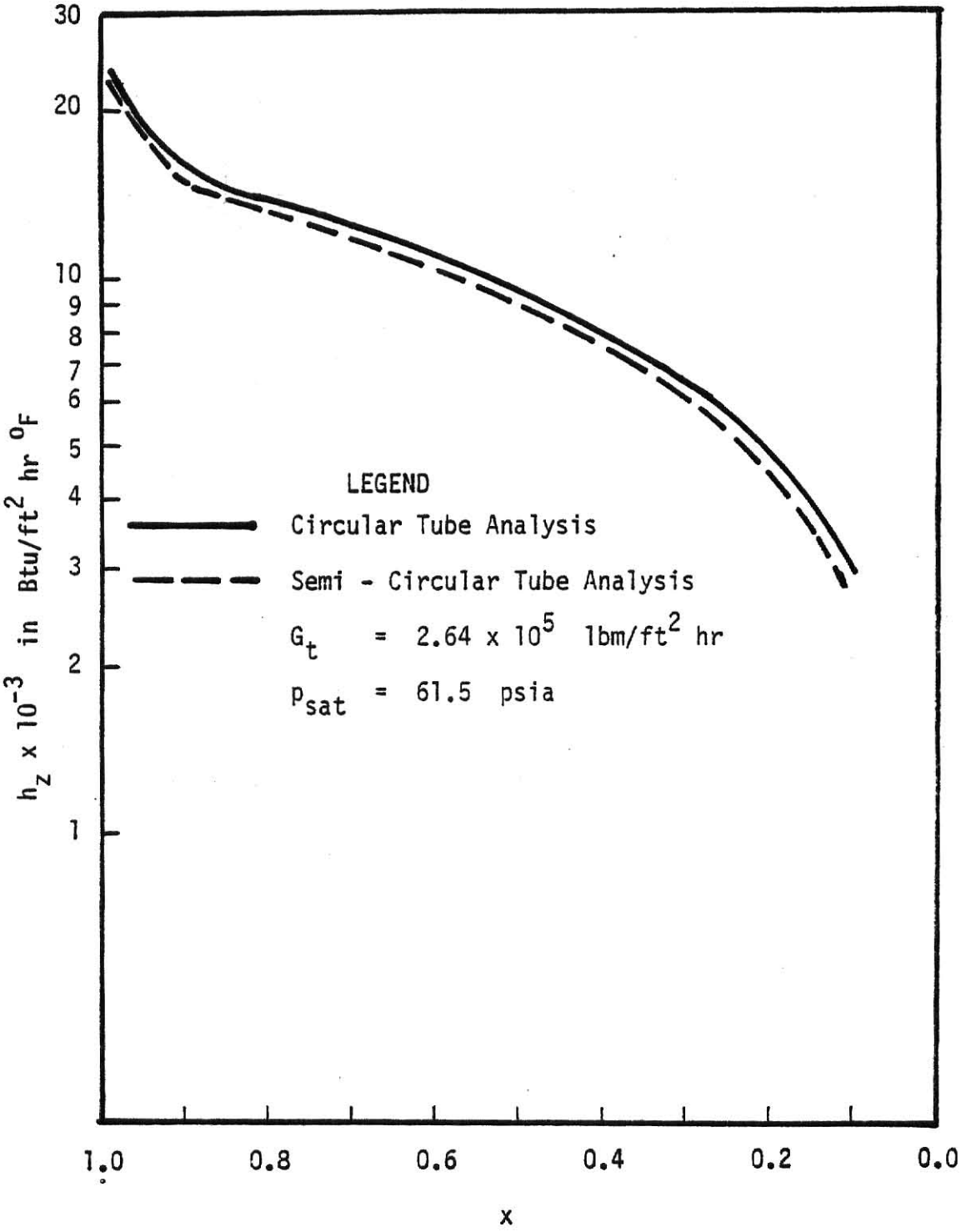

Fig (4-11) Comparison Between the Predictions of Local Heat Transfer Coefficents for Circular and Semi - Circular Tubes During Condensation of Steam.

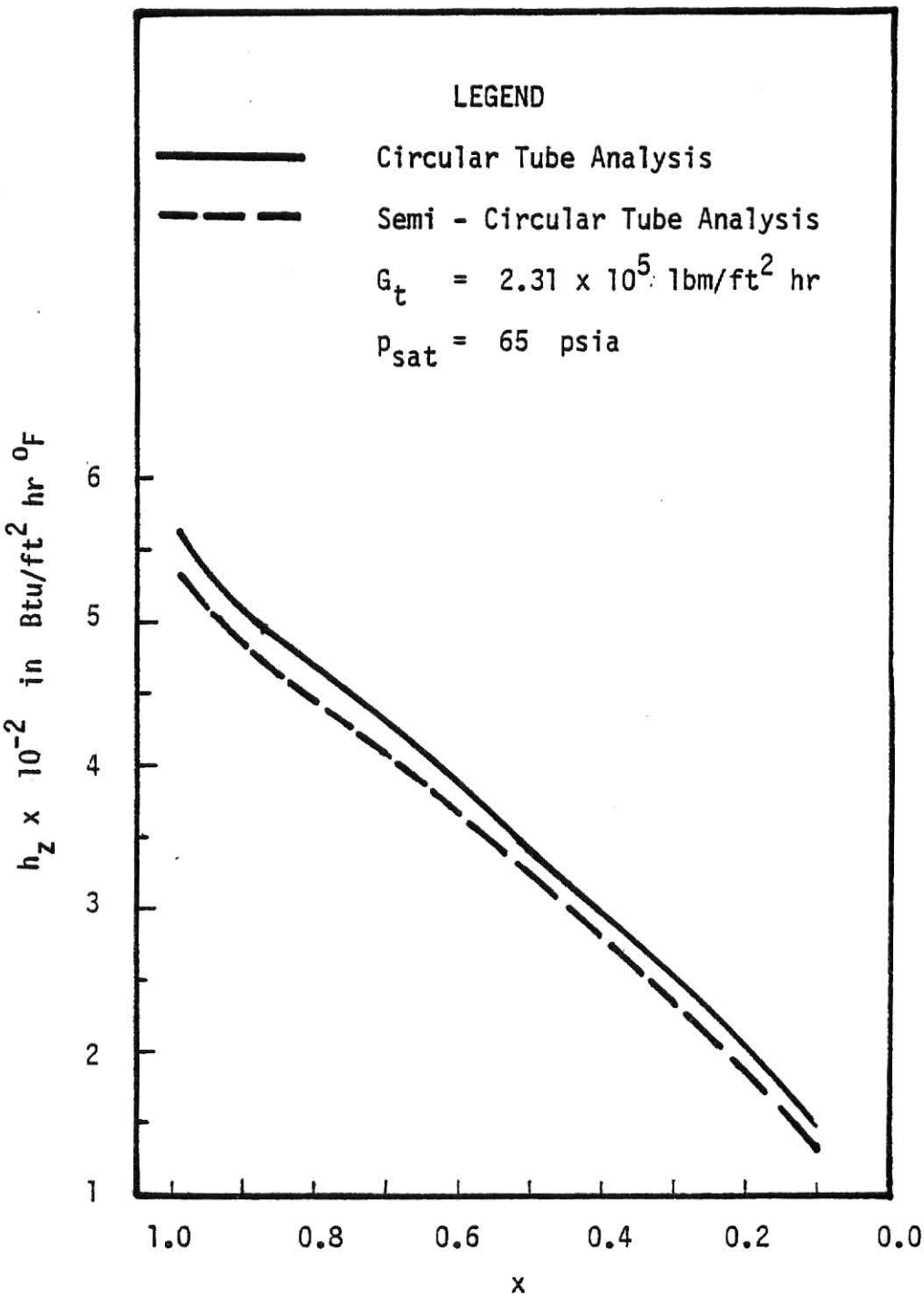

Fig (4-12) Comparison Between the Predictions of Local Heat Transfer Coefficents for Circular and Semi-Circular Tubes During Condensation of R - 113.

flow conditions Re_{TP} is higher for semi-circular tube than for circular tube, the shear velocity, V*, for semi-circular tube is lower than for circular tube. According to numerical computations the dimensionless temperature drop is nearly constant for circular and semi-circular tubes under same flow conditions. The combined effects of V* and t_δ^+ on h_z is, therefore, to reduce its value over circular tube value.

No experimental data exist, at the present time, for condensation heat transfer coefficients, local or mean, inside semi-circular tubes. The only data cited in the literature were for condensation inside tubes with twisted tape inserts of finite twist ratio [59,61]. As the twist ratio increases, the tape becomes flatter and for infinite twist ratio of the tape the flow inside a tube with tape is similar to the flow inside a semi-circular tube. The swirl induced and the secondary effects due to the presence of a twisted tape insert of finite twist ratio in the tube increase the heat transfer coefficients, local and mean, over the semi-circular tube values. Therefore, it was originally assumed that the present analysis for semi-circular tube yields a lower bound for heat transfer coefficients. This means that all the experimental heat transfer data with twisted tapes of finite twist ratio are higher than the predictions of semi-circular tube analysis for the same flow conditions.

Figs (4-13) and (4-14) show comparisons between the mean heat transfer coefficients during condensation of R-113 inside a horizontal tube with twisted tape inserts, as reported by

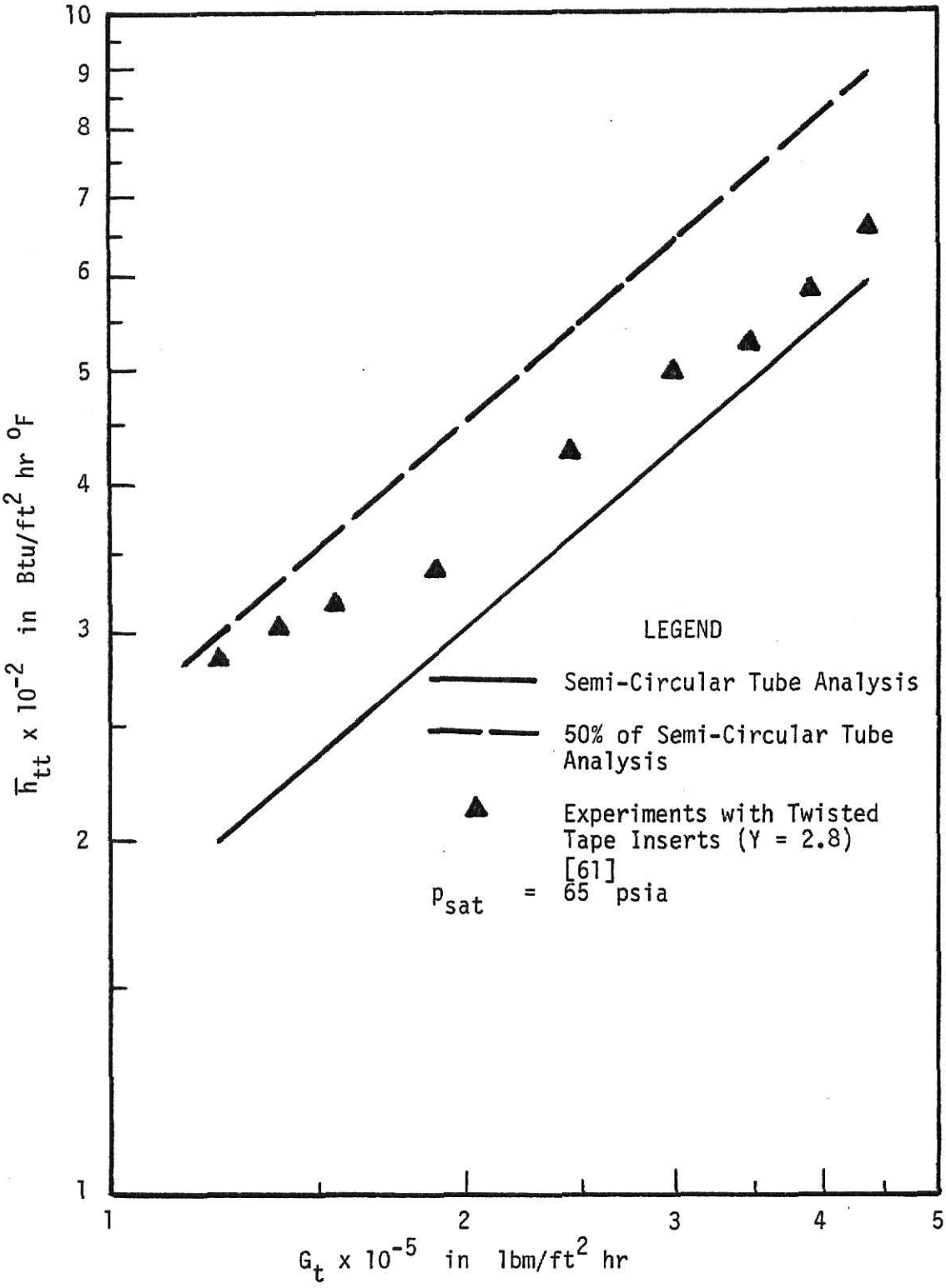

Fig (4-13) Comparison Between the Predicted Mean Heat Transfer Coefficents of Semi-Circular Tube Analysis and Experiments of Twisted Tape Inserts During Condensation of R - 113 at p_{sat} = 65 psia [61].

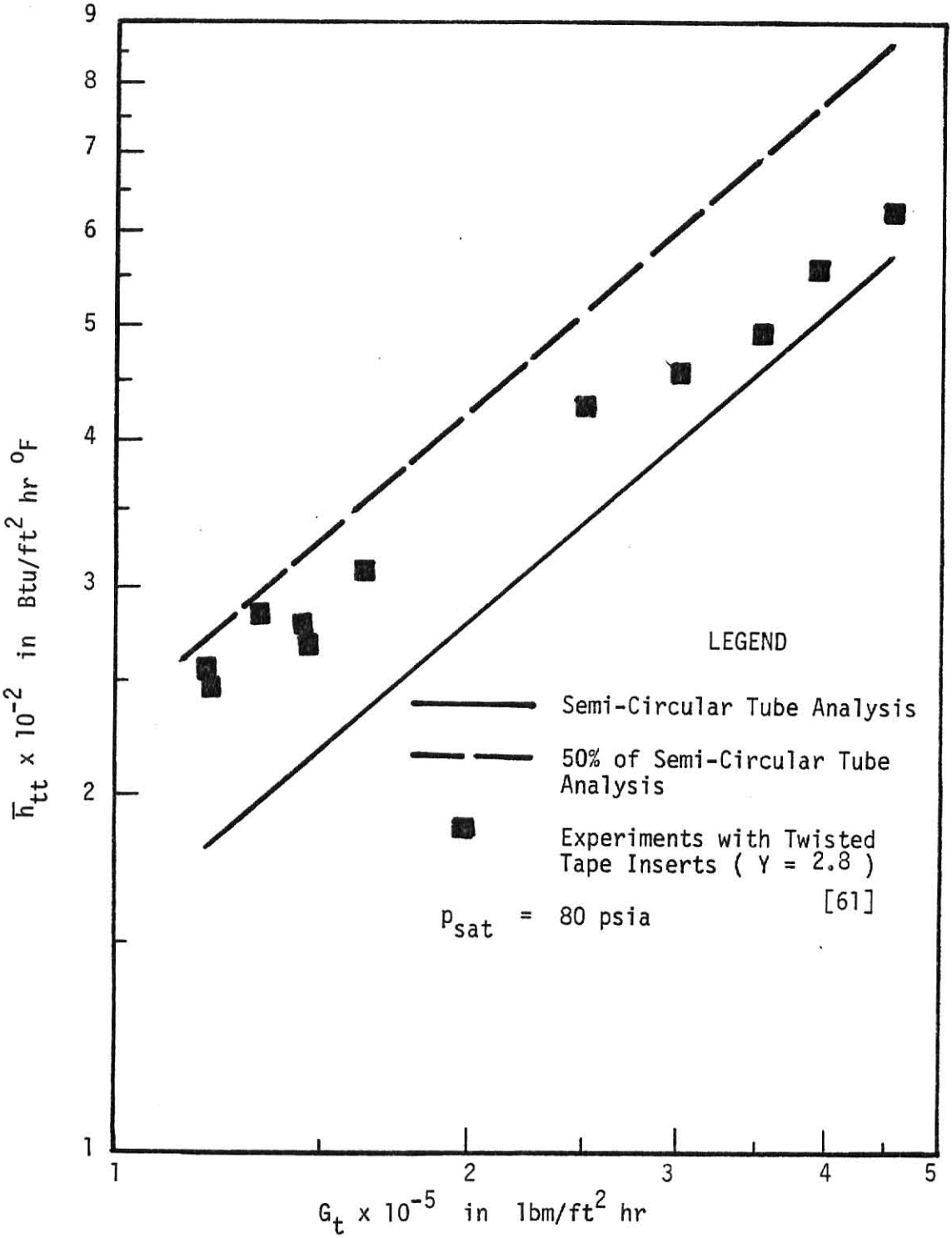

Fig (4-14) Comparison Between the Predicted Mean Heat Transfer Coefficents of Semi-Circular Tube Analysis and Experiments of Twisted Tape Inserts During Condensation of R - 113 at p_{sat} = 80 psia [61].

Luu [61], and the analytical predictions of the semi-circular tube of present analysis. The predictions are lower than the experimental data as it was originally anticipated. It is to be recalled that an annular flow model was assumed for the entire length of the semi-circular tube analysis. In reality annular flow occurs only near the upstream section of the tube and it eventually changes to wavy or slug flow towards the exit section. The overall effect should result in predicted values for the mean heat transfer coefficients lower than the predictions shown in Figs (4-13) and (4-14). Inspite of the fact that the predictions in these two comparisons are lower than the experimental measurements, the assumption that the present predictions represent a lower bound for experimental data is not totally realistic. Unless the analysis takes into account the changes in flow pattern it cannot be considered to represent the lower bound for the experimental measurements.

Figs (4-15) and (4-16) show comparisons between the mean heat transfer coefficients during condensation of steam inside horizontal tubes with twisted tape inserts reported by Royal [59] and the analytical predictions of the semi-circular tube of the present analysis. The results show that the predictions are higher than the measurements. This trend is opposite to the trend exhibited by the comparisons for R-113, Figs (4-13) and (4-14), where the predictions are lower than the experimental data. The only explanation one can present for such inconsistency in the analytical results is the fact that predictions in Fig (4-15) and (4-16) do not necessarily represent a lower

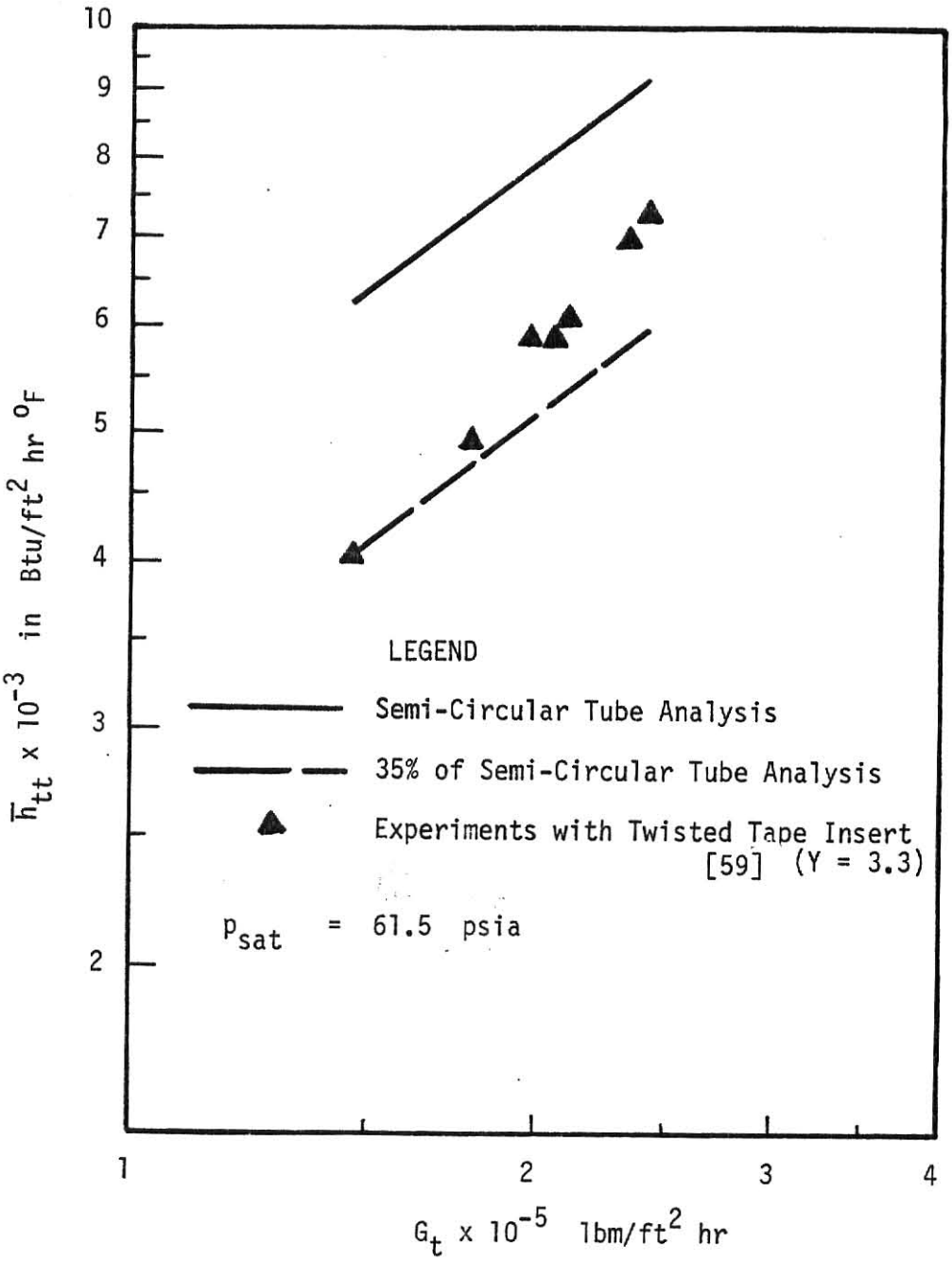

Fig (4-15) Comparison Between the Predicted Mean Heat Transfer Coefficents of Semi-Circular Tube Analysis and the Experiments with Twisted Tape Inserts During Condensation of Steam at p_{sat} = 61.5 psia.

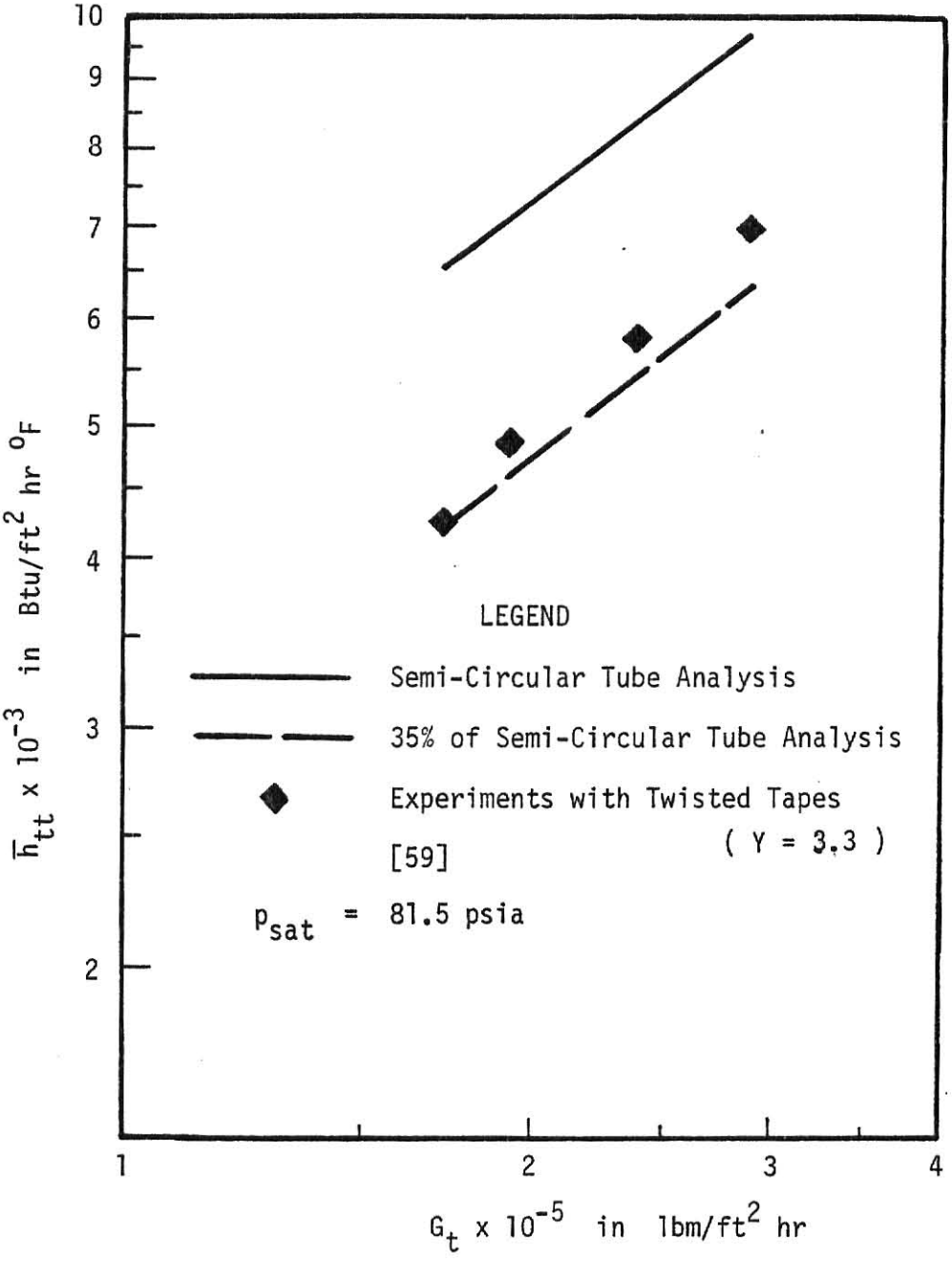

Fig (4-16) Comparison Between the Predicted Mean Heat Transfer Coefficents of Semi-Circular Tube Analysis and Experiments with Twisted Tape Inserts During Condensation of Steam at p_{sat} = 81.5 psia [59].

bound for the experimental data as discussed above.

4.4 SUMMARY

The analysis developed in the present study for annular flow condensation inside horizontal semi-circular tubes was used to predict local and mean heat transfer coefficients for R-12, R-113 and steam. The analytical predictions for circular tube for local heat transfer coefficients were within ±30% for R-12 inspite of the uncertainities in flow regime assumption and the correlations used in calculating local pressure gradients. The circular tube analysis, in general, over-predicted the mean heat transfer coefficients during condensation of R-113 by 30% and by 50% for steam. This was in accordance with what was expected. However, in a few instances, at low mass velocities, the analysis under-predicted heat transfer coefficients by 15% for R-113.

The analytical, local heat transfer coefficients for the semi-circular tube were lower than the circular tube values due to a lower shear velocity for semi-circular tube, under the same flow conditions. The mean heat transfer coefficients from semi-circular tube analysis were lower than the experimental values of R-113 with tapes of finite twist ratios. A reversed behaviour was observed for steam condensation.

4.5 CONCLUSIONS

The analysis developed in this chapter for condensation inside horizontal semi-circular tubes represents the first attempt ever made to tackle this problem. This problem

represents the condensation inside a circular tube with a twisted tape insert having an infinite twist ratio. The analysis was based on assumptions that were not verified experimentally. For example, the two-phase pressure drop correlations for adiabatic two-phase flow were used for calculating the local two-phase pressure gradients inside the semi-circular tube by replacing the diameter by the equivalent diameter. Also, void fraction correlations used for circular tubes were assumed to apply to semi-circular tubes. In addition annular flow pattern was assumed to exist along the entire length of the semi-circular tube. Despite these uncertainities, the predictions of the analysis for condensation of R-113 were lower than the experimental measurements as was originally anticipated. However, this trend was reversed for steam results. Reasonable explanations were given for such behaviour. Until the reliability of the correlations used for pressure gradients and void fractions is established, no claim can be made about reliability of the analysis. When this is accomplished, the effect of the twist ratio can be incorporated as a modifier to the predicted heat transfer coefficients from the analysis of the problem of condensation inside a semi-circular tube. Such modifier should reflect the effect of secondary flows which are produced by the swirl flow associated with the twisted tape.

CHAPTER V

RECOMMENDATIONS FOR FUTURE STUDY

In the present study an attempt was made to analyse the problem of condensation inside a semi-circular tube assuming an annular flow model to exist along the entire length of tube. This case approximates the case of condensation inside a circular tube with a twisted tape insert having an infinite twist ratio or a tube with a flat tape insert of width equal to the inside diameter of the tube. The approach followed in the analysis was similar to the approach adopted in earlier studies in the analysis of annular flow condensation inside circular tubes by Azer et al. [70]. In the present analysis, the frictional pressure gradient and void fraction correlations, originally developed for circular tube analysis, were used also in the semi-circular tube analysis by replacing the tube diameter, whenever it occurred in these correlations, by the equivalent diameter of the semi-circular tube. Several uncertainities about this approach were identified and outlined in Chapter IV. Before the validity of this approach can be evaluated certain problems related to in-tube condensation need to be investigated. The following recommendations are made for future studies.

1. None of the presently available frictional pressure gradient correlations are very accurate in their predictions for condensation inside smooth tubes. They were originally developed for adiabatic, two-phase, two-component flow systems where the flow is fully developed.

Even then specific correlations apply to specific flow patterns and not to others. Due to the fact that during condensation the flow pattern changes in the direction of flow from the inertia controlled flow (annular) to gravity controlled (wavy or slug) flow, no single frictional pressure gradient correlation can be expected to successfully correlate the condensation data along the entire condensation tube. Experimental pressure drop measurements need to be taken during condensation under different flow patterns and proper correlations need to be developed for each pattern. Such correlations need to be tested for different fluids, tube diameters before their validity can be established.

2. Additional studies are needed to establish the criteria for transition between the different flow patterns during condensation inside horizontal tubes. During the past few years flow pattern maps were developed for this purpose. Their reliability in predicting flow pattern changes have not yet been established. When this is accomplished, it is possible to predict the changes that occur in the flow patterns during condensation, for a given fluid with specified flow parameters. It is then by dividing the tube length into subsections where a specific flow pattern is dominant, and by applying the proper frictional pressure gradient correlation to that subsection, it will be possible to predict the pressure drop.
3. Void fractions correlations are needed to calculate the

pressure gradient due to momentum change, in the analysis of condensation inside tubes. Most of the presently used correlations are empirical in nature and their applicability to condensation has not been established. Different void fractions for different flow patterns are needed.

4. No realistic analysis of the problem of condensation inside tubes with twisted tape inserts can be done without the understanding of basic flow characteristics of the swirl flow produced by the tape. If such an analysis is to be successful the flow pattern need to be observed, understood, before the governing equations of the flow can be formulated. Several questions need to be answered. For example: What is a flow pattern? Can the swirl flow be treated as homogeneous flow? How can a void fraction be defined in such a case?

Until such questions are answered, it appears that the approach followed in Chapter 3 in the development of pressure drop and heat transfer correlations will be one to pursue until the desired correlations are found.

NOMENCLATURE

NOTE: Any definition, for a symbol, given in the text of the thesis over-rides the definition given in this section.

Symbol	Definition
A	Flow cross-sectional area
A_r, A_1	Areas as defined in Eqs (4-12) and (4-13)
a	Flow acceleration
a'	Thickness of tube wall
a_o, a_1	Constants in Eq (3-61)
Bo	Boiling number, Eq (3-5b)
C	Specific heat, or, A constant
C_1, C_2, c_1, c_2	Constants in Eq (3-23)
Co	Convection number, Eq (3-5c)
D	Inside diameter of the tube
D_e	Equivalent diameter
$(\frac{dp}{dz})$	Pressure gradient
F	Force
F_2	Variable defined by Eqs (A-27) to (A-29) and (A-47)
F_f	Wall shear correction factor, Eq (3-53)
F_t	Tangential velocity correction factor, Eq (3-50)
F_{tt}	Tape fin effect correction factor, Eq (3-52)
f	Friction factor
Fr	Froude number

Symbol	Definition
G	Mass velocity
g	Acceleration due to gravity 32.2 ft/sec^2
g_c	Gravitional constant 4.17×10^8 lb_m ft/lb_f hr^2
Ga	Galileo number, Eq (A-9)
h	Heat transfer coefficient
h_{fg}	Latent heat of vaporisation,or condensation
K	Thermal conductivity ,or, Flow parameter, Eq (C-4)
L	Condenser tube length
ℓ	Characteristic length
M	Parameter defined in Eq (A-30)
$\dot{M}$	Momentum flux
m	A constant
n	A constant
Nu	Nusset number
p	Pressure ,or, A constant
p_r	Reduced Pressure (= system pressure p/ critical pressure of condensing fluid)
Pr	Prandtl number
Q	Volumetric flow rate
q	Heat Flux ,or, A constant
R	Ratio of experimental mean heat transfer coefficient with twisted tape insert to the predicted mean heat transfer coefficient for smooth tube at the same flow

Symbol	Definition
	conditions, Eq (3-60)
r	Radius from tube axis ,or, A constant
S	Wetted perimeter
s	A constant
t	Temperature
u	Velocity
V	Velocity
W	Mass flow rate
X	Lockhart-Martinelli parameter
x	quality (= ratio of mass of vapor to the total mass)
Y	Twist ratio defined as the ratio of the twisted tape pitch per 180° rotation of tape helix to the inside diameter of the tube
y	Radial distance from the wall
Z	Parameter defined in Eqs (3-8) and (C-5)
z	Axial co-ordinate
Greek Symbols	
α	Ratio of two-phase friction factor to the single phase friction factor at two-phase Reynolds number, Eq (3-34) ,or, Thermal diffusivity
α'	Parameter defined by Eq (4-49)
β	Ratio of two-phase density to no-slip density ,or, Ratio of velocity of condensing particles entering the liquid phase to the mean liquid film velocity, Eq (4-21) ,or, A constant in Eqs (A-6) and (E-7)
γ	A constant in Eq (C-13)

Symbol	Definition
δ	Thickness of liquid film (if there is no subscript) ,or, Thickness in general (if there is subscript)
ε	Turbulent eddy diffusivity
ζ	Parameter defined in Eq (3-36)
η	Efficiency of tape as a fin
θ	Inclination of tube axis to horizontal
λ	Ratio of liquid volumetric flow rate to the total volumetric flow rate
μ	Dynamic viscosity
ν	Kinematic viscosity
ρ	Density
τ	Shear stress
ϕ	Ratio of local two-phase heat transfer coefficient to superficial single phase liquid heat transfer coefficient ,or, Peripheral angle measured from the top of the tube.
ϕ_V	Lockhart-Martinelli parameter

Subscripts

a	Axial
ad	Adiabatic
anal	Analytical
c	condensation
cal	predicted through correlation
e	Equivalent

Symbol	Definition
expt	Experimental
f	Frictional
H	Energy
i	Interfacial
in	Inlet to the tube
L	Liquid alone flowing at total mass flow rate
l	Liquid ,or, Liquid phase alone flowing in the tube
$\dot{M}$, M	Momentum
m	Mean ,or, Two-phase mixture
NS	No-slip
o	Inside surface of the tube wall ,or, Single phase
out	exit from the tube
sat	Saturation condition
t	Total ,or, Tangential
TP	Two-phase ,or, Smooth tube
TPF	Two-phase frictional
tt	Twisted tape ,or, Turbulent-turbulent
V	Vapor alone flowing at total mass flow rate
v	Vapor ,or, Vapor phase alone flowing in tube
z	Local ,or, Axial

Symbol	Definition
δ	At liquid-vapor interface ,or, At a distance from wall
ϕ	Peripheral
Superscripts	
-	Mean
+	Non-dimensional quantity

BIBLIOGRAPHY

1. Gouse Jr., S.W.,
"An Index to the Two-Phase Gas-Liquid Flow Literature",
MIT Rept. No. 9, MIT Press, Cambridge, Massachusetts (1966).

2. Bergles, A.E.,
"Survey and Evaluation of Techniques to Augment Convective Heat and Mass Transfer" in "Progress in Heat and Mass Transfer" Eds. U. Grigull and E. Hahne, 1 ed., 1, pp. 331-424, Pergamon Press, N.Y. (1969).

3. Bergles, A.E.,
"Techniques to Augment Heat Transfer" in "Handbook of Heat Transfer", Eds. W.M. Rohsenow and J.P. Hartnett 1 ed., Sec. 10, Mc Graw Hill Co., N.Y. (1973).

4. Bergles, A.E.,
"Recent Developments in Convective Heat Transfer Augmentation", App.Mech.Reviews, 26 (6), pp. 675-682 (1973).

5. Bergles, A.E., R.L. Webb, G.H. Junkhan and M.K. Jensen,
"Bibliography on Augmentation of Convective Heat and Mass Transfer", HTL-19, ISU-ERI-AMES-79206, Engg. Research Inst., Iowa State Univ., Ames, Iowa (1979).

6. Larson, R.L., G.W. Quaint and W.L. Bryan,
"Effects of Turbulence Promoters in Refrigerant Evaporator Coils", J. of ASRE, Refrigerating Engg., pp. 1193-1195 (1949).

7. Goldman, K.,
"Improved Heat Transfer by Application of Centrifugal Forces", NDA-2-79 (1958).

8. Oppenheimer, E.,
"The Effect of Spinning Flow on Boiling Burnout in Tubes", NDA-80-1 (1957).

9. Gambill, W.R. and N.D. Greene,
"A Study of Burnout Heat Fluxes Associated with Forced Convection, Sub-Cooled and Bulk Nucleate Boiling of Water in Source Vortex Flow", ORNL Central Files, CF-57-10-118 (1957).

10. Gambill, W.R., and N.D. Greene,
"Boiling Burnout with Water in Vortex Flow", Chem. Engg. Prog., 54 (10), pp. 68-76 (1958).

11. Hoffman, H.W., W.R. Gambill, J.J. Keyes Jr., and G.J. Kidd Jr.,
"Fundamental Studies in Heat Transfer and Fluid Mechanics", ORNL Central Files, CF-60-10-6 (1960).

12. Gambill, W.R., R.D. Bundy and R.W. Wansbrough, "Heat Transfer, Burnout and Pressure Drop for Water in Swirl Flow Through Tubes with Internal Twisted Tapes", Chem. Engg. Prog. Symp. Series, 57 (32), pp. 127-137 (1961).

13. Gambill, W.R. and R.D. Bundy, "An Evaluation of Present Status of Swirl Flow Heat Transfer", ORNL Central Files, CF-61-4-61 (1961); Also available as ASME paper No. 62-HT-42 (1962).

14. Hoffman, H.W., "Studies in Two-Phase Flow and Boiling Heat Transfer at ORNL", Proc. of the Meeting of the Working Group Heat Transfer. Sponsored by EURATOM-US Joint R and D Board, Brussels, EUR-352.e (Oct. 19-21, 1962); Also in TDR-7694.

15. Poppendiek, H.F., N.D. Greene, F.R. Macdonald, H.R. Wright, C.M. Sabin and A.S. Thompson, "High Acceleration Heat Transfer for Auxiliary Space Nuclear Power Systems", Annual Tech. Rept., Geoscience Ltd., TID-18028 (1962).

16. Gambill, W.R., and R.D. Bundy, "High Heat Flux Heat Transfer Characteristics of Pure Ethylene Glycol in Axial and Swirl Flow", A I Ch E J. 9 (1), pp. 55-59 (1963).

17. Kutateladze, S.S., "Heat Transfer in Condensation and Boiling", 2 ed. Ch.10, Moscow-Leningrad (1952); Also in AEC-Translations-3770 (Aug. 1959). As cited in reference [16].

18. Gambill, W.R., "Sub-Cooled Boiling and Burnout with Electrically Heated Twisted Tapes and Zero Wall Flux", Tran ASME, J. of Heat Transfer, Series C, 87 (3), pp. 342-348 (1965); Also in ORNL-TM-894 (1964).

19. Poppendiek, H.F., and W.R. Gambill, "Helical, Forced Flow Heat Transfer and Fluid Dynamics in Single and Two-Phase Systems", Proc. Intl. Conf. on Peaceful Uses of Atomic Energy, UNO, N.Y., 8, pp. 274-282 (1965).

20. Foure, C., "Improvement of Heat Transfer in Boiling Water Reactors", SNECMA Quarterly Rept. No. 1, France, EURAEC-33 (1960).

21. Foure, C., "Improvement of Heat Transfer in Boiling Water Reactors", SNECMA Quarterly Rept. No.2, France, EURAEC-34 (1960).

22. Foure, C., A. Beghin and B. Bernard,
"Study of Two-Phase Flows (Air-Water) with Vortex and Annular Flows", SNECMA Special Rept. No.3, France, EURAEC-144 (1961).

23. Foure, C.,
"Influence of Centrifugal Twisted Tapes on Freon Burnout Flux-Review of Tests", SNECMA Special Rept. No. 4, France, EURAEC-145 (1961).

24. Foure, C., A. Rousel and G. Souriox,
"Influence on Burnout Flux of Vortices Induced in Boiling Water at Atomspheric Pressure", SNECMA Special Rept.No.5, France, EURAEC-146 (1961).

25. Moussez, C.,
"Synthesis of Thermal Tests", SNECMA Special Rept.No.6, France, EURAEC-147 (1961).

26. Anonymus,
"Swirl Flow Boiling Water : Test Loop for Studying Swirl Flow in Boiling Water at a Pressure of 70 bars", SNECMA Special Rept. No.15, France,EURAEC-899 (1963).

27. Ibid., Special Report No. 16, EURAEC-900 (1963).

28. Anonymus
"Swirl Flow in Boiling Water : Synthesis of Tests Relative to Two-Phase Adiabatic Vertical Flows (Air-Water) with and without Twisted Tapes", SNECMA Special Rept.No. 14, France, EURAEC-898 (1963).

29. Lottes, P.A., R.P. Anderson, B.M. Hoglund, J.F. Marchaterre, M. Petrick, G.F. Popper and R.J. Weatherhead,
"Boiling Water Technology Status of Art Report. Volume 1: Heat Transfer and Hydraulics", ANL Rept.No. 6561.

30. Mondin, M.,
"L'Ebullition et le Transfert de Chaleur", Rappt Ge'ne'ral "Bulles et Gouttes", Compte Rendu des Te'me's Journ des de l' Hydraulique, Paris (1962).

31. Moussez, C.,
"Adaptation of Vortex Flow to a Biphase Liquid-Gas Mixture", Proc. of the Meeting of Working Group Heat Transfer. Sponsored by EURATOM-US Joint R and D Board, Brussels, pp. 89-107 (Oct. 19-21, 1962) TDR-7694; Also in EUR-352 e.

32. Volterras, J. and G. Tournier,
"Influences of Critical Fluxes of Vortices Induced in Boiling Water at Low Pressure", SNECMA Rept-S12, France, EURAEC-810 (1963).

33. Foure, C., C. Moussez and D. Eidelman,
"Techniques for Vortex Type Two Phase Flow in Water Reactors", (In French), Proc. of Intl. Conf. on Peaceful Uses of Atomic Energy, UNO, N.Y., 8 pp. 255-261 (1965). English abstract is available.

34. Allen, C.F.,
"Boiling of Freon-114 in a Three Foot Straight Tube Evaporator", Oak Ridge Gaseous Diffusion Plant, K-1487 (1961); Also in ANL-6734-261.

35. Viskanta, R.,
"Critical Heat Fluxes for Water in Swirling Flow", Nuclear Sci. and Engg., 10,pp. 202-203 (1961).

36. Gido, R.G., and A. Koestel,
"The SNAP II Power Conversion System. Mercury Boiling Research", Topical Rept. No. 17, NAA-SR-6309 (1962).

37. Blatt, T.A., and R.R. Adt Jr.,
"The Effects of Twisted Tape Swirl Generators on Heat Transfer Rate and Pressure Drop of Boiling Freon 11 and Water", ASME Paper 63-WA-42 (1963).

38. Bernstein, E., J.P. Petrek and J. Meregian,
"Evaluation and Performance of Once-through, Zero Gravity Boiler with Two Phase Water", Pratt and Whitney Aircraft Co., PWAC-428 (1964).

39. Moeck, E., G.A. Wikhammer, I.P.L. Macdonald and J.G. Collier,
"Two Methods of Improving the Dryout Heat Flux for High Pressure Steam-Water Flow", Atomic Energy of Canada Ltd., Ontario, Canada, AECL-2109 (1964).

40. Pai, R.H. and D. Pasint,
"Research at Foster and Wheeler Advances Once-through Boiler Design", Electric Light and Power, 43 (1), pp.66-70 (1965).

41. Hassida, A., G.C. Manzoni and R. Ravetta,
"Heat Transfer Crisis with Steam-Water Mixtures : An Experimental Study on the Critical Power with Local Swirl Promoters in Round Tubes", Energia Nucleare, 13 (11), pp.589-640 (1966).

42. Herbert, H.S. and U.J. Sterns,
"An Experimental Investigation of Heat Transfer to Water in Film Flow : Part II. Boiling Runs with and without Induced Swirl", Canadian J. of Chem. Engg, 46, pp. 408-412 (1968).

43. Rousel, A. and X. Rouvillois,
"Twisted Tapes for Increased Power Density", Nuclear Engg., 13 (1), pp. 43-45 (1968).

44. Bergles, A.E., W.D. Fuller and S.J. Hynek, "Dispersed Flow Film Boiling of Nitrogen with Swirl Flow", Intl. J. of Heat and Mass Transfer, 14, pp. 1343-1354 (1971).

45. Hunsbedt, A., "Sodium Heated Steam Generator Model Tests at SGTR. Volume 2 : Thermal-Hydraulic Performance Data and Analysis", GEAP-10580-2 (1972).

46. Hunsbedt, A., and J.M. Roberts, "Thermal-Hydraulic Performance of a 2 MW_t Sodium-Heated, Forced Recirculation Steam Generator Model", Trans ASME, J. of Engg. for Power, Series A, 96 (1), pp. 66-76 (1974).

47. Lopina, R.F., and Bergles, A.E., "Sub-Cooled Boiling of Water in Tape Generated Swirl Flow", Trans ASME, Series C, J. of Heat Transfer, 95 (2), pp. 281-283 (1973).

48. Cumo, M., G.E. Farello, G. Ferrari and G. Palazzi, "The Influence of Twisted Tapes in Subcritical, Once-through Vapor Generators in Counter Flow", Trans ASME, J. of Heat Transfer, Series C, 96 (3), pp. 365-370 (1974).

49. Nooruddin, A.F., and P.S. Murti, "Heat Transfer to Gas-Liquid Mixtures in a Vertical Tube Fitted with Twisted Tape", Intl. J. of Heat and Mass Transfer, 10, pp. 2655-1657 (1974).

50. Vander Mast, V.C., S.M. Read and L.A. Bromley, "Boiling of Natural Sea Water in Falling Film Evaporators", Desalination, 18,pp. 71-94 (1976).

51. Ornatskiy, A.P., V.A. Chernobay, A.P. Vasil'yev and S.V. Perkov, "Critical Heat Fluxes in Annuli with Swirl", Heat Transfer-Soviet Research, 7 (2), pp. 6-9 (1975).

52. Subbotin, V.I., S.P. Kaznovskiy and A.P. Sapankevich, "An Experimental Study of Methods for Augmenting the Critical Capacity of Steam Generating Tubes", Heat Transfer - Soviet Research, 7 (5), pp. 85-95 (1975).

53. Domanskiy, I.V., and V.N. Sokolov, "Heat Transfer in Turbulent Ascending Gas-Liquid Flow in a Vertical Tube with Twisted-Tape Turbulence Promoter", Heat Transfer-Soviet Research, 8 (6), pp. 70.75 (1976).

54. Osipenko, Yu.I, "Heat and Mass Transfer in a Cylindrical Tube with Secondary Swirling of One- and Two-Phase Liquid-Gas Flows", Heat Transfer-Soviet Research, 8 (6), pp.60-64 (1976).

55. Ryabov, A.N., F.T. Kamen'schikov, V.N. Filipov, A.F. Chalykh, T. Yugay, Ye.V. Stolyarov, T.I. Blagovestova, V.M. Mandrazhitskiy and A.I. Yemel'yanov, "Boiling Crisis and Pressure Drop in Rod Bundles with Heat Transfer Enhancement Devices", Heat Transfer-Soviet Research, 9(1), pp. 112-122 (1977).

56. Drizus, M.R.M., R.K. Skema and A.A. Slanciauskas, "Boiling Crisis in Swirled Flow of Water in Pipes", Heat Transfer-Soviet Research, 10 (4), pp. 1-7 (1978).

57. Lin, S.T., "Augmentation of Two-Phase Heat Transfer with In-line Static Mixers", Ph.D. Dissertation, Dept. of Mech. Engg., Kansas State Univ., Manhattan, Kansas (1979).

58. Royal, J.H. and A.E. Bergles, "Experimental Study of the Augmentation of Horizontal In-Tube Condensation", ASHRAE Trans, 82 (Pt II), pp. 919-931 (1976).

58a. Royal, J.H., and A.E. Bergles, "Augmentation of Horizontal In-Tube Condensation by Means of Twisted Tape Inserts and Internally Finned Tubes", Trans ASME, Series C, J. of Heat Transfer, 100 (1), pp. 17-24 (1978).

59. Royal, J.H., "Augmentation of Horizontal In-Tube Condensation of Steam", Ph.D. Dissertation, Dept. of Mech. Engg., Iowa State Univ., Ames, Iowa (1975).

60. Luu, M. and A.E. Bergles, "Experimental Study of Augmentation of In-Tube Condensation of R-113",ASHRAE Trans,85(Pt II), pp.132-145 (1979).

61. Luu, M., "Augmentation of In-Tube Condensation of R-113", Ph.D. Dissertation, Dept. of Mech. Engg., Iowa State Univ., Ames, Iowa (1980).

62. Carpenter, E.F. and A.P. Colburn, "The Effect of Vapor Velocity on Condensation inside Tubes", Proc. of the General Discussion on Heat Transfer, Inst. of Mech. Engrs. and ASME, pp. 20-26 (1951).

63. Akers, W.W., H.A. Deans and O.K. Crosser, "Condensing Heat Transfer within Horizontal Tubes", Chem. Engg. Prog. Symp. Series, Heat Transfer-Chicago, 55 (29), pp. 171-176 (1959).

64. Rosson, H.F., and J.A. Meyers, "Point Values of Condensing Film Coefficients inside a Horizontal Pipe", Chem. Engg. Prog. Symp. Series, 61 (59), pp. 190-199 (1961).

65. Boyko, L.D., and G.N. Kruzhilin,
"Heat Transfer and Hydraulic Resistance During Condensation of Steam in a Horizontal Tube and Bundle of Tubes", Intl. J. of Heat and Mass Transfer, 10, pp. 361-373 (1967).

66. Soliman, M., J.R. Schuster and P.J. Berenson,
"A General Heat Transfer Correlation for Annular Flow Condensation", Trans ASME, J. of Heat Transfer, 90 (2), Series C, pp. 267-276 (1968).

67. Azer, N.Z., L.V. Abis and T.B. Swearingen,
"Local Heat Transfer Coefficients During Forced Convection Condensation Inside Horizontal Tubes", ASHRAE Trans, 77 (Pt I), pp. 182-201 (1971).

68. Bae, S., J.S. Maulbetsch and W.M. Rohsenow,
"Refrigerant Forced Convection Condensation Inside Horizontal Tubes", ASHRAE Trans, 77 (Pt II), pp. 104-116 (1971).

69. Cavallini, A., and R. Zecchin,
"High Velocity Condensation of Organic Refrigerants Inside Tubes", Proc. of the XIII Intl. Congress of Refrigeration, Intl. Institute of Refrigeration, Brussels, Belgium, 2, pp. 193-200.

70. Azer, N.Z., L.V. Abis and H.M. Soliman,
"Local Heat Transfer Coefficients During Annular Flow Condensation", ASHRAE Trans, 78 (Pt I), pp. 135-143 (1972).

71. Murthy, V.N. and P.K. Sarma,
"Condensation Heat Transfer Inside Horizontal Tubes", Canadian J. of Chem. Engg., 50, pp. 547-549 (1972).

72. Traviss, D.P., W.M. Rohsenow and A.B. Baron,
"Forced Convection Condensation Inside Tubes : A Heat Transfer Equation for Condenser Design", ASHRAE Trans, 79 (Pt I), pp. 157-165 (1972).

73. Cavallini, A., and R. Zecchin,
"A Dimensionless Correlation for Heat Transfer in Forced Convection Condensation", Fifth Intl. Heat Transfer Conf., Tokyo, Heat Transfer 1974, Japanese Soc. of Mech.Engrs., 3, pp. 309-313 (1974).

74. Izumi, R., T. Ishimaru and W. Aoyagi,
"Heat Transfer and Pressure Drop for Refrigerant R-12 Condensing in a Horizontal Tube", Heat Transfer - Japanese Research, 5 (4), pp. 44-52 (1976).

75. Vrable, D.L., W.J. Yang and J.A. Clark,
"Condensation of Refrigerant-12 Inside Horizontal Tubes with Internal Axial Fins", Fifth Intl. Heat Transfer Conf., Tokyo, Heat Transfer 1974, Japanese Soc. of Mech. Engrs., 3, pp. 250-254 (1974).

76. Shah, M.M.,
"A General Correlation for Heat Transfer During Film Condensation Inside Pipes", Intl. J. of Heat and Mass Transfer, 22, pp. 547-556 (1979).

77. Luu, M., and A.E. Bergles,
"Enhancement of Horizontal In-Tube Condensation of R-113", Paper presented at the Session on Condensation Heat Transfer, Natl Heat Transfer Conf., ASME (1979).

78. Luu, M., and A.E. Bergles,
"Enhancement of Horizontal In-Tube Condensation of R-113", ASHRAE Trans, 86, (Pt I), (1980).

79. Shah, M.M.,
"A New Correlation for Heat Transfer During Boiling Flow Through Pipes", ASHRAE Trans, 82, (Pt II), pp. 66-86 (1976).

80. ASME - Steam Tables, ASME, N.Y. (1967).

81. ASHRAE Handbook of Fundamental, ASHRAE, N.Y. (1977).

82. Royal, J.H., and A.E. Bergles,
"Pressure Drop and Performance Evaluation of Augmented In-Tube Condensation", Sixth Intl. Heat Transfer Conf., Heat Transfer 1978, National Research Council of Canada, Toronto, 2, pp. 459-464 (1978).

83. Lockhart, R.W., and R.C. Martinelli,
"Proposed Correlation of Data for Isothermal Two-Phase, Two-Component Flow in Pipes", Chem. Engg. Prog., 45 (1), pp. 39-48 (1949).

84. Hughmark, G.A.,
"Pressure Drop in Horizontal and Vertical Co-Current Gas-Liquid Flow", I & EC Fundamentals, 2 (4), pp.315-321 (1963).

85. Dukler, A.E., M. Wick III,and R. Cleveland,
"Frictional Pressure Drop in Two-Phase Flow : Part A : A Comparison of Existing Correlations For Pressure Loss and Hold up", AIChE J. 10 (1), pp. 38-43 (1964).

86. Dukler, A.E., M. Wick III, and R. Cleveland,
"Frictional Pressure Drop in Two-Phase Flow : Part B : An Approach Through Similarity Analysis", AIChE J. 10 (1), pp. 44-51 (1964).

87. Martinelli, R.C., and D.B. Nelson,
"Prediction of Pressure Drop During Forced Circulation Boiling of Water", Trans. ASME, 70, pp.695-702 (1948).

88. Chisholm, D.,
"The Influence of Mass Velocity on Friction Pressure

Gradients During Steam Water Flow", Paper 35 presented at 1968 Thermodynamics and Fluid Mechanics Convention, Inst. of Mech. Engrs., Bristol, U.K. (1968).

89. Miropol'skii, R.I., R.I. Shneerova and L.M. Ternakova, "Heat Transfer and Hydraulic Resistance with Condensation of Superheated and Saturated Vapor Inside a Tube", Thermal Engg. 22 (4), pp. 115-118 (1975).

90. Hughmark, G.A., "Hold Up in Gas-Liquid Flow", Chem. Engg. Prog., 58 (4), pp. 62-65 (1962).

91. Baroczy, C.J., "Correlation of Liquid Fraction in Two-Phase with Applications to Liquid Metals", North American Aviation Report SR-8171, El Segundo, California (1963).

92. Thom, J.R.S., "Prediction of Pressure Drop During Forced Circulation Boiling Water", Intl. J. of Heat and Mass Transfer, 7, pp. 709-724 (1964).

93. Zivi, S.M., "Estimation of Steady-State Steam Void Fraction by Means of the Principle of Minimum Entropy Production", Trans ASME, J. of Heat Transfer, Series C, 86 (2), pp. 247-252 (1964).

94. Turner, J.M., and G.B. Wallis, "The Separate-Cylinders Model of Two-Phase Flow", Thayer School Engineering Report NYO-3114-6, Dartmouth College, Hanover, New Hampshire (1965).

95. Collier, J.G., "Convection Boiling and Condensation", 1 ed., pp.28-32, Mc-Graw Hill Co., London (1972).

96. Ginoux, J.J., (Ed), "Two-Phase Flows and Heat Transfer with Applications to Nuclear Reactor Design Problems", 1 ed., pp.19-20, A von Karman Institute Book, Hemisphere Publishing Corp., Washington (1978).

97. Linehan, J.H., M. Petrick, and M.M. El-Wakil, "On the Interface Shear Stress in Annular Flow Condensation", Trans ASME, J. of Heat Transfer, Series C, 91 (3), pp.450-453 (1969).

98. Silver, R.S., and G.B. Wallis, "A Simple Theory for Longitudinal Pressure Drop in the Presence of Lateral Condensation", Proc. Inst. of Mech. Engrs., 180 (Pt 1, No.1), pp. 36-42 (1965-66).

99. Eckert, E.R.G., and R.M. Drake, Jr., "Analysis of Heat and Mass Transfer", 1 ed., pp. 78-82, Mc-Graw Hill, N.Y. (1972).

100. Lopina, R.F., and A.E. Bergles, "Heat Transfer and Pressure Drop in Tape-Generated Swirl Flow of Single Phase Water", Trans. ASME, J. of Heat Transfer, Series C, 91 (3), pp. 434-442 (1969).

101. Lopina, R.F., and A.E. Bergles, "Heat Transfer and Pressure Drop in Tape Generated Swirl Flow", MIT, Engg. Projects Lab Rept. No. DSR 70281-47, Dept. of Mech. Engg., MIT, Cambridge, Massachusetts (1967).

102. Hong, S.W., and A.E. Bergles, "Augmentation of Laminar Flow Heat Transfer in Tubes by Means of Twisted-Tape Inserts", Tech. Rept. HTL-5, ISU-ERI-Ames-75011, Engg. Research Inst., Iowa State Univ., Ames, Iowa (1974).

103. System/360. Scientific Subroutine Package (SSP), Version III, Programmer's Manual, GH 20-02050-4, IBM Co., White Plains, N.Y.

104. Abis, L.V., "Forced Convection Condensation Inside Horizontal Tubes", Ph.D. Dissertation, Dept. of Mech. Engg., Kansas State Univ., Manhattan, Kansas (1969).

105. Bae, S., J. Maulbetsch, and W.M. Rohsenow, "Refrigerant Forced Convection Condensation Inside Horizontal Tubes", Rept. No. DSR-79760-64, Engg. Projects Lab, Dept. of Mech. Engg., MIT, Cambridge, Massachusetts (Nov. 1, 1969).

106. Traviss, D.P., A.B. Baron, and W.M. Rohsenow, "Forced Convection Condensation Inside Tubes", Rept. No. DSR-72591-74, Engg. Projects Lab, Dept. of Mech Engg., MIT, Cambridge, Massachusetts (July 1, 1971).

107. Soliman, H.M., "Analytical and Experimental Studies of Flow Patterns During Condensation Inside Horizontal Tubes", Ph.D. Dissertation, Dept. of Mech. Engg., Kansas State Univ., Manhattan, Kansas (1974).

108. Butterworth, D., "A Comparison of Some Void Fraction Relationship", AERE, Harwell, U.K., AERE-M 2619 (1974).

109. Bankoff, S.G., "A Variable Density Single-Fluid Model for Two-Phase Flow With Particular Reference to Steam-Water Flow", Trans. ASME, Series C, J. of Heat Transfer, 82 (4), pp. 265-270 (1960).

110. Martinelli, R.C., L.M.K. Boelter, T.H.M. Taylor, E.G. Thomsen and E.H. Morrin,
"Isothermal Pressure Drop for Two-Phase, Two-Component Flow in a Horizontal Pipe", Trans ASME, 66, pp. 139-151 (1944).

THIS BOOK CONTAINS NUMEROUS PAGES THAT WERE BOUND WITHOUT PAGE NUMBERS.

THIS IS AS RECEIVED FROM CUSTOMER.

APPENDICES

APPENDIX A

CORRELATIONS TO PREDICT HEAT TRANSFER COEFFICIENTS IN SMOOTH TUBE DURING CONDENSATION

1. Akers et al. correlation [63]:

The mean heat transfer coefficient is given by:

$$\bar{h}_{TP} = C \frac{K_l}{D} \left(\frac{G_e D}{\mu_l}\right)^n Pr_l^{1/3} \qquad \text{(A-1)}$$

where

$C = 0.0265$ and $n = 0.8$

for $\left(\frac{G_e D}{\mu_l}\right) > 5 \times 10^4$

$C = 5.03$ and $n = 0.333$

for $\left(\frac{G_e D}{\mu_l}\right) < 5 \times 10^4$

$$G_e = G_t \left\{ (1-\bar{x}) + \bar{x} \left(\frac{\rho_l}{\rho_v}\right)^{0.5} \right\} \qquad \text{(A-2)}$$

$\bar{x}$ = Arithmetic average of inlet and outlet qualities.

When Eqs (A-1) and (A-2) are applied to the entire tube, the mean quality, $\bar{x}$, used in Eq (A-2) is the arithmetic average of inlet and outlet qualities. When Eqs (A-1) and (A-2) are used to calculate local heat transfer coefficients, the tube length is divided into a number of sections and the mean quality, $\bar{x}$, in Eq (A-2) is the mean for the section in question.

All properties are to be evaluated at saturation temperature.

2. Rosson and Meyers correlation [64]:

The correlation is for local heat transfer coefficients which vary in peripheral direction. Making use of experimental data, three different equations were developed for local (peripheral) heat transfer coefficients. The equations correspond to: a. The top of the tube b. The bottom of the tube and c. The middle of the tube.

a. <u>Top of the Tube:</u> The local heat transfer coefficient is independent of amount of vapor in the pipe and is given by:

$$h_{z,\phi} = C \frac{K_l}{D} \left[\frac{D^3 \rho_l (\rho_l - \rho_v) g h_{fg}}{K_l \mu_l \Delta t} \right]^{0.25} \qquad (A-3)$$

where

h_{fg} = latent heat of vaporisation

Δt = temperature drop across the liquid film

= $(t_{sat} - t_o)$

C = constant which is a function of vapor Reynolds number

By using the experimental data C is given as:

$$C = 0.31 \, Re_v^{0.12} \qquad (A-4)$$

where

$$Re_v = \left[\frac{G_t x D}{\mu_v} \right]$$

b. <u>Bottom of the Tube:</u> Using von Karman analogy between momentum and heat transfer the local heat transfer coefficient at the bottom of the tube is given by:

$$h_{z,\phi} = \frac{\left[0.5656\ \phi_v\ Re_l^{0.5}\ K_l\right]}{\left[D\left\{1 + \frac{\ln(5Pr_l+1)}{Pr_l}\right\}\right]} \qquad (A-5)$$

where

ϕ_v = Lockhart-Martinelli parameter whose exact form depends on the type of flow of liquid and vapor [83]

$$Re_l = \frac{G_t(1-x)D}{\mu_l}$$

c. Middle of the Tube: From the experimental data it was observed that the local peripheral heat transfer coefficient decreases linearly with angle from the top to the bottom where it is constant. This linear relation may be defined by the location of the middle point, angle ϕ_M, and the slope at that point. At ϕ_M the local peripheral heat transfer coefficient is an arithmetic average of the heat transfer coefficients at the top and bottom.

Define

$$\beta = \frac{\phi_M}{\pi} \qquad (A-6)$$

β can be determined from the following equations:

$$\beta = 0.27\ Re_v^{0.1}$$

$$\text{for } \left[\frac{Re_v^{0.6}\ Re_l^{0.5}}{Ga}\right] < 6.4 \times 10^{-5} \qquad (A-7)$$

$$\beta = \frac{\left[1.74 \times 10^{-5} Ga\right]}{(Re_v\ Re_l)^{0.5}}$$

$$\text{for} \left[\frac{Re_v^{0.6}\, Re_l^{0.5}}{Ga}\right] \geq 6.4 \times 10^{-5} \qquad \text{(A-8)}$$

where the Galileo number, Ga, can be expressed as:

$$Ga = \frac{\left[D^3 \rho_l (\rho_l - \rho_v) g\right]}{\mu_l^2} \qquad \text{(A-9)}$$

The slope of the straight line, $h_{z,\phi}$ vs. ϕ, was correlated using experimental data and was given by:

$$\left(\frac{dh_{z,\phi}}{d\phi}\right) = \frac{12000}{(Re_v \Delta T)^{0.6}} \qquad \text{(A-10)}$$

where ΔT is in degrees ^{o}F.

3. Boyko and Kruzhilin correlation [65]:

The mean heat transfer coefficient during condensation inside a tube is given as:

$$\bar{h}_{TP} = 0.024 \frac{K_l}{D} Re_L^{0.8} Pr_l^{0.43} \left[\frac{(\rho/\rho_m)_{in}^{0.5} + (\rho/\rho_m)_{out}^{0.5}}{2}\right] \qquad \text{(A-11)}$$

where $Re_L = \left[\frac{G_t D}{\mu_l}\right]$

$$\rho/\rho_m = 1 + x\left(\frac{\rho_l}{\rho_v} - 1\right) \qquad \text{(A-12)}$$

When applied to the entire tube length the inlet and exit qualities are to be used in Eq (A-12). When local heat transfer coefficients are needed the entire condenser length is divided into a number of sections and the inlet and outlet qualities

used in Eq (A-12) are those of a particular section in question. All properties are evaluated at saturation temperature.

4. Soliman et al. correlation [66]:

Using the Carpenter and Colburn [62] equation Soliman et al. [66] arrived at a relation for local heat transfer coefficients through an analysis that derived equations for, friction, momentum and gravity forces in two phase annular flow. The local heat transfer equation is given by:

$$h_z = 0.036 \frac{K_l \rho_l^{0.5}}{\mu_l} Pr_l^{0.65} F_o^{0.5} \qquad (A-13)$$

where the exponent 0.5 for F_o was retained from the Carpenter and Colburn [62] equation. The exponent 0.65 for the Prandtl number and the constant 0.036 in Eq (A-13) were obtained from the experimental data during condensation of several fluids.

F_o in Eq (A-13) is given by:

$$F_o = F_{TPF} + F_M^* \pm F_g \qquad (A-14)$$

where

$$F_{TPF} = 0.0225 \frac{G_t^2}{\rho_v} Re_v^{-0.2} \left[\{ x^{1.8} + 5.7 \left(\frac{\mu_l}{\mu_v}\right)^{0.0523} (1-x)^{0.47} \right.$$

$$x^{1.33} \left(\frac{\rho_v}{\rho_l}\right)^{0.261} + 8.11 \left(\frac{\mu_l}{\mu_v}\right)^{0.105} (1-x)^{0.94}$$

$$\left. x^{0.86} \left(\frac{\rho_v}{\rho_l}\right)^{0.522} \right] \qquad (A-15)$$

Re_V = Reynolds number assuming all the mass is flowing vapor.

$$= \frac{G_t D}{\mu_v}$$

$$F_M = 0.25 \frac{G_t^2}{\rho_v} D \frac{dx}{dz} \left[2(1-x) \left(\frac{\rho_v}{\rho_l}\right)^{2/3} + \left(\frac{1}{x} + 2x - 3\right) \right.$$

$$\left. \left(\frac{\rho_v}{\rho_l}\right)^{4/3} + 2(1-x-\beta+\beta x) \left(\frac{\rho_v}{\rho_l}\right) \right] \qquad \text{(A-16)}$$

where

$$\beta = \frac{u_i}{\bar{u}_l}$$

u_i = velocity with which the condensing particles leave the vapor core

$\bar{u}_l$ = liquid film average velocity

β = 1.25 for turbulent liquid film

= 2.0 for laminar liquid film

$$F_g = 0.25 \frac{G_t^2}{Fr} \left[1 - \left\{ 1 + \left(\frac{1-x}{x}\right) \left(\frac{\rho_v}{\rho_l}\right)^{2/3} \right\}^{-1} \right] \qquad \text{(A-17)}$$

where Froude number, Fr, is defined as:

$$Fr = \frac{G_t^2}{\left[aD\rho_v(\rho_l - \bar{\rho}_v) \right]} \qquad \text{(A-18)}$$

$$a = g \sin \bar{\theta} \qquad \text{(A-19)}$$

g = acceleration due to gravity

θ = angle of inclination of the tube axis to the horizontal

In Eq (A-19) only absolute value of sin has to be

considered.

If the tube is horizontal F_g equals to zero. This correlation can predict the onset of liquid runback in the presence of an adverse gravitational field. This criterion can be obtained by equating F_o to zero. This amounts to setting wall shear stress to zero.

5. Azer et al. correlation [67,70]:

Analysing horizontal in-tube condensation for annular flow conditions and using a modified Lockhart-Martinelli parameter, ϕ_v, Azer et al. [70] arrived at an equation for local heat transfer coefficient as given below.

$$h_z = 0.153 \frac{K_l}{D} Pr_l Re_V^{0.9} \left(\frac{\mu_v}{\mu_l}\right) \left(\frac{\rho_l}{\rho_v}\right)^{0.5} x^{0.9} \frac{\phi_v}{t_\delta^+} \qquad \text{(A-20)}$$

where

$$\phi_v = \text{Modified Lockhart-Martinelli parameter [104]}$$
$$= 1 + 1.09\, X_{tt}^{0.039} \qquad \text{(A-21)}$$

$$X_{tt} = \left(\frac{1-x}{x}\right)^{0.9} \left(\frac{\rho_v}{\rho_l}\right)^{0.5} \left(\frac{\mu_l}{\mu_v}\right)^{0.1}$$

$$t_\delta^+ = 3.88\, Pr_l^{0.663} (4.67-x) \qquad \text{(A-22)}$$

and

$$Re_V = \left[\frac{G_t D}{\mu_v}\right]$$

The expression given for ϕ_v in Eq (A-21) was developed using R-12 data [104].

6. Bae et al. correlation [68]:

The local heat transfer coefficients can be calculated from the following equation:

$$h_z = \frac{\rho_l \, C_l \, V^*}{F_2} \qquad \text{(A-23)}$$

where

V^* = friction velocity based on wall shear stress

$$= (\tau_o \, g_c / \rho_l)^{0.5} \qquad \text{(A-24)}$$

$$\tau_o = -\frac{A}{S} \left(\frac{dp}{dz}\right)_{TPF} \qquad \text{(A-25)}$$

A = flow cross-sectional area

S = wetted perimeter

$\left(\frac{dp}{dz}\right)_{TPF}$ in Eq (A-25) can be obtained by using Lockhart-Martinelli correlation [83]. The Lockhart-Martinelli correlation can be given by

$$\left(\frac{dp}{dz}\right)_{TPF} = \frac{-0.09 G_t^{\,2}}{g_c \rho_v D} \left[\frac{G_t D}{\mu_v}\right]^{-0.2} \left[x^{1.8} + 5.7 \left(\frac{\mu_l}{\mu_v}\right)^{0.0523} (1-x)^{0.47} \, x^{1.33} \left(\frac{\rho_v}{\rho_l}\right)^{0.261} + 8.11 \left(\frac{\mu_l}{\mu_v}\right)^{0.105} (1-x)^{0.94} \, x^{0.86} \left(\frac{\rho_v}{\rho_l}\right)^{0.522} \right] \qquad \text{(A-26)}$$

F_2 in Eq (A-23) is given by:

$$F_2 = \delta^+ \, Pr_l \quad \text{for} \quad 0 < \delta^+ < 5 \qquad \text{(A-27)}$$

$$F_2 = 5Pr_l + 5\ln\{1 + Pr_l(\frac{\delta^+}{5} + 1)\}$$

$$\text{for } 5 < \delta^+ < 30 \qquad \text{(A-28)}$$

$$F_2 = 5Pr_l + 5\ln(1 + 5Pr_l) + \left\{\frac{2.5}{\{1 + \frac{10M}{Pr_l \delta^+}\}^{0.5}}\right\}$$

$$* \ln \left\{ \frac{\left[2M - 1 + (1 + \frac{10M}{Pr_l \delta^+})^{0.5} \frac{60M}{\delta^+} - 1 - (1 + \frac{10M}{Pr_l \delta^+})^{0.5}\right]}{\left[2M - 1 - (1 + \frac{10M}{Pr_l \delta^+})^{0.5} \frac{60M}{\delta^+} - 1 + (1 + \frac{10M}{Pr_l \delta^+})^{0.5}\right]} \right\}$$

$$\text{for } 30 < \delta^+ \qquad \text{(A-29)}$$

M in Eq (A-29) is given by:

$$M = \frac{F_o \delta^+ \nu_l}{\tau_o V^*} \qquad \text{(A-30)}$$

where

$$F_o = -\left(\frac{dp}{dz}\right) + \frac{a}{g_c} \rho_l - \frac{G_t^2}{g_c \rho_v} \frac{dx}{dz}$$

$$\left[\frac{1}{(1-\psi)} (\frac{\rho_v}{\rho_l})^{2/3} - \{\frac{(1-x)(2-\beta)}{(1-\psi)^2}\} \frac{\rho_v}{\rho_l}\right] \qquad \text{(A-31)}$$

The void fraction, ψ, is calculated using Zivi's expre-

ssion [93] given in Appendix C by Eq (C-15). The second term in Eq (A-31) is the gravity contribution to F_o and equals to zero for horizontal tubes. For other orientations,

$$a = g \sin \theta \qquad \text{(A-32)}$$

where

g = acceleration due to gravity

θ = tube axis inclination from horizontal

β in Eq (A-31) is the ratio of velocity condensate particles at the interface, u_i, to the average liquid velocity $\bar{u}_l$. β was obtained by Bae et al. [68] using Fig. (3) in that reference.

$\left(\frac{dp}{dz}\right)$ in Eq (A-31) is given by:

$$\left(\frac{dp}{dz}\right) = \left(\frac{dp}{dz}\right)_{TPF} + \left(\frac{dp}{dz}\right)_M + \left(\frac{dp}{dz}\right)_g \qquad \text{(A-33)}$$

where

$\left(\frac{dp}{dz}\right)_{TPF}$ is calculated by using Eq (A-26)

The momentum pressure gradient $\left(\frac{dp}{dz}\right)_M$ is given by:

$$\left(\frac{dp}{dz}\right)_M = -\frac{G_t^2}{g_c \rho_v}\frac{dx}{dz}\left[2x + (1-2x)\left(\frac{\rho_v}{\rho_l}\right)^{1/3} + (1-2x)\left(\frac{\rho_v}{\rho_l}\right)^{2/3} - 2(1-x)\left(\frac{\rho_v}{\rho_l}\right)\right] \qquad \text{(A-34)}$$

The pressure gradient due to gravity is given by:

$$\left(\frac{dp}{dz}\right)_g = \frac{G_t^2}{g_c \rho_v D Fr^2} \left[\left(\frac{\rho_l}{\rho_v}\right) - \psi \left(\frac{\rho_l}{\rho_v} - 1\right) \right] \qquad \text{(A-35)}$$

where Froude number, Fr, in Eq (A-35) is based on the total flow and is given by:

$$Fr = \frac{(G_t/\rho_v)}{(a\ D)^{0.5}} \qquad \text{(A-36)}$$

where a is given by Eq (A-32) and is always taken as positive.

By using Eqs (A-34) to (A-36) and Eq (A-26), $\left(\frac{dp}{dz}\right)$ can be calculated from Eq (A-33).

In this correlation δ^+ is calculated by trial and error from one of the following equations.

$$Re_l = 2(\delta^+)^2 \qquad \text{for} \quad 0 < \delta^+ < 5 \qquad \text{(A-37)}$$

$$Re_l = 50 - 32.2\delta^+ + 20\ \delta^+ \ln \delta^+$$

$$\text{for} \quad 5 < \delta^+ < 30 \qquad \text{(A-38)}$$

and

$$Re_l = -256 + 12\ \delta^+ + 10\ \delta^+ \ln \delta^+$$

$$\text{for} \quad 30 < \delta^+ \qquad \text{(A-39)}$$

where

$$Re_l = \left[\frac{G_t(1-x)D}{\mu_l}\right] \qquad \text{(A-40)}$$

Alternatly, Fig (4) of the reference [68] can be used to calculate δ^+ by using Re_l from Eq (A-40).

7. Cavillini and Zecchin correlation [69,73]:

$$\bar{h}_{TP} = 0.05 \frac{K_l}{D} \bar{Re}_e^{0.8} \bar{Pr}_l^{0.33} \qquad (A-41)$$

where

$$Re_e = Re_v \left(\frac{\mu_v}{\mu_l}\right) \left(\frac{\rho_v}{\rho_l}\right)^{-0.5} + Re_l \qquad (A-42)$$

$$Re_v = \frac{G_t \times D}{\mu_v}$$

$$Re_l = \frac{G_t (1-x) D}{\mu_l}$$

The mean equivalent Reynolds number $\bar{Re}_e$ used in Eq (A-41) is calculated using Eq (A-42) as an arithmetic average of equivalent Reynolds number at inlet and exit of the tube. The mean Prandtl number in Eq (A-41) is the arithmetic mean of inlet and exit Prandtl numbers each being determined at the corresponding pressure.

8. Murthy and Sarma correlation [71]:

Using a homogeneous model for horizontal condensation inside the tubes Murthy and Sarma gave the following equation for mean heat transfer coefficient:

$$\frac{\bar{Nu}_{TP}}{\bar{Nu}_o} = 16.3 \left(1 + Pr_l \frac{h_{fg}}{C_l \Delta t}\right) \left(\frac{D}{L}\right)^{0.72} \qquad (A-43)$$

where

$\overline{Nu}_{TP}$ = mean condensation Nusselt number defined as

$$= \frac{\bar{h}_{TP}\, D}{K_l}$$

D = inside diameter of the tube

$\overline{Nu}_o$ = mean single phase Nusselt number given by:

$$= 0.023\, Re_L^{0.8}\, Pr_l^{0.333} \qquad \text{(A-44)}$$

Re_L = Reynolds number assuming all the mass is flowing as liquid

$$= \frac{4W_t}{\pi D\, \mu_l} \qquad \text{(A-45)}$$

h_{fg} = latent heat of condensation (or vaporisation)

C_l = specific heat of liquid

Δt = temperature difference between saturated vapor and tube wall

and L = length of condenser tube.

The ranges of applicability of Eqs (A-43) and (A-44) are as given below:

$$1 \leq Pr_l \leq 5$$

$$1.3 \leq \frac{h_{fg}}{C_l\, \Delta t} \leq 24$$

$$90 \leq \frac{L}{D} \leq 400$$

$$3500 \leq Re_L \leq 1.5 \times 10^5$$

9. Traviss, Rohsenow and Baron correlation [72]:

The local heat transfer correlation is given by:

$$h_z = 0.15 \frac{K_l}{D} \frac{Re_l^{0.9} Pr_l}{F_2} \left(X_{tt}^{-1} + 2.85\, X_{tt}^{-0.476}\right) \qquad \text{(A-46)}$$

where

$$Re_l = \left[\frac{G_t(1-x)D}{\mu_l}\right]$$

X_{tt} = Lockhart-Martinelli parameter

$$= \left(\frac{1-x}{x}\right)^{0.9} \left(\frac{\mu_v}{\mu_l}\right)^{0.5} \left(\frac{\rho_l}{\rho_v}\right)^{0.1}$$

and

$$F_2 = 0.707\, Pr_l\, Re_l^{0.5} \qquad 0 \le Re_l \le 50 \qquad \text{(A-47a)}$$

$$F_2 = 5Pr_l + 5\ln\left[1 + Pr_l(0.09636\, Re_l^{0.585} - 1)\right]$$

$$50 < Re_l \le 1125 \qquad \text{(A-47b)}$$

$$F_2 = 5Pr_l + 5\ln\left[1 + 5Pr_l\right] + 2.5\ln(0.00313\, Re_l^{0.812})$$

$$1125 < Re_l \qquad \text{(A-47c)}$$

Eqs (A-46) and (A-47) were derived for refrigerants in annular flow inside a horizontal tube where both the phases are in turbulent flow.

The mean heat transfer coefficient can be obtained from:

$$\frac{1}{\bar{h}_{TP}} = \frac{1}{(x_{in}-x_{out})} \int_{x_{out}}^{x_{in}} \frac{dx}{h_z} \qquad \text{(A-48)}$$

10. Izumi et al. correlation [74]:

The mean heat transfer correlation is given by:

$$\bar{h}_{TP} = C_1 \, Re^{0.5} \, Pr_l^{0.333} \quad \text{For} \quad Re \leq 850 \tag{A-49}$$

$$\bar{h}_{TP} = C_2 \, Re^{0.8} \, Pr^{0.333} \quad \text{For} \quad 850 < Re \tag{A-50}$$

where

$$Re = Re_l \, (1 - \psi) \tag{A-51}$$

$$Re_l = \left[\frac{G_t (1-\bar{x}) D}{\mu_l} \right]$$

$\bar{x}$ = mean quality

ψ = void fraction

$$= \frac{1}{\left[1 + \left(\frac{1-\bar{x}}{\bar{x}} \right) \left(\frac{\rho_v}{\rho_l} \right)^{3/4} \right]} \tag{A-52}$$

$$C_1 = 0.16 \, D^{0.65}$$

$$C_2 = 0.069 \, D^{0.65} \tag{A-53}$$

where the nominal diameter, D, is expressed in millimeters.

APPENDIX B

FRICTIONAL PRESSURE DROP CORRELATIONS FOR TWO PHASE FLOW

The correlations of Lockhart-Martinelli [83] and Dukler et al. [86] are described in section (3.2.2).

Hughmark correlation [84]:

Through the use of lost work Hughmark gave the following correlation for frictional pressure gradient in two-phase flow

$$\left(\frac{dp}{dz}\right)_{TPF} = \frac{f_{TP}\, V^2\, \rho_{TP}^2}{2 g_c D} \qquad \text{(B-1)}$$

where

V = velocity of homogeneous two-phase mixture

$$= G_t \left[\frac{(1-x)}{\rho_l} + \frac{x}{\rho_v}\right]$$

ρ_{TP} = Two-phase density

$$= \{\, \rho_l(1-\psi) + \rho_v \psi \,\}$$

The void fraction, ψ, is calculated by means of Hughmark correlation [90] given in Appendix C.

Using $Re_{TP}(\frac{\rho_v}{\rho_l})\ (\frac{0.085}{D})$ as a parameter Hughmark [84] presented a family of curves using (f_{TP}/f_o) and the liquid volume fraction (λ) as the coordinates. f_o is the single phase friction factor corresponding to two-phase Reynolds number as given below:

$$\lambda = \frac{1}{\left[1 + \frac{x}{(1-x)}\left(\frac{\rho_v}{\rho_l}\right)\right]} \qquad \text{(B-2)}$$

$$Re_{TP} = \frac{G_t D}{\{ \mu_l (1-\psi) + \mu_v \psi \}} \qquad (B-3)$$

and

$$f_o = \frac{0.045}{Re_{TP}^{0.2}} \qquad (B-4)$$

APPENDIX C

CORRELATIONS FOR TWO-PHASE VOID FRACTION

1. Lockhart-Martinelli correlation [83]:

The correlation was developed using the experimental data on two-phase, two-component systems through the use of the following parameters:

$$X = \left[\left(\frac{dp}{dz}\right)_{f,l} \Big/ \left(\frac{dp}{dz}\right)_{f,v}\right]^{0.5} \qquad \text{(C-1)}$$

where

$\left(\frac{dp}{dz}\right)_{f,l}$ = frictional pressure gradient assuming liquid alone is flowing inside the pipe

$\left(\frac{dp}{dz}\right)_{f,v}$ = fractional pressure gradient assuming vapor alone is flowing inside the pipe

It can be shown that Eq (C-1) is equivalent to:

$$X^2 = \frac{Re_{vp}^{\,m}}{Re_{lp}^{\,n}} \frac{C_l}{C_v} \left(\frac{W_l}{W_v}\right)^2 \left(\frac{\rho_v}{\rho_l}\right) \qquad \text{(C-2)}$$

Re_{vp}, Re_{lp} = Reynolds numbers assuming each one of the phases is flowing alone in the pipe

m, n, C_l, C_v = constants in the Fanning friction factor equation

$$f = \frac{C}{Re^q}$$

For turbulent flow of both phases Eq (C-2) reduces to:

$$X_{tt} = \left(\frac{1-x}{x}\right)^{0.9} \left(\frac{\rho_v}{\rho_l}\right)^{0.5} \left(\frac{\mu_l}{\mu_v}\right)^{0.1} \qquad \text{(C-3)}$$

The transition from laminar to turbulent flow for each one of the phases was given by Lockhart and Martinelli [83] to correspond to Re_{vp} and Re_{lp} values between 1000 and 2000.

Once the type of flow, laminar or turbulent flow, in each of the phases is determined X can be calculated from Eq (C-2). The void fraction can then be determined from Fig (4) of reference [83] corresponding to the calculated, X.

2. Hughmark correlation [90]:

Following the single phase variable density model of Bankoff [109] the void fraction can be written as:

$$\psi = \frac{K}{\left[1 + \frac{(1-x)}{x}\left(\frac{\rho_v}{\rho_l}\right)\right]} \qquad (C-4)$$

where K is a flow parameter.

Hughmark [90] developed a correlation between K and a parameter Z using experimental data. The parameter Z is given by:

$$Z = \left[\frac{Re^{1/6}\ Fr^{1/8}}{\lambda^{1/4}}\right] \qquad (C-5)$$

where

$$Re = \frac{G_t D}{\left[(1-\psi)\mu_l + \psi\mu_v\right]} \qquad (C-6)$$

$$Fr = \frac{V^2}{g\ D} \qquad (C-7)$$

V = Homogeneous velocity of two phase mixture

$$= G_t \left[\frac{(1-x)}{\rho_l} + \frac{x}{\rho_v} \right] \qquad \text{(C-8)}$$

g = acceleration due to gravity

λ = liquid volume fraction

$$= \frac{1}{\left[1 + \frac{x}{(1-x)} \left(\frac{\rho_v}{\rho_l}\right)\right]} \qquad \text{(C-9)}$$

By using experimental data Hughmark [90] tabulated the values of K and Z. The tabulated values can be approximated by the following expressions:

$$K = \exp [-1.98 + 0.666 \ln Z + 2.635 (\ln Z)^2 - 4.5 (\ln Z)^3 + 3.611 (\ln Z)^4 - 1.148 (\ln Z)^5 + 0.243 (\ln Z)^6] \qquad 0 < Z \leq 7 \qquad \text{(C-10)}$$

$$K = \exp [-4.707 + 9.149 \ln Z - 7.817 (\ln Z)^2 + 3.503 (\ln Z)^3 - 0.861 (\ln Z)^4 + 0.11 (\ln Z)^5 - 0.0058 (\ln Z)^6] \qquad 7 < Z < 130 \qquad \text{(C-11)}$$

$$K = 0.98 \qquad 130 \leq Z \qquad \text{(C-12)}$$

Calculation of void fraction using this correlation involves an iteration process as the value of void fraction is needed in Eq (C-6). Assuming an initial value for void fraction, ψ, Z can be calculated from Eqs (C-5) to (C-9).

Depending on the value of Z, K is calculated from Eqs (C-10) to (C-12). Using the value of K in Eq (C-4) a new value of void fraction, ψ, is calculated. This procedure is repeated until two successive values of ψ are within an error criterion.

3. Baroczy correlation [91]:

Using air-water and mercury-nitrogen hold up data Baroczy showed that ratios of liquid and vapor densities and viscosities are also parameters in hold up correlation, in addition to Lockhart-Martinelli parameter, Eq (C-1). For turbulent flow of both the phases, using X_{tt} as a parameter Baroczy presented a family of curves plotted with hold up, $(1-\psi)$, and $(\mu_l/\mu_v)^{0.2}$ (ρ_v/ρ_l) as the co-ordinates.

Calculation procedure for void fraction is summarised as follows:

1. Calculate X_{tt}, using local quality, from Eq (C-3)
2. Calculate $(\mu_l/\mu_v)^{0.2}$ (ρ_v/ρ_l)
3. Read hold up, $(1-\psi)$, from Fig (3) of reference [91].
4. $\psi = 1 - (1-\psi)$

Range of variables for this correlation are:

$$0.01 \leq X_{tt} \leq 100$$

$$0.0001 \leq \left(\frac{\mu_l}{\mu_v}\right)^{0.2}\left(\frac{\rho_v}{\rho_l}\right) \leq 1$$

4. Thom correlation [92]:

Using steam-water data Thom correlated local void fraction through the use of a dimensionless slip factor, which is a function of saturation pressure. The void fraction can be

given by:

$$\psi = \frac{\gamma x}{\left[1 + x(\gamma - 1)\right]} \qquad (C\text{-}13)$$

where γ is the dimensionless slip factor.

Using the tabulated data for γ and system saturation pressure, γ,can be written as:

$$\gamma = 258.8 - 0.875\ p \qquad (C\text{-}14)$$

$$14.7 \leq p \leq 250$$

where p is in psia.

5. Zivi Correlation [93]:

Formulating the kinetic energy in a steady,two-phase flow in a finite length of conduit in terms of void fraction and applying the principle of minimum entropy production, Zivi could derive an expression for void fraction as given below:

$$\psi = \frac{1}{\left[1 + \frac{(1-x)}{x}\left(\frac{\rho_v}{\rho_l}\right)^{2/3}\right]} \qquad (C\text{-}15)$$

The flow regime assumed was annular.

6. Turner-Wallis correlation [94]:

Turner and Wallis showed that two-phase two-component void fraction data of Martinelli et al. [110] can best be described by:

$$\psi = \left[\frac{1}{1 + X_{tt}^{0.8}}\right]^{\frac{1}{2.65}} \qquad \text{(C-16)}$$

where X_{tt} is given by Eq (C-3).

APPENDIX D

DERIVATION OF Eq (4-23)

The average liquid velocity and the liquid mass flow rate at a given axial location can be written in terms of local quality and void fraction as given below:

$$u_l = \frac{(1-x)\, W_t}{(1-\psi)\, \rho_l A} \tag{D-1}$$

$$W_l = (1-x)\, W_t \tag{D-2}$$

Therefore

$$u_l \frac{dW_l}{dz} = - \frac{(1-x) W_t^2}{(1-\bar{\psi}) A \rho_l} \frac{dx}{dz} \tag{D-3}$$

and

$$\frac{d}{dz}(u_l W_l) = \frac{W_t^2}{A\rho_l} \frac{d}{dz} \left\{ \frac{(1-x)^2}{(1-\psi)} \right\} \tag{D-4}$$

The void fraction given by Zivi's [93] expression is:

$$\psi = \frac{1}{\left[1 + \left(\frac{1-x}{x}\right) \left(\frac{\rho_v}{\rho_l}\right)^{2/3}\right]} \tag{D-5}$$

By the use of Eq (D-5), it can be shown that:

$$\frac{d}{dz}(u_l W_l) = \left\{ \frac{-2(1-x)\, W_t^2}{(1-\bar{\psi}) A \rho_l} \frac{dx}{dz} \right\} \left\{ 1 - \frac{1}{2} \frac{(1-x)}{(1-\psi)} \right.$$

$$\left. \frac{(\rho_v/\rho_l)^{2/3}}{\left[x + (1-x) \left(\frac{\rho_v}{\rho_l}\right)^{2/3}\right]^2} \right\} \tag{D-6}$$

Substituting Eqs (D-3) and (D-6) in the momentum change term in Eq (4-20)

$$\{1.25\, u_l \frac{dW_l}{dz} - \frac{d}{dz}(u_l W_l)\} = -\frac{(1-x)\, W_t^2}{(1-\psi)A\rho_l} \frac{dx}{dz}$$

$$\left[-0.75 + \frac{(1-x)}{(1-\psi)} \frac{(\rho_v/\rho_l)^{2/3}}{\{ x + (1-x)(\frac{\rho_v}{\rho_l})^{2/3} \}^2} \right]$$

(D-7)

Substituting (D-7) into right hand side of Eq (4-20) and rearranging terms, the first term on the right hand side of Eq (4-23) is obtained.

APPENDIX E

DERIVATION OF TWO-PHASE MOMENTUM PRESSURE GRADIENT

$$\left(\frac{dp}{dz}\right)_M = -\frac{1}{Ag_c}\frac{d}{dz}\left(u_l W_l + u_v W_v\right) \tag{E-1}$$

The local phase velocities are given by:

$$u_l = \frac{W_t(1-x)}{\rho_l A(1-\psi)} \tag{E-2a}$$

and

$$u_v = \frac{W_t x}{\rho_v A \psi} \tag{E-2b}$$

The local mass flow rate for each phase is given by:

$$W_l = (1-x)W_t \tag{E-3a}$$

$$W_v = x\, W_t \tag{E-3b}$$

Using Eqs (E-2) and Eqs (E-3) in Eq (E-1)

$$\left(\frac{dp}{dz}\right)_M = -\frac{G_t^2}{g_c}\frac{d}{dz}\left\{\frac{1}{\rho_l}\frac{(1-x)^2}{(1-\psi)} + \frac{1}{\rho_v}\frac{x^2}{\psi}\right\}$$

$$= -\frac{G_t^2}{g_c}\left\{\frac{1}{\rho_l}\frac{d}{dz}\left[\frac{(1-x)^2}{(1-\psi)}\right] + \frac{1}{\rho_v}\frac{d}{dz}\left(\frac{x^2}{\psi}\right)\right\} \tag{E-4}$$

Now

$$\frac{d}{dz}\left[\frac{(1-x)^2}{(1-\psi)}\right] = -\frac{2(1-x)}{(1-\psi)}\frac{dx}{dz} + \frac{(1-x)^2}{(1-\psi)^2}\frac{d\psi}{dx}\frac{dx}{dz} \tag{E-5a}$$

and

$$\frac{d}{dz}\left(\frac{x^2}{\psi}\right) = \frac{2x}{\psi}\frac{dx}{dz} - \frac{x^2}{\psi^2}\frac{d\psi}{dx}\frac{dx}{dz} \qquad \text{(E-5b)}$$

Substituting Eqs (E-5) into Eq (E-4)

$$\left(\frac{dp}{dz}\right)_M = -\frac{G_t^2}{g_c}\frac{dx}{dz}\left[-\frac{2(1-x)}{\rho_l(1-\psi)} + \frac{2x}{\rho_v\psi} + \frac{d\psi}{dx}\right.$$

$$\left.\left\{\frac{(1-x)^2}{(1-\psi)^2\rho_l} - \frac{x^2}{\psi^2\rho_v}\right\}\right] \qquad \text{(E-6)}$$

According to Butterworth [108] the void fraction can in general be written as:

$$\psi = \frac{\beta}{\left\{1 + p\left(\frac{1-x}{x}\right)^q \left(\frac{\rho_v}{\rho_l}\right)^r \left(\frac{\mu_l}{\mu_v}\right)^s\right\}} \qquad \text{(E-7)}$$

where β, p, q, r and s are constants.
Let

$$\phi = p\left(\frac{1-x}{x}\right)^q \left(\frac{\rho_v}{\rho_l}\right)^r \left(\frac{\mu_l}{\mu_v}\right)^s \qquad \text{(E-8)}$$

Therefore,

$$\psi = \frac{\beta}{1+\phi} \qquad \text{(E-9)}$$

Then

$$\frac{d\psi}{dx} = \frac{d\psi}{d\phi}\frac{d\phi}{dx} \qquad \text{(E-10)}$$

$$\frac{d\psi}{d\phi} = -\frac{\beta}{(1+\phi)^2} \qquad \text{(E-11)}$$

and

$$\frac{d\phi}{dx} = p \frac{d}{dx} \left\{ \left(\frac{1-x}{x}\right)^q \right\} \left(\frac{\rho_v}{\rho_l}\right)^r \left(\frac{\mu_l}{\mu_v}\right)^s$$

$$= -\frac{pq}{x^2} \left(\frac{1-x}{x}\right)^{q-1} \left(\frac{\rho_v}{\rho_l}\right)^r \left(\frac{\mu_l}{\mu_v}\right)^s$$

Therefore,

$$\frac{d\phi}{dx} = -\frac{pq}{x(1-x)} \left(\frac{1-x}{x}\right)^q \left(\frac{\rho_v}{\rho_l}\right)^r \left(\frac{\mu_l}{\mu_v}\right)^s \qquad \text{(E-12)}$$

Substituting Eqs(E-11) and (E-12) into Eq (E-10) yields

$$\frac{d\psi}{dx} = \frac{pq \left(\frac{1-x}{x}\right)^q \left(\frac{\rho_v}{\rho_l}\right)^r \left(\frac{\mu_l}{\mu_v}\right)^s}{x(1-x)\ (1+\phi)^2} \qquad \text{(E-13)}$$

Substituting Eqs (E-7) and (E-8) into Eq (E-13) yields

$$\frac{d\psi}{dx} = \left\{ \frac{\psi q}{x(1-x)} \right\} \left\{ \frac{\phi}{1+\phi} \right\} \qquad \text{(E-14)}$$

Now

$$(1-\psi) = \frac{(1+\phi-\beta)}{(1+\phi)} \qquad \text{(E-15)}$$

If $\beta = 1$ then,

$$(1-\psi) = \frac{\phi}{(1+\phi)} \qquad \text{(E-16)}$$

Substituting Eq (E-16) into Eq (E-14) yields

$$\frac{d\psi}{dx} = \frac{\psi q\ (1-\psi)}{x(1-x)} \qquad \text{(E-17)}$$

Using Eq (E-17) in Eq (E-6)

$$\left(\frac{dp}{dz}\right)_M = -\frac{G_t^2}{g_c}\frac{dx}{dz}\left[\frac{-2(1-x)}{\rho_l(1-\psi)} + \frac{2x}{\rho_v\psi} + q\left\{\frac{\psi(1-x)}{\rho_l x(1-\psi)} - \frac{x(1-\psi)}{\rho_v\psi(1-x)}\right\}\right] \qquad \text{(E-18)}$$

For q = 1, Eq (E-18) reduces to Eq (4-32)

Derivation of Eq (4-32) from Zivi's Expression:

The void fraction expression of Zivi [93] is given by:

$$\psi = \frac{1}{\left[1 + \left(\frac{1-x}{x}\right)\left(\frac{\rho_v}{\rho_l}\right)^{2/3}\right]} \qquad \text{(E-19)}$$

Comparing Eqs (E-7) and (E-19) it can be shown that:

$$\beta = 1 = p = q$$

$$r = 2/3$$

and $$s = 0$$

Now it will be shown that (4-32) can be derived using Zivi's expression for void fraction, namely Eq (E-19).

Let

$$\phi = 1 + \left(\frac{1-x}{x}\right)\left(\frac{\rho_v}{\rho_l}\right)^{2/3} \qquad \text{(E-20)}$$

Using Eq (E-20) the void fraction can be written as:

$$\psi = \frac{1}{(1+\phi)} \qquad \text{(E-21)}$$

Then

$$\frac{d\psi}{dx} = \frac{d\psi}{d\phi}\,\frac{d\phi}{dx} \qquad \text{(E-22)}$$

$$\frac{d\psi}{d\phi} = -\frac{1}{(1+\phi)^2} \qquad \text{(E-23)}$$

and

$$\frac{d\phi}{dx} = -\frac{1}{x^2}\left(\frac{\rho_v}{\rho_l}\right)^{2/3} = -\left(\frac{1-x}{x}\right)\frac{1}{x(1-x)}\left(\frac{\rho_v}{\rho_l}\right)^{2/3} \qquad \text{(E-24)}$$

$$\frac{d\psi}{dx} = \frac{\left(\frac{1-x}{x}\right)\;\frac{1}{x(1-x)}\;\left(\frac{\rho_v}{\rho_l}\right)^{2/3}}{(1+\phi)^2} \qquad \text{(E-25)}$$

Using Eqs (E-20) and (E-21), Eq (E-25) can be rewritten as:

$$\frac{d\psi}{dx} = \frac{\psi}{x(1-x)}\;\frac{\phi}{(1+\phi)} \qquad \text{(E-26)}$$

and

$$(1-\psi) = \frac{\phi}{(1+\phi)} \qquad \text{(E-27)}$$

Using Eq (E-27) in Eq (E-26)

$$\frac{d\psi}{dx} = \frac{\psi(1-\psi)}{x\,(1-x)} \qquad \text{(E-28)}$$

Using Eq (E-28) in Eq (E-6)

$$\left(\frac{dp}{dz}\right)_M = -\frac{G_t^2}{g_c}\,\frac{dx}{dz}\left[\frac{-2(1-x)}{\rho_l(1-\psi)} + \frac{2x}{\rho_v\psi} + \frac{(1-x)}{\rho_l\,x(1-\psi)} - \frac{x\,(1-\psi)}{\rho_v\psi(1-x)}\right] \qquad \text{(4-32)}$$

APPENDIX F

SUMMARY OF COMPUTATIONAL STEPS

Step No.	Quantity to be calculated	Remarks
1	$D_e = D/(1 + 2/\pi)$	For smooth tube $D_e = D$
2	$\frac{dx}{dz} = -\frac{1}{L}$	assumed
3	$A = \pi D^2/4$	
4	$G_t = W_t/A$	If G_t is known $W_t = G_t A$
5	$\psi = \frac{1}{\{1 + (\frac{1-x}{x})(\frac{\rho_v}{\rho_l})^{2/3}\}}$	Given by Zivi [93]
6	$\lambda = \frac{Q_l}{Q_l+Q_v} = \frac{1}{\{1 + (\frac{x}{1-x})(\frac{\rho_l}{\rho_v})\}}$	

Step No.	Quantity to be calculated	Remarks
7	$\rho_{NS} = \lambda\rho_l + (1-\lambda)\rho_v$ $\mu_{NS} = \lambda\mu_l + (1-\lambda)\mu_v$ $Re_{NS} = \frac{4W_t}{\pi D_e \mu_{NS}}$	From Dukler et al. [86]. No slip parameters.
8	$\rho_{TP} = \frac{\rho_l \lambda^2}{(1-\psi)} + \frac{\rho_v (1-\lambda)^2}{\psi}$ $\beta = \rho_{TP}/\rho_{NS}$ $Re_{TP} = Re_{NS}\beta$	From Dukler et al. [86]. Separated flow parameters.
9	$\alpha = \frac{f_{TP}}{f_o} = 1 + \frac{(-\ln\lambda)}{[1.281 - 0.478(-\ln\lambda) + 0.444(-\ln\lambda)^2 - 0.094(-\ln\lambda)^3 + 0.00843(-\ln\lambda)^4]}$	From Dukler et al. [86].

Step No.	Quantity to be calculated	Remarks
10	$f_o = 0.0014 + 0.125/Re_{TP}^{0.32}$	From Dukler et al. [86] Single phase friction factor
11	$\left(\frac{dp}{dz}\right)_{TPF} = \frac{-2 G_t^2 f_o \alpha \beta}{g_c D_e \rho_{NS}}$	From Dukler et al. [86]
12	$\left(\frac{dp}{dz}\right)_M = -\frac{G_t^2}{g_c}\frac{dx}{dz}\left[\frac{-2(1-x)}{\rho_l(1-\psi)} + \frac{2x}{\rho_v \psi} + \frac{\psi(1-x)}{\rho_l x(1-\psi)} - \frac{x(1-\psi)}{\rho_v \psi(1-x)}\right]$	
13	$\left(\frac{dp}{dz}\right) = \left(\frac{dp}{dz}\right)_{TPF} + \left(\frac{dp}{dz}\right)_M$	
14	$\tau_o = -\frac{r_o}{2}\left(\frac{dp}{dz}\right)_{TPF}/(1 + 2/\bar{\pi})$	With $\tau_o = -\frac{r_o}{2}\left(\frac{dp}{dz}\right)_{TPF}$ and $D_e = D$ all the steps hold good for smooth tube.

Step No.	Quantity to be calculated	Remarks
15	$V^* = \tau_o g_c/\rho_l$	
16	$r_o^+ = r_o V^*/\nu_l$	
17	$u^+ = y^+ \quad 0 \le y^+ < 5$ $u^+ = 3.05 + 5 \ln y^+ \quad 5 \le y^+ \le 30$ $u^+ = 5.5 + 2.5 \ln y^+ \quad 30 < y^+$	von Karman velocity profile
18	$W_t = \frac{2\pi \rho_l \nu_l^2}{(1-x) V^*} \int_0^{\delta^+} u^+(r_o^+ - y^+)dy^+$	
19	$\tau_V = [\tau_o + \frac{r_o}{2}\frac{dp}{dz}\{1 - (1-\delta^+/r_o^+)^2\} + \{\frac{G_t^2 r_o(1-x)}{2\rho_l g_c(1-\psi)}$ $\frac{dx}{dz}\{-0.75 + \frac{(1-x)}{(1-\psi)} \frac{(\frac{\rho_v}{\rho_l})^{2/3}}{x+(1-x)(\frac{\rho_v}{\rho_l})^{2/3}} 2\}]/(1-\delta^+/r_o^+)$	

Step No.	Quantity to be calculated	Remarks

20

$$\tau/\tau_o = \{ \frac{(1-y^+/\delta^+)}{(1-y^+/r_o^+)} \left[\frac{-G_t^2 r_o (1-x)}{2\rho_l g_c (1-\psi)} \frac{dx}{dz} \right]$$

$$\left[-0.75 + \frac{(1-x)}{(1-\psi)} \frac{(\rho_v/\rho_l)^{2/3}}{\{ x + (1-x)(\frac{\rho_v}{\rho_l})^{2/3} \}^2} \right]$$

$$- \frac{r_o}{2} \frac{dp}{dz} \left[(1-\delta^+/r_o^+) \{ \frac{(1-y^+/r_o^+)}{(1-\delta^+/r_o^+)} \right.$$

$$\left. - \frac{(1-\delta^+/r_o^+)}{(1-y^+/r_o^+)} \} \right] + \tau_v \frac{(1-\delta^+/r_o^+)}{(1-y^+/r_o^+)} \} / \tau_o$$

Step No.	Quantity to be calculated	Remarks
21	$\alpha' = \frac{G_t \, r_o}{4\rho_l V^* \delta^+} \frac{dx}{dz}$	Solve this equation to obtain t^+
	$\frac{dt^+}{dy^+} = \frac{[1 + \alpha' y^+ t^+]}{[1 - y^+/r_o^+][\frac{1}{Pr_l} \frac{\tau/\tau_o}{(\frac{du^+}{dy^+})} - 1]}$	$t^+ = t_{\delta}^+$ at $y^+ = \delta^+$
	and $t^+ = 0 \quad y^+ = 0$	
22	$h_z = \frac{\rho_l C_l V^*}{t^+_{\delta}}$	
	$Nu_z = \frac{h_z D_e}{K_l}$	

Step No.	Quantity to be calculated	Remarks
23	$(\bar{h}_{tt})_{anal} = \frac{1}{(x_{in}-x_{out})} \int_{x_{out}}^{x_{in}} h_z dx$	

APPENDIX G

ALTERNATE APPROACH TO DETERMINE δ^+

According to Traviss et al. [106] the local superficial Reynolds number can be defined, assuming liquid alone is flowing, as follows:

$$Re_l = \frac{G_t(1-x)D_e}{\mu_l} \qquad (G-1)$$

since $G_t = 4W_t/\pi D^2$ (G-2)

$$Re_l = \frac{4W_t(1-x)\ D_e}{\mu_l \pi D^2} \qquad (G-3)$$

Neglecting the curvature effects, the liquid film flow inside the pipe can be considered as flow past a flat plate of width equals to the pipe circumference. Considering an elemental area (πD x dy), at a distance y from the surface of the plate, the liquid continuity equation can be written as:

$$W_l = \pi D \rho_l \int_0^{\delta} u_l \, dy \qquad (G-4)$$

Since,

$$W_l = W_t (1-x) \qquad (G-5)$$

Eq (G-4) can be rewritten as:

$$W_t = \frac{\pi D \mu_l}{(1-x)} \int_0^{\delta} u^+ \, dy^+ \qquad (G-6)$$

Substituting Eq (G-6) into Eq (G-3), it can be written

that:

$$Re_1 = \frac{4D_e}{D} \int_0^{\delta} u^+ \, dy^+ \qquad (G-7)$$

The integral in Eq (G-7) was evaluated using von Karman velocity for the liquid film, Eq (4-7) . The following results were obtained for the superficial Reynolds number, Re_1:

$$Re_1 = 2 \frac{D_e}{D} \delta^{+2} \qquad 0 \leq \delta^+ < 5 \qquad (G-8)$$

$$Re_1 = \frac{D_e}{D} [50 - 32.2 \, \delta^+ + 20 \, \delta^+ \ln \delta^+]$$

$$5 \leq \delta^+ \leq 30 \qquad (G-9)$$

$$Re_1 = \frac{D_e}{D} [-256 + 12 \, \delta^+ + 10 \, \delta^+ \ln \delta^+]$$

$$30 < \delta^+ \qquad (G-10)$$

Neglecting the area occupied by the flat tape and the tape thickness the equivalent diameter, defined as four times the hydraulic radius, can be written as:

$$D_e = \frac{D}{(1 + 2/\pi)} \qquad (G-11)$$

Using (G-11) and (G-1) δ^+ can be obtained from Eqs (G-8) to (G-10) by iteration as they are non-linear. Or, Eq (G-8) to (G-10) can be approximated by straight lines on a log-log graph. Using Eq (G-11) and these piecewise curve fits δ^+ can be written as an explicit function of Re_1 as:

$$\delta^+ = 0.902 \; Re_1^{0.5} \qquad 0 \leq Re_1 < 30 \qquad (4\text{-}55)$$

$$\delta^+ = 0.6133 \; Re_1^{0.5907} \qquad 30 \leq Re_1 \leq 685 \qquad (4\text{-}56)$$

$$\delta^+ = 0.121 \; Re_1^{0.8284} \qquad 685 \leq Re_1 < 23{,}000 \qquad (4\text{-}57)$$

The error involved in calculating δ^+ using Eqs (4-55) to (4-57) and using Eqs (G-8) to (G-10) is less than 8%. The error involved in calculating the heat transfer coefficient, using Eqs (4-55) to (4-57) to calculate δ^+ and using iteration procedure to calculate δ^+ as in section (4.2.3), was found to be negligible.

APPENDIX H

COMPUTER PROGRAM

ILLEGIBLE DOCUMENT

THE FOLLOWING DOCUMENT(S) IS OF POOR LEGIBILITY IN THE ORIGINAL

THIS IS THE BEST COPY AVAILABLE

```
C
C
C     $$$$$$$$$$$$$$$$$$$$$$$$$$$$$$$$$$$$$$$$$$$$$$$$$$$$$$$$$$$$$$$$$$$$
C
C     THIS PROGRAM IS WRITTEN TO IMPLEMENT THE PRESENT ANALYSES
C     OF HORIZONTAL,FORCED CONVECTION,ANNULAR FLOW CONDENSATION
C     INSIDE CIRCULAR AND SEMI-CIRCULAR TUBES
C
C     THIS PROGRAM CALCULATES THE FOLLOWING LOCAL QUANTITIES :
C
C     1)  VOID FRACTION,
C     2)  LIQUID FILM THICKNESS,
C     3)  PRESSURE GRADIENTS,
C     4)  WALL AND INTERFACIAL SHEAR STRESSES,
C     5)  NON-DIMENSIONAL TEMPERATURE DROP ACROSS THE LIQUID
C         FILM,
C     6)  HEAT TRANSFER COEFFICENT          AND,
C     7)  NUSSELT NUMBER
C
C     IN THIS PROGRAM THE FOLLOWING RELATIONS ARE USED :
C
C     1)  ZIVI'S CORRELATION FOR LOCAL VOID FRACTION
C     2)  DUKLER ET AL. CORRELATION FOR LOCAL FRICTIONAL
C         PRESSURE GRADIENT
C     3)  TRAVISS - ROHSENOW APPROXIMATION FOR THE
C         NON-DIMENSIONAL LIQUID FILM THICKNESS, DELTA +
C     4)  DX/DZ = - 1 / L
C
C     $$$$$$$$$$$$$$$$$$$$$$$$$$$$$$$$$$$$$$$$$$$$$$$$$$$$$$$$$$$$$$$$$$$$
C
C     *************************************************************
C
C     DEFINITIONS OF THE VARIABLE NAMES USED IN THIS PROGRAM
C
C     *************************************************************
C
C     A1 - A5       VARIABLE NAMES USED IN THE COMPUTATION OF
C                   SHEAR STRESSES
C     A6 & A7       FUNCTION SUBPROGRAMS USED TO CALCULATE CERTAIN
C                   LOCAL QUANTITIES
C     A             NATURAL LOGARITHM OF LAMDA
C     AAL           = 1 - LAMDA
C     AL            LAMDA
C     ALFA          PARAMETER DEFINED IN THE DIFFERENTIAL EQUATION
C                   FOR NON-DIMENSIONAL TEMPERATURE DROP
C     ALPHA         RATIO OF TWO-PHASE FRICTION FACTOR TO THE
C                   CORRESPONDING SINGLE PHASE FRICTION FACTOR
C     AREA          CROSS SECTIONAL AREA OF THE CIRCULAR TUBE
C     AVNU          MEAN ANALYTICAL NUSSELT NUMBER
C     BETA          RATIO OF TWO-PHASE DENSITIES
C     CL            SPECIFIC HEAT OF SATURATED LIQUID
C     D             INSIDE DIAMETER OF THE CONDENSER TUBE
C     DDP           DP
C     DE            EQUIVALENT DIAMETER
C                   = D                   FOR CIRCULAR TUBE
C                   = D/(1+2/PI)          FOR SEMI-CIRCULAR TUBE
C     DEL           DTAPLS
C     DELTA         LOCAL LIQUID FILM THICKNESS
C     DP            TOTAL TWO-PHASE LOCAL PRESSURE GRADIENT
C     DPF           LOCAL TWO-PHASE FRICTIONAL PRESSURE GRADIENT
```

```
C       DPM         LOCAL TWO-PHASE MOMENTUM PRESSURE GRADIENT
C       DTAPLS      LOCAL NON-DIMENSIONAL LIQUID FILM THICKNESS
C       DUDY        FIRST DERIVATIVE OF LIQUID VELOCITY PROFILE
C       DXBYDZ      QUALITY GRADIENT
C       DY          FIRST DERIVATIVE OF TPLUS WITH RESPECT TO
C                   YPLUS
C       ERROR       PERCENTAGE DEVIATION BETWEEN EXPERIMENTAL AND
C                   ANALYTICAL MEAN HEAT TRANSFER COEFFICENTS
C       EXPTNU      EXPERIMENTAL MEAN NUSSELT NUMBER
C       FO          SINGLE PHASE FRICTION FACTOR EVALUATED AT RETP
C       GC          GRAVITATIONAL CONSTANT
C       GT          TOTAL MASS VELOCITY
C       H           LOCAL HEAT TRANSFER COEFFICENT
C       HEXPT       EXPERIMENTAL MEAN HEAT TRANSFER COEFFICENT
C       HFG         LATENT HEAT OF CONDENSATION ( OR VAPORISATION)
C       HTP         MEAN ANALYTICAL HEAT TRANSFER COEFFICENT
C       KL          THERMAL CONDUCTIVITY OF THE SATURATED LIQUID
C       L           CONDENSING LENGTH OF THE TUBE
C       LAMDA       RATIO OF LOCAL LIQUID VOLUMETRIC FLOW RATE TO
C                   THE TOTAL VOLUMETRIC FLOW RATE
C       N4          NUMBER OF STEPS USED IN THE NUMERICAL
C                   INTEGRATION OF THE DIFFERENTIAL EQUATION
C       NEQ         NUMBER OF SIMULTANEOUS DIFFERENTIAL EQUATIONS
C                   SOLVED BY THE RKG SCHEME
C       NG          NUMBER OF DATA POINTS WITH DIFFERENT MASS
C                   VELOCITIES FOR EACH INLET SATURATION PRESSURE
C       NP          NUMBER OF DIFFERENT INLET SATURATION PRESSURES
C                   FOR EACH TWIST RATIO OR FOR EACH SMOOTH TUBE
C       NU          LOCAL NUSSELT NUMBER
C       NX          NUMBER OF AXIAL LOCATIONS FOR COMPUTATION OF
C                   LOCAL QUANTITIES
C       NY          NUMBER OF TWISTED TAPE INSERTS EXPERIMENTALLY
C                   INVESTIGATED FOR EACH FLUID
C       PI          A CONSTANT
C       PIN         INLET PRESSURE OF THE CONDENSING FLUID
C       POUT        EXIT PRESSURE OF THE CONDENSING FLUID
C       PRL         PRANDTL NUMBER OF THE SATURATED LIQUID
C       PSAT        INLET SATURATION PRESSURE
C       Q           LOCAL QUALITY
C       QQ          A VARIABLE NAME USED IN THE RKG SCHEME
C       RO          INSIDE RADIUS OF THE CONDENSER TUBE
C       ROPLUS      LOCAL NON-DIMENSIONAL, RO
C       RATDEN      RATIO OF DENSITY OF SATURATED VAPOR TO THE
C                   DENSITY OF THE SATURATED LIQUID
C       RATIO       RATIO OF THE EXPERIMENTAL TO THE ANALYTICAL
C                   MEAN HEAT TRANSFER COEFFICENTS
C       RE          REYNOLDS NUMBER ASSUMING THAT ALL THE MASS IS
C                   FLOWING AS LIQUID
C       REL         LOCAL REYNOLDS NUMBER ASSUMING THAT LIQUID
C                   ALONE IS FLOWING IN THE TUBE
C       RENS        REYNOLDS NUMBER OF TWO-PHASE MIXTURE FOR
C                   NO-SLIP CONDITIONS
C       RETP        REYNOLDS NUMBER FOR TWO-PHASE FLOW CONDITIONS
C       RG          LOCAL VOID FRACTION
C       RGDEF       LOCAL VOID FRACTION BY DEFINITION
C       RHOL        DENSITY OF SATURATED LIQUID
C       RHONS       DENSITY OF TWO-PHASE MIXTURE FOR NO-SLIP
C                   CONDITIONS
C       RHOV        DENSITY OF SATURATED VAPOR
C       RL          LOCAL LIQUID HOLD UP
```

```
C       RP              ROPLUS
C       SHEAR           FUNCTION SUBPROGRAM USED TO CALCULATE THE
C                       SHEAR STRESS DISTRIBUTION ACROSS THE LIQUID
C                       FILM
C       STEP            STEP SIZE USED IN THE RKG SCHEME
C       TO              TOUNOT
C       TOPLUS          NON-DIMENSIONAL TEMPERATURE DROP ACROSS THE
C                       LIQUID FILM
C       TOUNOT          LOCAL WALL SHEAR STRESS
C                       = - RO*DPF/2                FOR CIRCULAR TUBE
C                       = -RO*DPF/(2*(1+2/PI))  FOR SEMI-CIRCULAR TUBE
C       TOUV            LOCAL INTERFACIAL SHEAR STRESS
C       TPLUS           NON-DIMENSIONAL TEMPERATURE DROP UP TO A
C                       LOCATION YPLUS FROM THE WALL
C       TSAT            INLET SATURATION TEMPERATURE
C       TV              TOUV
C       UL              DYNAMIC VISCOSITY OF THE SATURATED LIQUID
C       UNS             VISCOSITY OF THE TWO-PHASE MIXTURE FOR NO-SLIP
C                       CONDITIONS
C       UV              DYNAMIC VISCOSITY OF THE SATURATED VAPOR
C       V               RG
C       VSTAR           LOCAL SHEAR VELOCITY
C       VV              RL
C       VVSTAR          VSTAR
C       WT              TOTAL MASS FLOW RATE
C       X               Q
C       XL              = 1 - X
C       YPLUS           NON-DIMENSIONAL DISTANCE FROM THE WALL
C       ZZ              A VARIABLE NAME USED IN THE CALCULATION OF
C                       MEAN HEAT TRANSFER COEFFICENTS
C
C       ++++++++++++++++++++++++++++++++++++++++++++++++++++++++++++++
C
C       SUBROUTINES USED IN THIS PROGRAM
C
C       ++++++++++++++++++++++++++++++++++++++++++++++++++++++++++++++
C
C       DERIV           SUBROUTINE CALLED BY RKG
C       QSF             SUBROUTINE TO CACULATE MEAN HEAT TRANSFER
C                       COEFFICENTS FROM THE LOCAL VALUES. THIS
C                       SUBROUTINE IS A FORM OF SIMPSON'S RULE OF
C                       NUMERICAL INTEGRATION
C       RKG             SUBROUTINE USED IN THE NUMERICAL INTEGRATION
C                       OF THE DIFFERENTIAL EQUATION FOR THE
C                       NON-DIMENSIONAL TEMPERATURE DROP ACROOS THE
C                       LIQUID FILM, TDPLUS
C
C
C       ==============================================================
C
C
        COMMON      A1,A3,A5,ALFA,DDP,DEL,PRL,RO,ROPLUS,TO,TV
        REAL        KL,L,LAMDA(20),NU(20)
        DIMENSION   DELTA(20),DP(20),DPF(20),DPM(20),DTAPLS(20)
        DIMENSION   H(20),Q(20),RP(20),RG(20),RGDEF(20),RL(20)
        DIMENSION   TDPLUS(20),TOUNOT(20),TOUV(20),VSTAR(20)
        DIMENSION   ZZ(11)
        DIMENSION   TITLE(20)
        DIMENSION   DY(1),QQ(1),TPLUS(1)
        N4=100
```

```
      NEQ=1
      PI=3.1415926
      GC=4.17312E08
      NY=2
                  DO  2  IY=1,NY
      READ  1000,  NP,NX
1000  FORMAT(2I5)
                  DO  1  I=1,NX
      IF (I.EQ.1)  Q(I)=.99
      IF (I.GE.2)  Q(I)=1.-(I-1)*.1
   1              CONTINUE
                  DO  2  IP=1,NP
      READ 1005, (TITLE(I),I=1,20)
1005  FORMAT(20A4)
      READ  1000,  NG
      READ 1010, D,L,KL,CL,HFG
1010  FORMAT(5F15.8)
      READ 1010, TSAT,PSAT
      READ 1010, RHOL,RHOV,UL,UV,PRL
      PRINT 5000, (TITLE(I),I=1,20)
5000  FORMAT(1H1//30X,20A4//)
      PRINT 5005,  L,D,TSAT,PSAT,PRL,KL,CL
5005  FORMAT(10X,'PIPE LENGTH = ',F5.2,1X,'FT',2X,'PIPE DIA = '
     1 ,F5.3,1X,'INCH'//10X,'SATURATION TEMP = ',F8.3,1X,'F',5X
     2 ,'SATURATION PRESSURE = ',F8.3,1X,'PSIA'//10X,
     3 'LIQUID PROPERTIES :   PR NO = ',F8.4,2X,
     4 'THERMAL CONDUCTIVITY = ',F8.5,1X,'BTU/FT HR F',2X,
     5 'CL = ',F7.4,1X,'BTU/LBM F'/)
      PRINT  5010,  RHOL,RHOV,UL,UV,HFG
5010  FORMAT(10X,'DENSITIES (LBM/FT ** 3) :     LIQUID : ',
     1 F12.6,2X,'VAPOR : ',F12.6//10X,'VISCOSITIES(LBM/FT S) :'
     2 ,5X,'LIQUID : ',F15.9,2X,'VAPOR : ',F15.9//10X,
     3 'LATENT HEAT = ',F8.3,2X,'BTU/LBM'/)
      UL=UL*3600.
      UV=UV*3600.
      D=D/12.
      RO=D/2.
      AREA=PI*RO*RO
      DE=D/(1.+2./PI)
      RATDEN=RHOV/RHOL
      DXBYDZ=-1./L
                  DO  3  I=1,NX
      LAMDA(I)=1./(1.+Q(I)/((1.-Q(I))*RATDEN))
      RG(I)=1./(1.+(1.-Q(I))*RATDEN**.6667/Q(I))
      RL(I)=1.-RG(I)
   3              CONTINUE
                  DO  2  IG=1,NG
      READ  1015,  GT,HEXPT,POUT,PIN
1015  FORMAT(4F10.3)
      WT=GT*AREA
                  DO  11  I=1,NX
      X=Q(I)
      XL=1.-X
      AL=LAMDA(I)
      AAL=1.-AL
      V=RG(I)
      VV=RL(I)
C     LIQUID FILM THICKNESS
      REL=GT*XL*DE/UL
      IF  (REL-30.)  4,4,5
```

```
    4     DEL=.902*SQRT(REL)
                    GO  TO  6
    5     IF   (REL-685.)   8,8,9
    8     DEL=.6133*REL**.5907
                    GO  TO  6
    9     DEL=.121*REL**.8284
    6     DTAPLS(I)=DEL
          STEP=DEL/FLOAT(N4)
C       PRESSURE GRADIENTS
          RHONS=RHOL*AL+RHOV*AAL
          UNS=UL*AL+UV*AAL
          RENS=4.*WT/(PI*DE*UNS)
          BETA=(RHOL*AL*AL/VV+RHOV*AAL*AAL/V)/RHONS
          RETP=RENS*BETA
          A=-ALOG(AL)
          ALPHA=1.0+A/(1.281-0.478*A+0.444*A*A-0.094*A**3+0.00843*
     1    A**4)
          FO=.0014+.125/(RETP**.32)
          DPF(I)=-2.*GT*GT*FO*ALPHA*BETA/(GC*DE*RHONS)
          DPM(I)=-GT*GT*DXBYDZ/GC*(-2.*XL/(RHOL*VV)+2.*X/(RHOV*V)+
     1    V*XL/(RHOL*X*VV)-X*VV/(RHOV*V*XL))
          DP(I)=DPF(I)+DPM(I)
          DDP=DP(I)
C       CALCULATION OF SHEAR STRESSES
          TOUNOT(I)=-.5*RO*DPF(I)/(1.+2./PI)
          TO=TOUNOT(I)
          VSTAR(I)=SQRT(TO*GC/RHOL)
          VVSTAR=VSTAR(I)
          ROPLUS=RO*VVSTAR*RHOL/UL
          RP(I)=ROPLUS
          DELTA(I)=DEL*UL/(VVSTAR*RHOL)
          A1=1.-DEL/ROPLUS
          A2=TO+.5*RO*DDP*(1.-A1*A1)
          A3=RO*GT*GT*XL*DXBYDZ/(2.*RHOL*GC*VV)
          A4=X+XL*RATDEN**.6667
          A5=-.75+XL*RATDEN**.6667/(VV*A4*A4)
          TOUV(I)=(A2+A3*A5)/A1
          TV=TOUV(I)
          RGDEF(I)=A1*A1
C       CALCULATION OF T DELTA +
          ALFA=GT*RO*DXBYDZ/(4.*RHOL*VVSTAR*DEL)
          TPLUS(1)=0.
          YPLUS=0.
          QQ(1)=0.
                    DO  10  KRKG=1,N4
   10     CALL   RKG   (NEQ,STEP,YPLUS,TPLUS,DY,QQ)
          TDPLUS(I)=TPLUS(1)
          H(I)=RHOL*CL*VVSTAR/TDPLUS(I)
          NU(I)=H(I)*DE/KL
   11               CONTINUE
          RE=GT*DE/UL
          CALL   QSF   (0.1,H,ZZ,NX)
          HTP=ZZ(NX)/(1.-C(NX))
          RATIO=HEXPT/HTP
          ERROR=100.*(HEXPT-HTP)/HEXPT
          AVNU=HTP*DE/KL
          EXPTNU=HEXPT*DE/KL
          PRINT 5020
 5020     FORMAT(   //30X,'PRESSURE GRADIENTS'//10X,'QUALITY',10X,
     1    'FRICTIONAL PRESSURE GRAD',5X,'MOMENTUM PRESSURE GRAD',
```

```
     2   'TOTAL PRESSURE GRAD'//30X,'LBF/FT**2/FT',17X,
     3   'LBF/FT**2/FT',17X,'LBF/FT**2/FT'/)
         PRINT 5025, (Q(I),DPF(I),DPM(I),DP(I),I=1,NX)
5025     FORMAT(10X,F7.5,15X,F15.6,13X,F15.6,12X,F15.6)
         PRINT 5030
5030     FORMAT(////30X,'WALL & INTERFACIAL SHEAR STRESSES'//10X
     1   ,'QUALITY',10X,'WALL SHEAR STRESS',10X,
     2   'INTERFACIAL SHEAR STRESS (TOUV)',5X,'SHEAR VELOCITY',7X
     3   ,'RO PLUS'//32X,'LBF/FT**2',18X,'LBF/FT**2',25X,'FT/HR'
     4   //)
         PRINT 5035, (Q(I),TOUNOT(I),TOUV(I),VSTAR(I),RP(I),I=1,
     1   NX)
5035     FORMAT(10X,F7.5,15X,F12.6,15X,F12.6,20X,F10.4,9X,F10.2)
         PRINT 5040
5040     FORMAT(1H1//10X,'QUALITY',12X,'VOID FRACTION',14X,
     1   'HOLD UP',10X,'LAMDA',10X,'VOID FRACTION BY DEFINITION'
     2   //)
         PRINT 5045, (Q(I),RG(I),RL(I),LAMDA(I),RGDEF(I),I=1,NX)
5045     FORMAT(10X,F7.5,15X,F8.6,15X,F8.6,10X,F8.6,10X,F8.6)
         PRINT 5050
5050     FORMAT(//10X,'QUALITY',10X,'NON-DIMENSIONAL TEMP DROP',
     1   2X,'(T DELTA +)'//)
         PRINT 5055, (Q(I),TDPLUS(I),I=1,NX)
5055     FORMAT(10X,F7.5,10X,F12.6)
         PRINT 5060
5060     FORMAT(    //10X,'QUALITY',5X,'DELTA',10X,'DELTA +',10X,
     1   ' H T COEFFICENT',5X,'NUSSELT NUMBER'//24X,'FT',28X,
     2   'BTU/FT ** 2 HR F'//)
         PRINT 5065, (Q(I),DELTA(I),DTAPLS(I),H(I),NU(I),I=1,NX)
5065     FORMAT(10X,F7.5,5X,F10.8,5X,F9.4,8X,F15.4,4X,F15.5)
         PRINT  5070,  HTP,AVNU,HEXPT,EXPTNU,ERROR,RATIO,GT,RE
5070     FORMAT(//10X,'AVE HT COEFFICENT = ',F10.4,2X,
     1   'BTU/FT ** 2 HR F',5X,' AVE NUSSELT NUMBER = ',F10.4//10
     2   X,' EXPT H T COEFFICENT = ',F10.4,2X,'BTU/FT ** 2 HR F',
     3   5X,'EXPT NUSSELT NUMBER = ',F10.4//10X,'% ERROR = ',F6.1
     4   ,5X,'RATIO OF EXPT HT COEFF(TAPE) TO THE ANALYTICAL HT '
     5   ,'COEFFICENT = ',F7.4//10X,'MASS VELOCITY = ',F8.1,2X,
     6   'LBM/FT ** 2 HR'//10X,'REYNOLDS NUMBER BASED ON UL & GT'
     7   ,' = ',F8.1)
         PRINT 5075
5075     FORMAT(1H1)
   2             CONTINUE
                 STOP
                 END
         SUBROUTINE   RKG    (NEQ,H,X,Y,DY,Q)
         DIMENSION  A(2)
         DIMENSION  Y(NEQ),DY(NEQ),Q(NEQ)
         A(1)=0.29289321881345247 5
         A(2)=1.70710678118654752
         H2=.5*H
         CALL    DERIV    (NEQ,X,Y,DY)
                 DO  1   I=1,NEQ
         B=H2*DY(I)-Q(I)
         Y(I)=Y(I)+B
   1     Q(I)=Q(I)+3.*B-H2*DY(I)
         X=X+H2
                 DO  2  J=1,2
         CALL    DERIV    (NEQ,X,Y,DY)
                 DO  2  I=1,NEQ
         B=A(J)*(H*DY(I)-Q(I))
```

```
      Y(I)=Y(I)+B
    2 Q(I)=Q(I)+3.*B-A(J)*H*DY(I)
      X=X+H2
      CALL    DERIV    (NEQ,X,Y,DY)
                  DO  3   I=1,NEQ
      B=0.16666666666666666*(H*DY(I)-2.*Q(I))
      Y(I)=Y(I)+B
    3 Q(I)=Q(I)+3.*B-H2*DY(I)
                RETURN
                END
      SUBROUTINE    DERIV    (NEQ,X,Y,DY)
      COMMON      A1,A3,A5,ALFA,DDP,DEL,PRL,RO,ROPLUS,TO,TV
      DIMENSION   DY(NEQ),Y(NEQ)
      A6(X)=1.-X/ROPLUS
      A7(X)=(1.-X/DEL)/A6(X)
      SHEAR(X)=(-A3*A5*A7(X)-.5*RO*DDP*(A1*(A6(X)/A1-A1/A6(X))
     1 )+TV*A1/A6(X))/TO
      IF   (X.LT.5.)   DUDY=1.
      IF   (X.GE.5..AND.X.LE.30.)   DUDY=X/5.
      IF   (X.GT.30.)   DUDY=X/2.5
      DY(1)=(1.+ALFA*X*Y(1))/(A6(X)*(1./PRL+SHEAR(X)*DUDY-1.))
                RETURN
                END
```

PREDICTION OF HEAT TRANSFER AND PRESSURE DROP DURING CONDENSATION INSIDE HORIZONTAL TUBES WITH AND WITHOUT TWISTED TAPE INSERTS

by

KONERU RAMAKRISHNA

B.E., Andhra University, Waltair, India, 1976
M. Tech., Indian Institute of Technology, Madras, India, 1978

AN ABSTRACT OF A MASTER'S THESIS

submitted in partial fulfillment of the

requirements for the degree

MASTER OF SCIENCE

Department of Mechanical Engineering

KANSAS STATE UNIVERSITY
Manhattan, Kansas

1980

ABSTRACT

The success of twisted tape inserts in augmenting the heat transfer in single phase flow and boiling inside tubes has lead recently to their use in augmenting in-tube condensation. No single heat transfer or pressure drop correlations are available at the present time to correlate the existing experimental data on condensation inside tubes with twisted tape inserts. The objective of this study was to develop such correlations.

To achieve this objective, two different approaches were attempted. In the first approach a suitable heat transfer correlation was identified, among the existing smooth tube correlations, which correlates both the steam and R-113 condensation data that were reported recently in the literature. Modifiers were applied to the chosen smooth tube heat transfer correlation to bring about the best agreement between the predicted and the existing experimental condensation data in tubes with twisted tape inserts. Similar procedure was followed to develop the pressure drop correlation.

The second approach was analytical in nature in which the analogy between momentum and heat transfer in the condensate liquid film was used. The model analysed was that of condensation inside a semi-circular tube where a continuous condensate film flows along the semi-circular boundary while the remaining straight boundary is insulated and no condensation occurs on it. This model represents the limiting case

of a twisted tape insert with an infinite twist ratio. This analysis was based on the assumption that the pressure drop correlations applicable to circular (smooth) tube condensation are also applicable to condensation inside semi-circular tubes by replacing the tube diameter by the semi-circular tube equivalent diameter. This is the first attempt ever made to analyse such a problem. No experimental data exist in the literature at the present time for the verification of the model analysed. However, a few comparisons were made between the heat transfer coefficients predicted by the analysis and existing experimental data of condensation inside tubes with twisted tape inserts having finite twist ratios. The reliability of the analytical predictions could not be established because of various uncertainities in the analysis. Therefore, no attempt was made to modify the analysis to account for the effect of twist ratio on heat transfer.